Atmospheric circulation, seasonal predictability and Britain's energy system

PhD in Atmosphere, Oceans and Climate

Department of Meteorology

Hazel E. Thornton

November 2018

Supervisors:

Prof. Sir Brian Hoskins

Prof. Adam Scaife

Dr. David Brayshaw

Declaration

I confirm that this is my own work and the use of all material from other sources has been properly and fully acknowledged.

- Hazel Thornton

Acknowledgements

First and foremost I'd like to thank my supervisors, Adam Scaife, Brian Hoskins and David Brayshaw. I have thoroughly enjoyed doing my PhD which is thanks to their commitment, encouragement and brilliance. I could not have asked for more. Secondly I'd like to thank colleagues at the Met Office, Doug Smith, Philip Bett, Nicky Stringer, Julia Lockwood, Jo Camp, Nick Dunstone, Simon Brown, Erika Palin, Kate Halladay and Kirsty Lewis, for useful discussions, computer wizardry and friendship. A big thank you to Rob and my family for listening to my running commentary on progress and for supporting me throughout. Finally, a special thank you to Emily for giving me the drive, motivation and deadline to complete this PhD.

'If at first you don't succeed, try, try, again.'
Thomas H. Palmer, 1840

Abstract

This PhD explores the influence of winter weather on the British energy system. It investigates the effect of weather variability on electricity and gas demand and on wind power generation. Weather-driven extremes of energy demand have a significant impact on the wider energy system, and therefore their risk is quantified and the driving circulation patterns identified. In addition, to potentially improve the energy sector's preparedness for winter, the skill of seasonal weather forecasts to predict winter energy demand is assessed.

The analysis indicates that energy demand has a strong anti-correlation with temperature, once socio-economic influences are removed. A 1°C reduction in temperature typically gives a 1% increase in daily electricity demand and a 3%-4% increase in gas demand. The risk of extreme demand is assessed using a long temperature record and the modern-day temperature-demand relationship. For example, the risk of a winter having at least as much energy demand as December 2010 is estimated to be one in ~34 years (95% confidence interval of 20-60 years).

To assess the ability of wind turbines to provide power during high electricity demand, the relationship between wind power and demand is characterised. In winter, average wind power availability reduces by a third between lower and higher demand. However, during highest demand there is a modest recovery in wind power. This relationship is driven by the large-scale weather patterns affecting Northern Europe. During high demand events, neighbouring countries may struggle to provide additional capacity due to concurrent low temperatures and reduced wind power.

Skilful predictions of winter mean gas demand and the number of extreme demand days over the winter period are possible from seasonal forecasts initialised in November. Use of such forecasts could help improve the security of gas supplies and reduce the impacts associated with extreme demand events.

Publications

The research in each of chapters 3, 4 and 5 of this thesis has been published:

Thornton, H.E., Hoskins, B.J. and Scaife, A.A., 2016: The role of temperature in the variability and extremes of electricity and gas demand in Great Britain. *Environmental Research Letters*, 11, doi:10.1088/1748-9326/11/11/114015.

Thornton, H.E., A.A. Scaife, B.J. Hoskins and D.J. Brayshaw, 2017: The relationship between wind power, electricity demand and winter weather patterns in Great Britain. *Environmental Research Letters*, 12, doi:10.1088/1748-9326/aa69c6.

Thornton, H.E., A.A. Scaife, B.J. Hoskins, D.J. Brayshaw, D. Smith, N. Dunstone, N. Stringer, and P.E. Bett, 2019: Skilful seasonal prediction of winter gas demand. *Environmental Research Letters*, 14, doi:10.1088/1748-9326/aaf338

Contents

Chapter 1

Introduction

1.1 Variability of Britain's winter climate

The variability of winter weather in Britain is widely discussed. Daily, country-wide average temperatures can range from below freezing to greater than 10°C within a matter of days. Equally a number of wet days can be followed by a week of very little rain. This variety of weather conditions reflects the geographical location of Britain, positioned between the Atlantic Ocean and the European continent and in proximity to the Arctic. With its lower thermal capacity, the European land mass loses its summer and autumn warmth much quicker than the ocean. Consequently, air flows from the east of Britain in winter are typically coldest, being on average five degrees cooler than air flows from the west and marginally cooler than air flows from the north (Osborn et al. 1999). In contrast, winter rainfall in Britain is more dependent on the vorticity than the wind direction, with higher accumulations during cyclonic flow.

Much of this daily weather variability is driven by the presence of synoptic weather systems. Britain is positioned at the eastern end of the North Atlantic storm track (Blackmon, 1976). Low pressure systems that form in the western Atlantic, develop and move across the ocean. During this process, the low-level air circulating in the systems is progressively moistened through evaporation from the warm underlying ocean. Upon reaching Britain low pressure systems can bring warm, wet and windy conditions. Related to its position at the end of the storm-track, Britain is also a region which can be strongly influenced by blocking high pressure systems (Rex, 1950). Blocking highs are typically larger in scale (∼2000km – 4000km across) than low pressure systems and they last for longer (6-11 days, Pinheiro et al. 2019). Low pressure systems are diverted to the north and south of such high pressure systems, and their passage over Britain is often ‘blocked’. During blocked conditions in winter, Britain is typically cooler, calmer and drier, with easterly or northerly winds.

Considering the winter as a whole, some winters have a higher number of low pressure systems, whilst others are more dominated by high pressure systems. For example during the winter of 2013/14 the UK experienced record average rainfall, associated with numerous wind storms (Knight et al., 2017). In contrast, winter 2009/10 was one of the coldest on record, with many days dominated by high pressure (Cattiaux et al., 2010). The North Atlantic Oscillation (‘NAO’) is a measure of the meridional pressure contrast across the North Atlantic (Wallace and Gutzler, 1981). The phase of the NAO influences the winter climate of Britain and the wider Atlantic basin, including the location, strength and number of storms and the associated wind, temperature and rainfall conditions (Hurrell 1995 and Hurrell and Deser 2009). Understanding what drives the phase of the NAO and the associated winter climate is complex and not fully-understood, and involves the influence of teleconnections to climate processes in different parts of the world. For example Atlantic sea surface temperatures (SST), the variability of climate in the Pacific, known as the El Nino Southern Oscillation (ENSO) or the phase of the winds in the equatorial region of the stratosphere (the Quasi Biennial Oscillation, QBO) can all influence the winter conditions experienced in Britain (Rodwell et al. 1999, Fraedrich and Muller 1992, Marshall and Scaife 2009). Although many of these drivers are now skilfully predicted at the seasonal timescale (Saha et al. 2006, Scaife et al. 2014b), the variety and combination of drivers that can influence Britain’s winter makes its seasonal prediction challenging.

1.2 The impact of weather on Britain’s energy system

All sectors of society are critically dependent upon the availability of energy, including health, housing and the economy. The primary aim of an energy system operator is to ensure a resilient supply of both electricity and gas, sufficient to meet the national demand. The variability and extremes of winter weather in Britain can cause problems for the provision of energy. For example low temperatures can compromise energy security, due to the strong dependence of energy demand on temperature (Bessec and Fouquau 2008, Szoplik 2015). A recent example occurred in March 2018, when very low temperatures associated with strong easterly winds (named the 'Beast from the East') produced high gas demand and caused the system operator to issue a gas deficit warning (National Grid, 2018). Other impacts include wind storm damage on transmission infrastructure and flooding of ground based assets such as sub-stations after heavy rainfall (McColl et al. 2012). The energy sector is, however, experienced in managing the impacts of weather on its operations, using a range of weather forecasts to increase its preparedness.

The influence of weather on the energy system is rapidly increasing, due to the changing energy landscape. With the global drive to reduce green-house gas emissions and in order to limit the effects of anthropogenic climate change, the development of renewable electricity generation has been widely promoted both in Britain and around the world (Wiser et al., 2011). Wind and solar power capacity in Britain has increased rapidly in the last decade and its growth is projected to continue (BEIS, 2018). Both wind and solar power generation are directly determined by daily weather conditions; consequently, as their installed capacity increases, the influence of weather on the supply of electricity will also increase. When balancing the network, weather variability must now be taken into account when estimating the demand, the generation and also the supply of energy.

1.3 Thesis aims

This PhD explores the influence of weather variability on certain aspects of the British energy system in winter. The focus is on understanding the impact of weather and atmospheric circulation on electricity and gas demand and on the availability of wind power. The magnitude, likelihood and drivers of extreme demand events are explored. Finally, the skill of current seasonal weather forecasts to predict winter energy demand is assessed.

1.3.1 Risk of high demand events

Balancing energy supply and demand is most challenging when demand is at its highest. The amount of generation capacity in Britain is dictated and financed by the market, with new generation sources only being built when there is sufficient demand for additional generation. Consequently, there is little additional capacity beyond what is normally required. This contrasts with for example France, where there is a large surplus in electricity generation capacity and where Government invests heavily in the building of additional capacity (International Energy Agency, 2016).

During peak demand in Britain, the grid operator requires energy generated from the full range of suppliers. If supplies are insufficient, there is a heightened risk of electricity black outs or gas shortages. The British Government stipulates that the energy system must be able to cope with a certain level of extreme demand, such as the 1 in 20 year peak daily demand (National Grid, 2016). A thorough understanding of the risk and magnitude of extreme demand events is therefore beneficial. Quantifying this risk is however made more difficult by the short length of many energy demand data sets (typically 15-30 years) and by society's changing demand patterns. However, the strong anti-correlation between demand and temperature offers the opportunity to use much longer temperature data series (>200 years) to estimate the risk of weather-driven extreme demand events.

This PhD investigates the variability of daily electricity and gas demand in Britain over the observed period (from 1975 onwards), exploring the role of both socio-economic and meteorological drivers. In addition, the magnitude and risk of weather-driven extreme demand events are quantified, and historical events are put into context.

1.3.2 Wind power availability during high demand

With the drive to de-carbonise the energy system, the ability of renewable energy sources to replace traditional generation sources needs to be understood. During the winter of 2010/2011 there were episodes where both temperatures and wind speeds in Britain were very low. This created days with extreme electricity demand but very little wind power. Individuals in the energy industry and sections of the media began questioning the ability of wind turbines to provide power when most needed (Royal Academy of Engineering 2013) and preliminary studies have given non-conclusive results (Zachary and Dent 2012, Brayshaw et al. 2012, Harrison et al. 2015). The British Government is keen to understand whether the conditions experienced during that winter were typical or anomalous. In addition they want to know if conditions were similar in neighbouring countries, to understand whether additional supplies of electricity can be sourced through interconnection when British supplies are stretched.

This PhD consequently explores the relationship between electricity demand and wind power supply in Britain, with a particular focus on extreme demand conditions. The role and importance of atmospheric circulation in this relationship is investigated. In addition, a basic assessment of the demand and wind power conditions in the rest of Europe during peak electricity demand in Britain is established, to determine whether inter-connectors could improve the security of Britain's electricity supplies.

1.3.3 Seasonal predictability of winter demand

Seasonal forecasting of winter climate in North-western Europe has improved in the last decade. The winter NAO can now be skilfully predicted by a number of seasonal prediction systems (Baker et al., 2018). This improvement has been attributed to having higher resolution models and a larger ensemble size (Scaife et al. 2014b, Eade et al. 2014). Studies have begun to demonstrate that current skill levels are sufficient to skilfully forecast the impacts of winter weather on different sectors of society (e.g. Svensson et al. 2015, Palin et al. 2016).

The use of seasonal forecast information by Britain's energy industry is currently limited. To ensure that the energy sector is as prepared as possible ahead of the winter, a 'Winter Outlook' report is compiled by the grid operator (National Grid, 2017). This details the operator's view on the security of supply of electricity and gas systems for the coming winter and is based on a survey of industry participants. The report is made publicly available and it is used by a range of different actors across the industry to help prepare for the winter. The outlook gives a forecast of total and peak winter demand, the likely supply margins and the expected availability of different supplies. These estimates are based on societal drivers of demand and supply, such as the strength of the economy and the availability of generation and storage infrastructure, however they do not currently take account of any weather forecast information. Rather, the influence of weather on these demand predictions is assessed by assuming standard winter weather conditions and by stress testing using historical meteorological extremes.

This PhD capitalises on the recent improvements in winter climate forecasting to assess whether seasonal forecasts can be used to predict winter energy demand. Specifically, the skill in predicting winter mean gas demand and the number of high gas demand days during winter is assessed.

1.3.4 Thesis questions

To summarise the key questions addressed in this PhD are:

- How has Britain's energy demand varied over the recent period and what has driven this variability? What is the risk and magnitude of weather-driven extreme demand events today?
- What is the relationship between wind power and electricity demand and to what extent can it be explained by meteorology? Can wind turbines provide power during high demand periods? Can interconnection help improve the security of energy supply?
- Can seasonal weather forecasts predict winter mean gas demand and the number of high gas demand days over the winter period?

Chapter 2

Literature Review

2.1 Climate of the North Atlantic and European region

2.1.1 Meridional radiation imbalance

The sun's radiation ultimately drives the climate system. Most of the sun's short wave-length radiative energy passes through the atmosphere and is either absorbed by the earth's surface or is reflected back out to space, depending on the albedo of the surface and cloud amount (Wallace and Hobbs, 1977). The short wave-length energy flux varies significantly with latitude and time, generating the diurnal and seasonal cycles. The oceans are heated by direct absorption of short wave-length radiation, while the atmosphere is mostly heated by either sensible heat from the earth's surface or by absorption of long-wavelength infra-red (IR) radiation emitted from the earth's surface. The release of latent heat into the atmosphere through condensation is another important source of atmospheric heating. At low latitudes there is a net gain in energy, with incoming solar radiation exceeding outgoing radiation. In contrast, in the polar regions there is a net loss of energy (Trenberth and Solomon, 1994). This net energy imbalance from the equator to pole can be considered to drive the circulations of the ocean and atmosphere.

2.1.2 Ocean heat transport

Figure 2.1 (Trenberth and Fasullo, 2017) shows the poleward energy transport in the oceans and atmosphere and highlights the variation in energy transport with latitude. Energy transport peaks around 35° North, and is dominated by transport within the atmosphere at this latitude. Nearer to the equator the ocean plays a more significant role. Even though the Atlantic Ocean is a smaller basin than the Pacific, it plays an important and unique role in climate variability (Trenberth and Fasullo, 2017). The Atlantic Meridional Overturning Circulation (AMOC) is responsible for most of the meridional transport of heat by the mid-latitude northern hemisphere oceans (see Figure 2.1 right). In addition to the direct transportation of heat northwards by the AMOC, the atmosphere is heated from below, with an upward surface heat flux of 80-100W/m^2 (Trenberth and Fasullo, 2017). Variations in AMOC strength are linked to multi-decadal variations in sea surface temperatures in the North Atlantic, referred to as the 'Atlantic Multi-decadal Oscillation' (AMO, Kerr 2000, Knight et al. 2005). The AMO can influence the climate of the Atlantic basin, with for example an increase in extratropical cyclonicity and rainfall during its positive (warmer) phase (Knight et al., 2006).

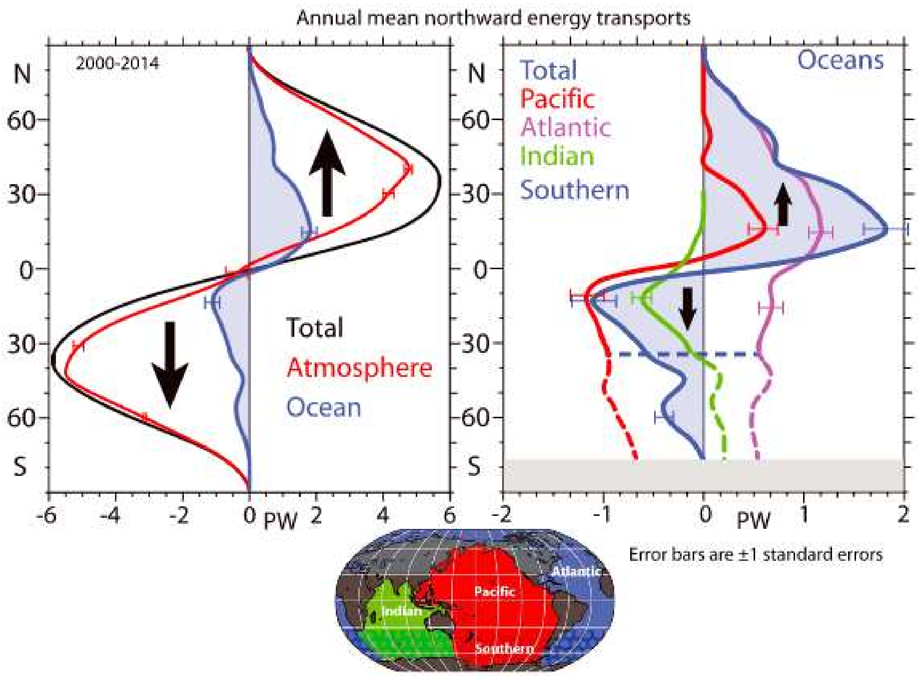

Figure 2.1: Northward energy transports. Left: The annual and zonal means of the northward energy transports for 2000-2014 in PW for the total Earth system (black), the atmosphere (red) and the ocean (blue). Right: The ocean component broken down into the contributions from the Atlantic (violet), Pacific (red), and Indian (green) Oceans which combine south of 35°S to give the southern ocean value, as given in the small map below. The error bars are 1 standard deviation. Trenberth and Fasullo (2017).

2.1.3 North Atlantic storm track

The meridional gradient in air temperature over the North Atlantic is strongest in the winter season. In mid-latitudes there is a balance between the horizontal pressure gradient and the Coriolis force, resulting in winds which are in approximate geostrophic balance. There is also a balance between the vertical pressure gradient and the gravity force, referred to as hydrostatic balance. As a result of these balances, vertical variations of the geostrophic wind are then proportional to the horizontal variations of the temperature field, through the thermal wind balance. The large decrease in temperature with latitude from equator to pole in winter is consequently accompanied by an increase in zonal wind speeds with height. In certain conditions, the shear in the flow can allow small disturbances to amplify and grow, through positive feedback between circulations at the surface and aloft (see Hoskins and James 2014 for a thorough description). This process is known as baroclinic instability and describes the conversion of available potential energy into eddy kinetic energy and is the basis for the development of cyclones and anticyclones (Woollings, 2010). These synoptic weather systems transport cold air southwards and warm air northwards, and contribute to the northwards flux of heat. Developing cyclones move across the Atlantic from the west to east, with a south-west north-east tilt, in a region known as the North Atlantic storm track (see Figure 2.2b). If these storms are still active when they reach the west coast of Europe, they can bring strong winds and heavy rainfall. As the low pressure systems decay, their eddy kinetic energy is partly converted into zonal kinetic energy. Momentum is consequently fed back to the underlying atmospheric flow (Woollings, 2010), creating a band of strong westerly winds, known as the eddy driven jet stream.

2.1.4 Jet streams

A jet stream is a band of very strong winds. In the northern hemisphere winter, strong winds are found near the tropopause, circling much of the globe, as shown in Figure 2.2a. Two jet streams are distinguished in the northern hemisphere winter, the subtropical jet stream and the eddy driven jet stream (Woollings et al., 2010). The subtropical jet is located at approximately 30-35°North, and arises from a thermal wind balance with the strong meridional temperature gradients at the edge of the Hadley cell (Vallis et al., 2004). This subtropical jet stream is limited to the upper troposphere. In contrast, the eddy driven jet stream occurs throughout the depth of the troposphere and results from the transfer of momentum from transient eddies to the large scale flow. At most longitudes the two jet streams overlap, whilst in the Atlantic, there is a clear separation, with the eddy driven jet 10-15° further north than the subtropical jet. Woollings (2010) state the separation of the two jets over the Atlantic as one of the underlying reasons why European weather is so unique. The position of the eddy driven jet stream varies significantly from week to week, and consequently on any given day the upper level winds will differ from the winter mean shown in Figure 2.2a. Woollings et al. (2010) found 3 main locations for the lower tropospheric Atlantic eddy driven jet, a southerly, mid and northerly latitude location (approximately 37°N, 45°N and 57°N). These relate closely to the three Atlantic atmospheric regimes (NAO negative, NAO positive and Atlantic ridging) discussed in section 2.2.2.

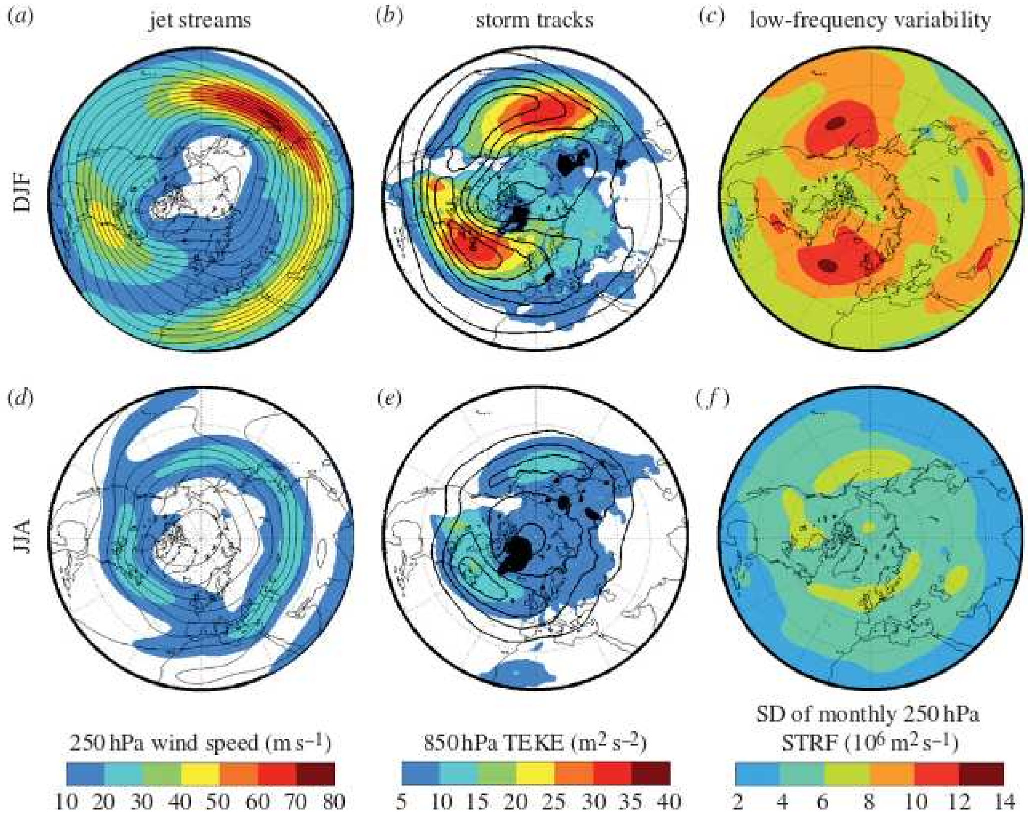

Figure 2.2: Northern Hemisphere climatology for December 1957 to August 2002 from the ERA-40 reanalysis. a) December-February (DJF) 250 hPa wind speed with streamfunction contoured every $1 \times 10^7 m^2 s^{-1}$. b) DJF transient eddy kinetic energy (TEKE) using 2-6 day bandpass filtered winds. Shading shows low level values (850 hPa) and contour lines show the upper level (250 hPa) values contoured every 20 $m^2 s^{-2}$. c) Standard deviation of monthly-mean 250 hPa streamfunction in DJF. d)-f) as a)-c) but for June-August (JJA). Woollings (2010).

2.1.5 Stationary waves

Figure 2.2a also shows the winter mean streamfunction over the Northern hemisphere. Troughs are seen over the western side of the Pacific and Atlantic Oceans, with a ridge over Europe. The zonal deviations in the winter mean flow can be described as large scale stationary Rossby waves, and are linked to the distribution of continents and oceans (Holton, 1992). The North Atlantic storm track (Figure 2.2b) is seen to follow the streamfunction lines over the Atlantic. Brayshaw et al. (2009) have attributed the location and orientation of the storm track to the configuration of the Rocky mountains and the orientation of the East coast of North America. The path of developing cyclones has been shown to be steered by the eddy-driven jet (Lau 1988, Branstator 1995). As mentioned above the eddies themselves, particularly through variation in eddy momentum flux convergence, drive the variability in strength and position of the jet stream (Vallis et al., 2004). The storm track and jet stream consequently feed back upon one another. The surface winds in the storm track region also drive the western boundary current in the Atlantic Ocean, which itself is crucial to the existence of the storm track. Hoskins and Valdes (1990) consequently describe the storm tracks as self-maintaining.

2.1.6 Blocking

Atmospheric blocking is a large-scale atmospheric flow regime which is observed to be both quasi-stationary and persistent in nature (Pelly, 2001). As the name suggests, blocking occurs when the westerly jet in the mid-latitudes is blocked, and cyclones moving within the jet are deflected either side of the blocking feature. A block was first described by Rex (1950) as the splitting of the basic westerly current into two branches extending over at least 45° of longitude and lasting for a period of ten days or more. Since then a wide range of blocking definitions have been developed (see Woollings et al. 2018 for a summary), and their breadth reflects the wide range of conditions interpreted as blocking. Three main types of block are frequently described, a dipole block, an omega block or an open ridge of high pressure. A key feature in all definitions, is a large area of high pressure with associated barotropic anti-cyclonic flow. In a dipole block, an area of low pressure also exists to the south of the high pressure, which helps to maintain the position of the block (Hoskins and James, 2014).

There is currently still no comprehensive theory of blocking (Woollings et al., 2018). However the importance of upper level dynamics in the generation of blocks is clear. When planetary scale Rossby waves, which propagate in a westwards direction relative to the upper level westerly flow, become extended in latitude and break, air parcels are cut off from their source regions. Once cut off, the structures can only disappear if either the air returns to its source location, or through frictional or heating processes (Hoskins and James, 2014). The stability of the blocking dipole means blocks often last for a week or longer, longer than would be expected given diabatic processes alone. During extreme blocking events, such as the blocking over Russia in the summer of 2010, anomalous convection in the tropics has been found to drive and maintain the Rossby wave forcing responsible for the development of a long lasting block (Trenberth and Fasullo, 2012). Others have found that upstream eddies can help maintain the block structure, by encouraging further wave breaking and by contributing vorticity anomalies into the block (e.g. Shutts 1983, Altenhoff et al. 2008). The importance of diabatic heating in blocking processes has only recently been emphasised (Croci-Maspoli and Davies 2009, Pfahl et al. 2015).

In the Northern hemisphere, blocking predominantly occurs over the eastern regions of the Atlantic and Pacific Oceans (Tibaldi and Molteni, 1990). The impact of blocking on European weather is significant and depends on the location of the block and time of year. For example in winter, Scandinavian blocking can produce cold, calm conditions over much of Northern Europe, whilst in summer, heat wave conditions can result. If a blocking anticyclone is particularly persistent, the deflection of low pressure systems around the block can lead to drought conditions beneath the high pressure system and increased rainfall elsewhere (Trigo et al., 2004).

2.2 Variability of North Atlantic winter climate

2.2.1 Low frequency variability: Teleconnection patterns

Analysis of long records of monthly mean atmospheric circulation reveal large scale correlations between the flow at remote locations. Such correlations are referred to as 'teleconnections' to stress the correlation-at-a-distance aspect of their nature (James, 1994). A teleconnection describes the contemporaneous and lagged variations in climate over distant parts of the globe. Teleconnections have fixed locations, with nodes and anti-nodes, which oscillate in parallel. At its simplest level, a teleconnection is identified by calculating the correlation between all individual grid points across the globe and then identifying regions which are distant (greater than a typical synoptic feature) and are strongly correlated with one another.

The two main large-scale teleconnection patterns of the Northern Hemisphere 500hPa geopotential height field are the Pacific-North American (PNA) pattern and the North Atlantic Oscillation (NAO) and are shown in Figure 2.3 (James 1994, following Wallace and Gutzler 1981). The PNA pattern has four centres of action, the central Pacific, northeast Pacific, northwest Canada and southeast USA. The NAO has two main centres of action, in the subtropical Atlantic and the northwest Atlantic. These teleconnections indicate connections between the tropics and mid-latitudes, and reflect meridionally propagating Rossby waves (James, 1994).

Another approach used to analyse low frequency climate variability is principal components analysis (PCA). Compared to correlation analysis described above, PCA has the benefit of giving information about the timescale of variability. The aim of PCA is to represent the maximum possible fraction of the variability contained in an original data set through a smaller set of orthogonal eigenvectors (known as EOFs, see Wilks 2006). The NAO is the first EOF of the North Atlantic region, explaining 39% of the variance of the winter sea level pressure field (see Figure 2.4, Hurrell and Deser 2009). A clear dipole in pressure between the northern and southern regions of the North Atlantic is seen.

The North Atlantic Oscillation

The North Atlantic Oscillation is the dominant mode of atmospheric variability in the North Atlantic and European region. In the positive phase of the NAO, atmospheric pressure is higher than normal in the region of the Azores high and lower than normal over the Icelandic region, leading to an anomalously strong pressure gradient over the North Atlantic basin. This strengthened pressure gradient is associated with stronger westerly winds and a more northerly and intense storm track (Rogers, 1990). Warmer wetter conditions are experienced over Northern Europe and Eastern US, whilst cooler, drier conditions occur over the Mediterranean and the Canadian Arctic (Wallace and Gutzler 1981, Hurrell 1995, Hurrell and Deser 2009). In contrast, during the NAO's negative phase, the pressure gradient across the North Atlantic is weaker than normal and at times even reversed. This leads to an increase in air flows over Europe from the east and north and a higher chance of anticyclonic blocking (Shabbar et al., 2001). Conditions in Northern Europe and the Eastern US are consequently colder and drier than normal, whilst the Mediterranean and Canadian Arctic are warmer and wetter than usual (Hurrell, 1995).

The NAO also influences the ocean. On interannual and sub-decadal timescales, variations in the NAO drive a tripole pattern of SST anomalies in the North Atlantic

(Marshall et al. 2001, Delworth et al. 2017). This SST pattern is a direct response of the ocean mixed layer to turbulent surface heat flux anomalies associated with the NAO. The strong coupling between the surface winds and the surface ocean means that the NAO also influences wave height, with larger waves in the northeast Atlantic and smaller waves south of 40° North during NAO positive conditions (Visbeck et al. 2003, Bacon and Carter 1993). On timescales longer than ten years, there is a lagged response of the ocean to the NAO. For example, a prolonged positive NAO anomaly will enhance the strength of the AMOC after a decadal-scale delay, leading to increased northwards heat transport and warmer basin wide SSTs (Delworth et al., 2017).

To a lesser extent, the ocean can also influence the atmosphere in the North Atlantic. Variability of the NAO at both shorter and longer timescales is found to be driven in part by the SST tripole in the North Atlantic and by ENSO in the Pacific (Rodwell et al. 1999, Czaja and Frankignoul 2002, Deser et al. 2007, Folland et al. 2012, Dunstone et al. 2016). These results highlight the two-way feedback between the ocean and atmosphere.

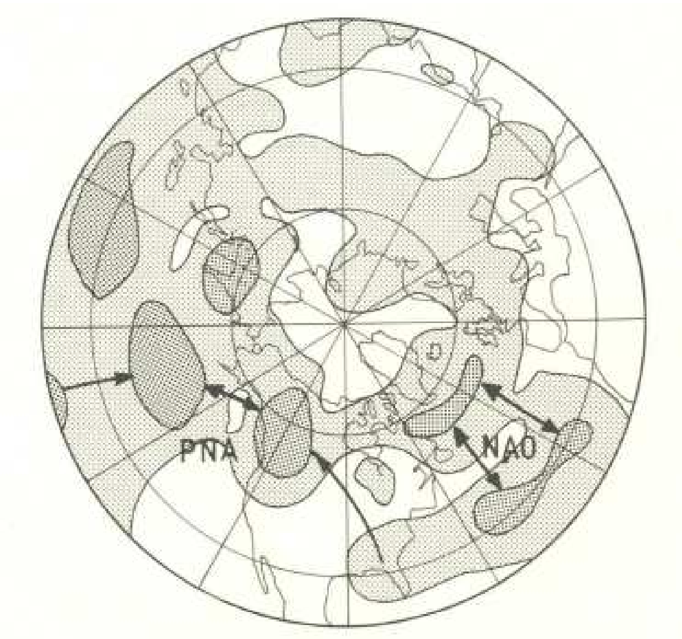

Figure 2.3: Summary of the main teleconnection patterns for the northern hemisphere winter, based on the monthly mean geopotential height fields. The heavy lines denote the 0.6 correlation contours. James (1994), after Wallace and Gutzler (1981)

Understanding of the dynamical drivers of the winter NAO has increased in recent decades. The Quasi-Biennial Oscillation, sudden stratospheric warmings,

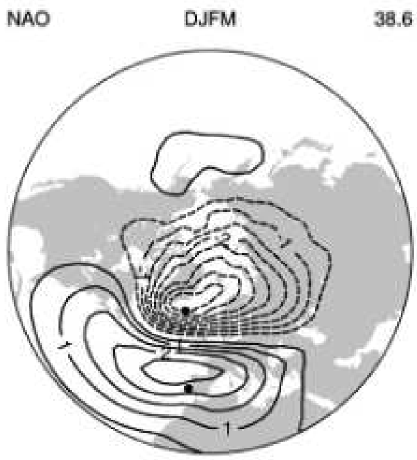

Figure 2.4: Leading empirical orthogonal function (EOF1) of the winter (December to March) mean sea level pressure anomalies over the North Atlantic sector and the percentage of the total variance explained. The data cover 1899-2006. Hurrell and Deser (2009).

Atlantic SSTs, the El Nino Southern Oscillation and tropical precipitation are all now considered to affect the winter NAO (Thompson et al. 2002, Baldwin and Dunkerton 2001, Czaja and Frankignoul 2002, Merkel and Latif 2002, Scaife et al. 2017). The response of the NAO to these dynamical drivers is discussed in the seasonal prediction section 2.6. In summary the NAO drives significant variations in weather and climate across the whole North Atlantic basin and across a range of timescales.

2.2.2 Synoptic variability: Weather regimes

To better understand North Atlantic synoptic (multi-day) climate variability, many studies have attempted to identify the dominant large-scale weather regimes present in winter. This approach assumes the atmosphere preferentially evolves between a number of dominant states or regimes and compared to PCA, it attempts to identify more physically meaningful patterns of climate variability. A number of statistical techniques have been used to identify possible regimes. Initial efforts involved subjectively grouping together patterns in synoptic weather charts, for example the Lamb weather types (Lamb, 1972). More recently methods have become objective and identify the weather or climate states which correspond to peaks in the probability density function of the climate phase space (see Fereday et al. 2008 for a thorough summary).

An objective regime classification method frequently used is cluster analysis.

Cluster analysis essentially sorts data into groups whose identities are not known in advance (Wilks, 2006). A number of clustering algorithms have been developed, based on either hierarchical or non-hierarchical methods. The former, reduces the number of groups by successively identifying and combining the two most similar members, until the desired number of groups is achieved. In contrast, non-hierarchical methods such as K-means clustering, specify the number of groups at the start and then move members between groups until each member in the group is closest to its own centroid and far from the centroids of neighbouring groups. To reduce the dimensionality of the data set being clustered, the data is often projected on the leading few EOFs prior to clustering. Clustering can be applied to daily, or temporally averaged data, such as monthly means.

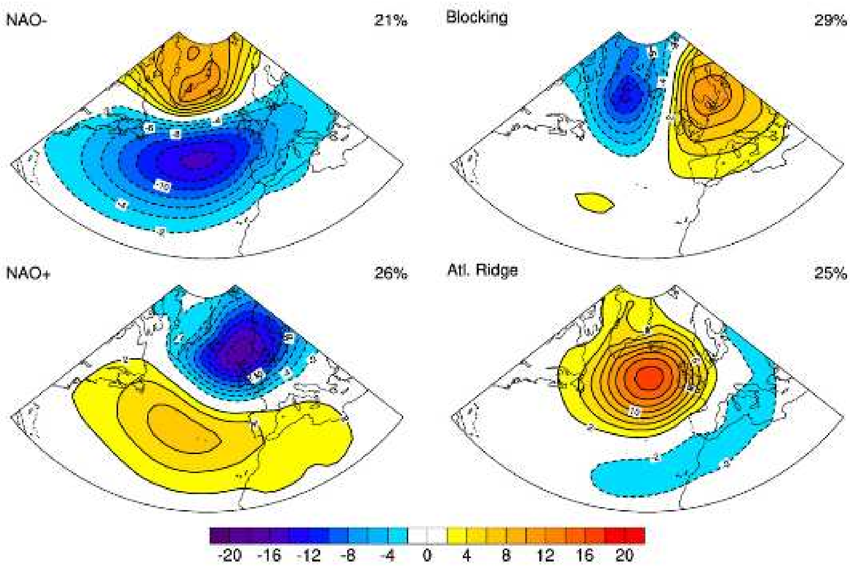

Figure 2.5: Winter (December-March) weather regimes in sea level pressure (hPa) over the North Atlantic domain using daily data from 1950-2006. The percentage at the top right of each panel expresses the frequency of occurrence of a cluster out of all winter days since 1950. Hurrell and Deser (2009) following Cassou et al. (2004).

Four weather regimes are typically found to summarise the daily variability of the atmospheric pressure field over the North Atlantic, shown in Figure 2.5 (Hurrell and Deser 2009, following Cassou et al. 2004). The four regimes comprise of the two phases of the NAO, and two further regimes dominated by a centre of high pressure located over either Scandinavia (referred to as 'Blocking') or to the west of the UK (the 'Atlantic ridge' regime). Cassou et al. (2004) and Hurrell and Deser (2009) show that the climatological frequency of each regime over winter is similar (occurring during 20-30% of days) and over the twentieth century some winters are more dominated by one regime than another. For example the winters of the 1960s were dominated by the NAO negative regime, whilst the 1990s had many more NAO positive days. However, for any given winter there is always a mix of regimes, highlighting that although the NAO is the dominant mode of variability in the North Atlantic, it does not explain all the variance seen (Hurrell and Deser, 2009).

The climate of the North Atlantic varies across a range of spatial and temporal scales, as exemplified in Figures 2.3 and 2.5. As highlighted, a range of methods exist to explore this variability and although the detailed behaviour seen can be method specific, the dominant features, such as the NAO remain.

2.3 Britain's winter climate

Britain is located to the North-west of the European continent. To the west of Britain is the Atlantic Ocean and to the east the North Sea. The ocean's higher heat capacity compared to the atmosphere, means that as the autumn leads into winter, the ocean keeps Britain warmer than in other more continental regions at the same latitude. Britain is positioned at the end of the North Atlantic Storm track, in a region where both low pressure systems and blocking anticyclones prevail. Winter climate in Britain is therefore very variable, with warmer wetter winters when the air flow is from the west or south-west and colder, drier winters when the air flow is from the north or east. Figure 2.6 shows the large variability in winter UK mean temperatures from 1910 to 2018, ranging from near freezing to approximately 6°C (NCIC, 2018). UK winter rainfall is shown in Figure 2.7, with winter accumulations ranging from approximately 100 to 550mm. Extreme winters can be identified, such as the cold and dry winter of 1963 (the year refers to the January and February of the winter period) or the very wet winter of 2014.

The weather experienced in a particular winter varies with location. Figure 2.8 shows the variation in winter mean temperature and precipitation across the UK in 2010 and 2014, presented as an anomaly from the 1961-1990 period. The winters of 2010 and 2014 were both recent extreme winters and give an indication of the range of winter weather conditions experienced in Britain. A description of each winter is given below.

2.3.1 Winter 2009/2010

Winter 2010 was the coldest winter in 31 years, with a winter mean temperature of only 1.6°C (Prior and Kendon 2011, see Figure 2.6) and cold anomalies in all

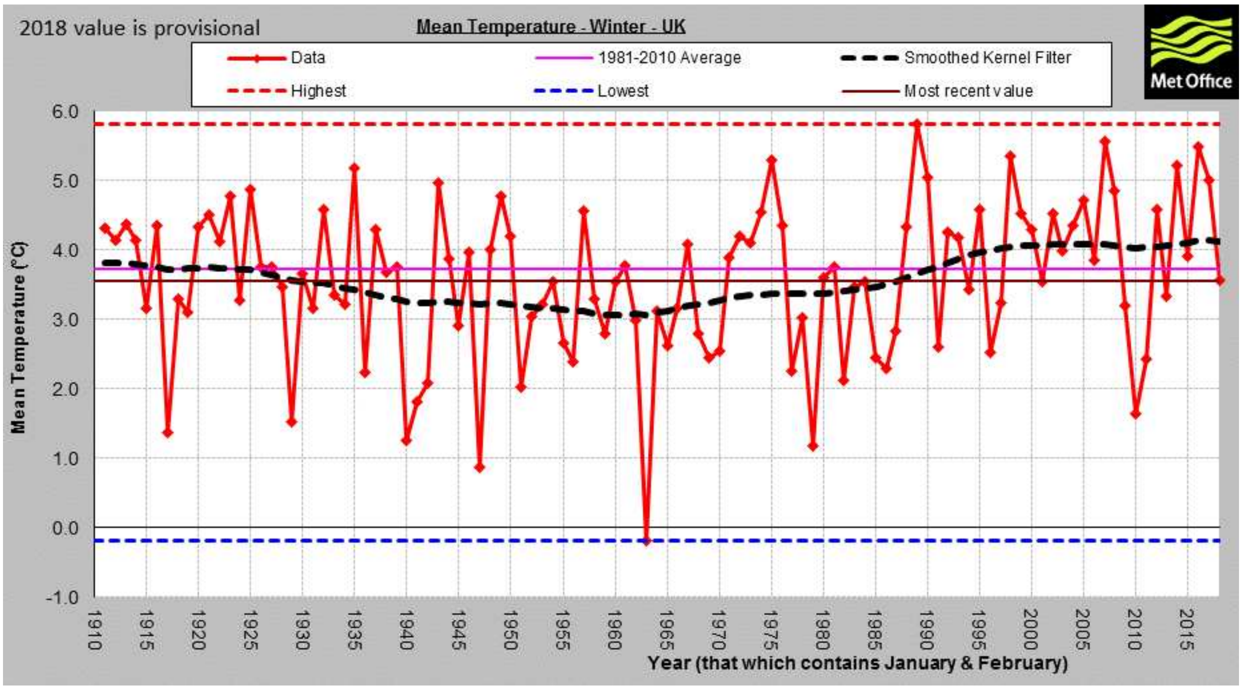

Figure 2.6: Winter mean UK temperature (°C), 1910 to 2018, NCIC (2018).

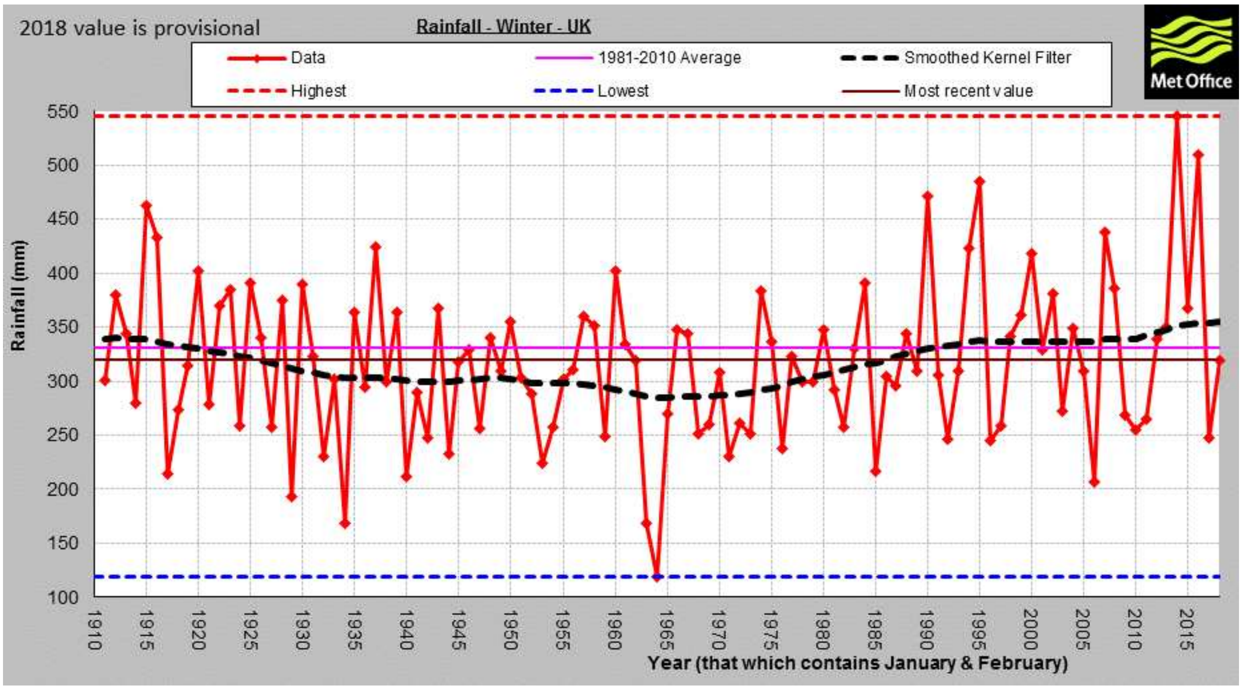

Figure 2.7: Winter mean UK rainfall (mm), 1910 to 2018, NCIC (2018).

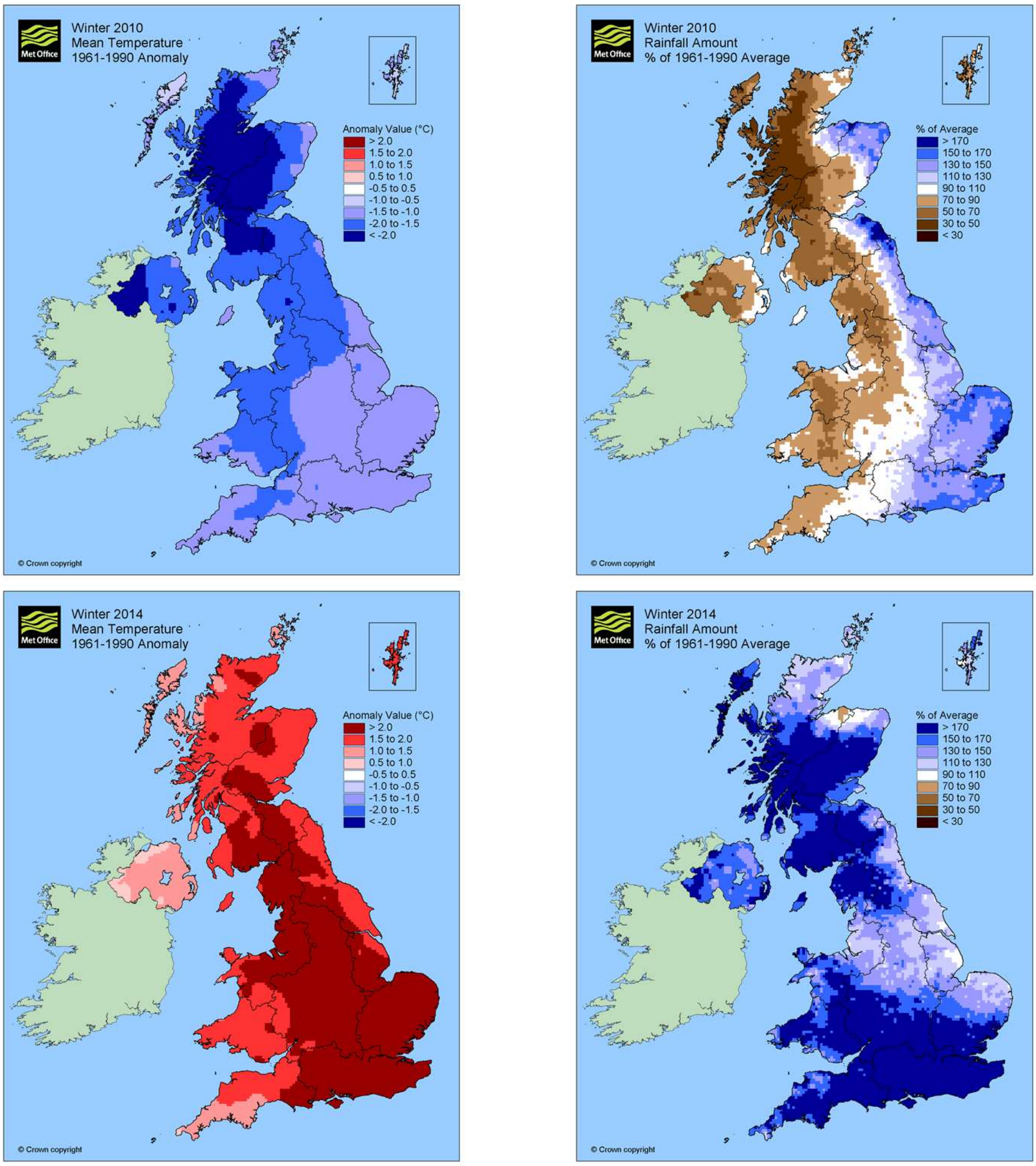

Figure 2.8: The winter mean temperature anomaly from the 1961-1990 average (°C, left) and winter rainfall amount (% of 1961-1990 average, right) for 2010 (upper) and 2014 (lower), NCIC (2018).

regions (Figure 2.8, upper left panel). The winter was characterised by prolonged cold spells, hard frosts and frequent snowfalls, with predominantly easterly and northerly winds bringing air from Northern Europe over the UK. Temperatures fell well below freezing in selected locations, for example -10°C occurred in the Scottish glens. Rainfall totals were higher than average over the eastern half of the UK, but lower over the western half, reflecting the dominance of easterly winds (Figure 2.8, upper right panel). In contrast, exceptionally warm and wet conditions occurred in parts of south-eastern Europe and the Mediterranean (Prior and Kendon, 2011).

In 2010, the 500hPa geopotential height anomaly field was strongly zonal, with anomalously high pressure over the pole and low pressure over mid-latitudes. This led to a record negative winter mean NAO index, almost 3 standard deviations below average (Cattiaux et al., 2010). Winter 2010 also had the second highest blocking frequency since 1949, with 33% of days being classed as blocked. The persistence of the NAO over the winter was notable, with approximately two-thirds of days classified as the NAO negative regime and very few NAO positive regime days (Cattiaux et al., 2010). Wang and Chen (2010) attribute the cold surface temperatures to warming of the stratosphere and its subsequent downwards propagation to the surface. In addition Fereday et al. (2012) also suggested that the easterly phase of the Quasi-Biennial Oscillation (QBO), the strong El Nino, anomalous snow cover and the solar minimum in 2010 may all have contributed to the extreme NAO index that winter. See section 2.4.2 for a description of these patterns of climate variability.

2.3.2 Winter 2013/2014

Winter 2014 was the wettest winter in the UK since records began in 1910, with 165% of average rainfall (see Figure 2.8, lower right panel, NCIC 2018). This was caused by a succession of deep Atlantic low pressure systems affecting the UK (Kendon and McCarthy, 2015). Matthews et al. (2014) found winter 2014 to be the stormiest winter for the UK and Ireland in a 143-year series. Exceptionally high river flows were experienced in many parts of the country, leading to impactful flooding events, particularly in southern regions (Huntingford et al., 2014). The westerly atmospheric flow regime, produced mild conditions across the UK (see Figure 2.8, lower left panel) and the average UK temperature was the fifth highest in a series from 1910. There was a marked absence of cold spells, with few air frosts and little or no snow in the southern half of the UK and at lower elevations (Kendon and McCarthy, 2015).

The winter mean sea level pressure was anomalously low over the UK and to the west of the UK. Such that the winter NAO index was 1.3 standard deviations above the average from 1981-2010. Knight et al. (2017) explored the drivers of winter 2014 and concluded that influences from the tropics were likely to have played a significant role in the development of the unusual extra-tropical circulation. In addition, the westerly phase of the QBO and the associated stronger and more stable stratospheric polar vortex appear to have contributed to the extreme conditions (Huntingford et al. 2014, Knight et al. 2017) .

2.4 Seasonal weather prediction

In 1963 Lorenz discovered the phenomenon of chaos. Even with a perfect model and essentially perfect initial conditions, forecasts lose all predictive information after a finite time. Small instabilities can grow in time and may eventually modify the large-scale flow and change the evolution of a developing circulation system in a distant part of the atmosphere (Hoskins and James, 2014). Lorenz noted that practical predictability is a function of the physical system under investigation, the available observations and the dynamical prediction models used to simulate the system. Based on atmospheric initialization alone, Lorenz found the limit of deterministic predictability for mid-latitude weather was about two weeks.

However, predictable aspects of the atmosphere beyond two weeks have been found to be possible using a combination of three different sources of predictability; inertia of the climate system, patterns of climate variability and the influence of external forcing factors. These sources of predictability are summarised in Figure 2.9 (National Academy of Sciences, 2010) and are described below.

2.4.1 Inertia of the climate system

The inertia of the climate system represents the influence of more slowly varying components of the climate system on the atmosphere. Initialisation of these components can lead to extended predictability. For example, the ocean has a heat capacity 3,500 times that of air, consequently anomalies in ocean heat content develop over much longer timescales than in the atmosphere and also last for much longer. Once such an anomaly has developed, it can have a large impact on the atmosphere over a number of months or years. Predictions of the evolution of European climate can therefore be improved by taking the ocean conditions into account (Rodwell and Doblas-Reyes, 2006).

Other components of the climate system have 'memory' and can be used for seasonal prediction of the atmosphere, including soil moisture, snow cover, vege-

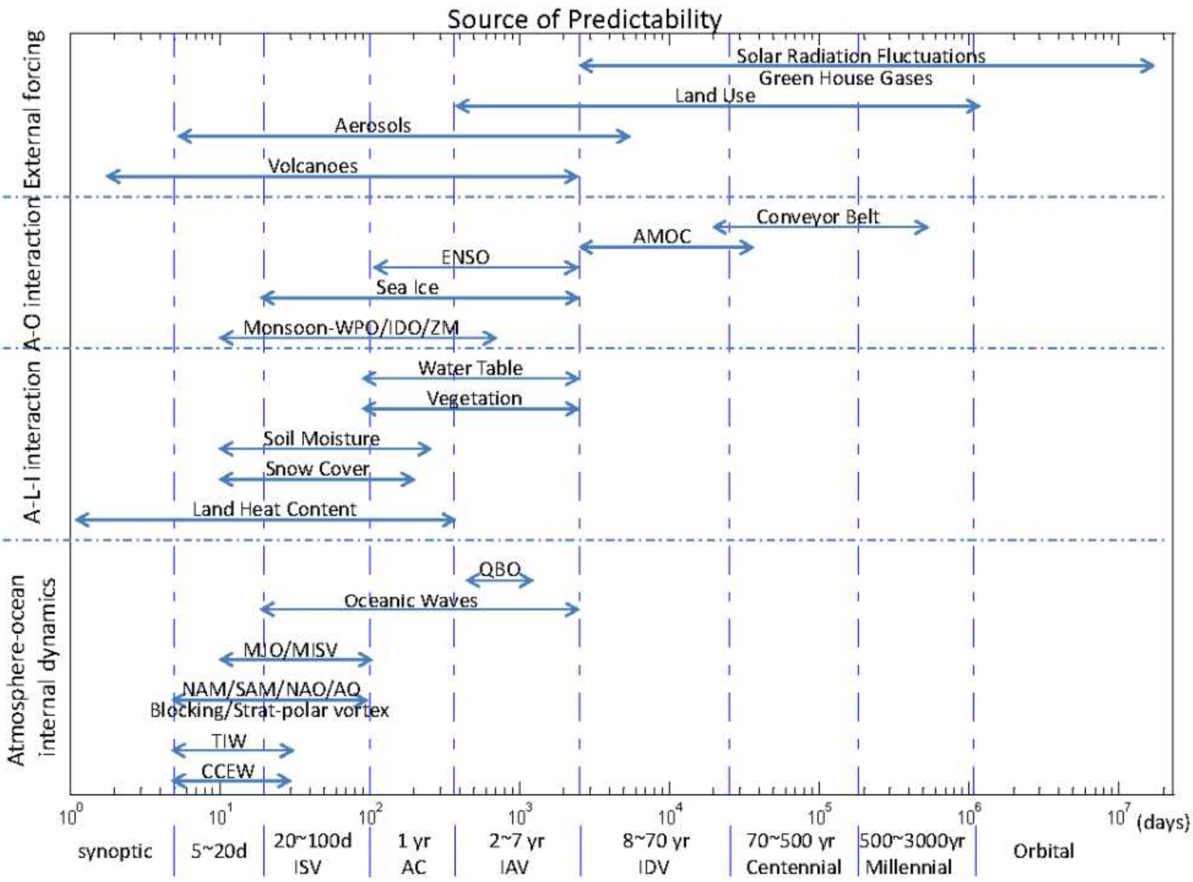

Figure 2.9: Processes that act as sources of interseasonal to interannual climate predictability extend over a wide range of timescales and involve interactions among the atmosphere, ocean and land, National Academy of Sciences (2010).

tation, land heat content and polar sea ice (National Academy of Sciences, 2010). For example, although the moisture content of soil is to a large extent determined by the amount of rainfall received, it varies on a much slower timescale than that of rainfall. Soil moisture integrates the effects of rainfall, evaporation and runoff and influences the atmosphere through impacting the surface energy budget. Soil moisture has been found to influence the evolution of atmospheric temperature and rainfall in certain regions and at certain times of year (Koster and Suarez, 2003). For example, Black et al. (2006) and Fischer et al. (2007) found the precipitation deficit in the preceding spring and the resultant dry soils led to an exacerbation of the European summer heat wave of 2003.

The health of vegetation can also outlive an atmospheric anomaly and influence the local climate long after the initial atmospheric anomaly has subsided (Zeng et al., 1999). Where vegetation is sparse or in higher latitude regions where soil moisture freezes, thermal energy stored in the land surface can also influence the overlying atmosphere over an extended period. The influence of Arctic sea ice on European climate has attracted considerable attention, with contrasting results. However a common conclusion is that a reduction in Arctic sea ice can increase the risk of the negative phase of the NAO in winter (Deser et al. 2004, Screen 2017). Current seasonal prediction systems now initialise sea ice conditions and include interactive sea ice physics to model such feedbacks (Scaife et al., 2014b).

2.4.2 Climate variability

The interaction between different components of the climate system, can lead to quasi-periodic variations in climate that give additional predictability at the seasonal timescale (National Academy of Sciences 2010, Smith et al. 2012). The El Nino Southern Oscillation (ENSO) is the largest-amplitude interannual pattern of climate variability on the planet, with every 2-7 years an oscillation involving the surface temperature of the ocean and atmosphere, rainfall and circulation in the tropical Pacific region (Philander, 1989). ENSO has a large impact on the surface weather in the regions directly affected by the oscillation, but also in regions far from the source region, through Rossby wave induced teleconnections (Wallace and Gutzler 1981, Hoskins and Karoly 1981). For example, the NAO is influenced by ENSO via both a direct tropospheric pathway and also a more remote stratospheric pathway, through the disruption of the stratospheric polar vortex and its subsequent surface impacts (Butler et al., 2014). With the exception of the spring predictability barrier (Duan and Wei, 2013), ENSO can be predicted one to a few seasons in advance using both statistical methods and coupled ocean-atmosphere models (Zebiak and Cane 1987, Saha et al. 2006, Wang et al. 2009, Luo et al. 2008). This skill leads to increased predictability of atmospheric conditions in many locations around the globe.

Other patterns of climate variability that can improve seasonal predictability involve different layers of the atmosphere, such as the influence of convection in the troposphere on the evolution of climate in the stratosphere. For example gravity waves created by tropospheric convection, propagate vertically and drive an oscillation in the tropical zonal winds in the stratosphere, known as the Quasi-Biennial Oscillation (QBO). Approximately every 14 months, the flow direction reverses and its phase is highly predictable (Pohlmann et al. 2013, Scaife et al. 2014a). The QBO has been found to affect the jets in both the stratosphere and the troposphere. During the westerly phase of the QBO, the stratospheric polar vortex is typically stronger, and the tropospheric jet stream often more intense and shifted poleward, increasing the meridional pressure gradient (Holton and Tan 1980, Kidston et al. 2015). This more positive NAO pattern, leads to stronger surface winds and more intense cyclones (Anstey and Shepherd 2014, Kidston et al. 2015). The opposite is true during the easterly phase of the QBO. Consequently, advance knowledge of the QBO phase can improve predictability of the surface conditions (Boer and Hamilton 2008, Scaife et al. 2014b). However, given the QBO is only one of many influencing factors, knowledge of its phase alone is not sufficient to give an accurate forecast of surface winter weather.

Planetary waves also influence the strength of the polar vortex in the stratosphere. Some winters have a strong and persistent westerly flow around the North Pole, whilst in every other winter on average, a sudden stratospheric warming (SSW) event can lead to a complete breakdown of the stratospheric westerlies. SSW are found to be less likely when the QBO is in its westerly phase (Holton and Tan, 1980). After a SSW the anomalously easterly winds move down through the troposphere leading to an increase in the likelihood of easterly flow conditions at the surface and cold air outbreaks (Baldwin and Dunkerton 2001, Thompson et al. 2002). In the weeks following a SSW event, increased predictability of surface conditions over Northern Europe is found (Marshall and Scaife 2010, Sigmond et al. 2013).

The third source of climate predictability at the seasonal timescale comes from the external forcing of climate. Natural external forcing factors include the variation in the sun's output and volcanic eruptions, whilst man-made external forcing includes green-house gas emissions, aerosols and land use change. For example, incoming solar radiation varies with an 11-year cycle and this can have an influence on atmospheric conditions (Haigh and Cargill, 2015), with maximum response lagged by a few of years (Gray et al., 2013). Ineson et al. (2011) find that during a solar minimum, negative NAO conditions and cold Northern European winters are more likely. While a large volcanic eruption can significantly cool the global atmosphere over the following few years (see review by Robock 2000). Human activities, such as the burning of fossil fuels for power generation, or the burning of forests to clear land for agriculture, influence the composition and radiation balance of the atmosphere. For example, GHG forcing leads to the warming of the troposphere, while aerosol forcing causes cooling (Myhre et al., 2013).

2.5 Seasonal prediction systems

Seasonal forecasts can be made using purely statistical techniques, dynamical models or a combination of both (Smith et al., 2012). Statistical analysis can enable an improved understanding of the climate system, which can then be incorporated into dynamical models, improving their forecasts. In addition, the combination of statistical and dynamical methods can allow the prediction of quantities directly relevant to society, such as transport impacts (Palin et al., 2016), which are not directly output from the climate model itself (National Academy of Sciences, 2010).

2.5.1 Prediction methods

Statistical methods are trained on historical data, modelling the relationship between climate fields in either space and/or time. A number of statistical methods can be used, including correlation and regression, empirical orthogonal functions and principal component analysis or constructed analogues (National Academy of Sciences, 2010). For example, Folland et al. (2012) and Hall et al. (2017) use multiple-linear regression to model and predict the influence of a number of climate drivers on European winter temperatures and rainfall, or the NAO.

Dynamical models are based on the fundamental laws of physics; the conservation of mass, Newton's second law and the laws of thermodynamics. In a dynamical model, the atmosphere and ocean are often represented on a horizontal and vertical grid, and the equations are solved at each grid point. The influence of processes that occur on scales smaller than the grid are modelled separately using physical parametrisations. Parametrised processes include short and long wave radiation, boundary layer processes, moist convection and sub grid-scale turbulent mixing.

The first attempts at longer range forecasting (beyond 2 weeks) were made in the late 1960s using an atmospheric general circulation model (AGCM, Miyakoda and Hembree 1969). The first successful dynamical predictions of ENSO used a model with a one-layer ocean representing the thermocline and a simple atmosphere (Cane et al., 1986). Hybrid schemes with either a more detailed ocean or atmosphere were then developed and a two-tier approach used. Coupled global circulation models (CGCM) were first used operationally in the 1990s and have developed to include detailed atmosphere, ocean, land and sea ice components. Initial conditions for seasonal forecasts are currently derived from separate atmosphere, ocean and land assimilation schemes (e.g. MacLachlan et al. 2015).

With better observations and understanding of the climate system, and the increase in computing power available, CGCMs are now able to spontaneously reproduce many of the observed features of the climate system with improved fidelity, such as jet streams, the Hadley circulation and ENSO (Smith et al., 2012). Since the 2000s ENSO prediction skill using a CGCM has improved significantly, such that forecasts are generally competitive or better than those based on statistical methods (Saha et al. 2006, Wang et al. 2009, Barnston et al. 2012).

2.5.2 Ensemble prediction

Systematic errors in the mean state, the annual cycle and in climate variability are however still present in CGCMs, impacting seasonal forecast skill. To better sample the uncertainty in a seasonal forecast an ensemble of forecasts is commonly produced. There are a number of methods for producing an ensemble. The ECMWF system 4 (Molteni et al., 2011) initialises all forecasts members on the same day, with small perturbations in the integrations generated by a stochastic physics scheme. The Met Office system in contrast uses a lagged ensemble approach, where each day, 2 ensemble members are run, and then the forecasts are gathered together over a period of time to give the ensemble (MacLachlan et al., 2015). The range of outcomes across the ensemble reflects the uncertainty in the forecast associated with initial condition and modelling uncertainty.

To represent model structural uncertainty, forecasts from more than one modelling system can be considered, as errors in one model may be uncorrelated to those of another. By combining the forecasts from different models, the impact from systematic errors are to some extent reduced and lead to an improvement in seasonal forecast skill. For example Palmer et al. (2004) found a multi-model seasonal forecast system to be more reliable than that based on any of the individual models included.

2.5.3 Met Office prediction systems

The Met Office seasonal and decadal prediction systems ('GloSea5' and 'DePreSys3') are used within this thesis and are described at length in MacLachlan et al. (2015) and Dunstone et al. (2016). Both systems use the Met Office's global environment model (HadGEM3-GC2) to evolve the climate forward in time. This model consists of an atmosphere, ocean, land surface and sea-ice component. It represents the full depth of the stratosphere (85 model levels), and has 3 hourly atmosphere-ocean coupling and assimilated sea-ice. The atmosphere and land components have a horizontal resolution of 0.8° longitude by 0.6° latitude (approximately 50km in mid-latitudes), while the ocean and sea-ice model resolution is 0.25° (approximately 27km on the equator). The recent increase in ocean resolution has improved the path of the North Atlantic Current, and has removed a cold bias in the North-west Atlantic (Scaife et al. 2011, MacLachlan et al. 2015). The frequency of blocking in Northern Europe was also found to improve (Scaife et al., 2011).

MacLachlan et al. (2015) summarises the seasonal forecast skill of GloSea5: ENSO skill is very high (the anomaly correlation coefficient is 0.8 for a 5 month lead time), the Arctic Oscillation is well predicted with a correlation of 0.63, the MJO is skilfully forecast out to 20 days, equivalent to other systems, and the distribution of storm tracks in the North Atlantic is well captured, but with too few storms.

Within this PhD, seasonal forecast skill is assessed by comparing observations with the ensemble mean of the combined GloSea5 and DePreSys3 hindcast sets. The GloSea5 hindcast set covers 23 years, from 1993 to 2016. Ten ensemble hindcast members are available for each calendar week, and the three nearest weeks of hindcasts centred around the desired start time are collected together. For a winter forecast, 30 ensemble members are therefore available. In contrast, the DePreSys3 system has 40 ensemble members available over the winter period, each initialised on the 1st November, covering the period 1981 to 2018. In both systems, ensemble member differences are created using a stochastic physics scheme (MacLachlan et al., 2015). The different methods of initialisation of the GloSea5 and DePreSys3 systems do not appear to influence the seasonal prediction skill of the NAO (Scaife et al. 2014b, Dunstone et al. 2016).

2.6 Predictability of the North Atlantic winter climate

As discussed earlier, the NAO is the dominant pattern of winter climate variability in the North-Atlantic and European region, and significantly influences temperature, rainfall and wind conditions in Britain. Predicting the correct phase of the NAO in advance is therefore critical for the skilful prediction of winter conditions in Britain. The NAO has been shown to be influenced by many of the climate processes described above, including the QBO, SSWs, Atlantic SSTs, ENSO and tropical precipitation (Thompson et al. 2002, Baldwin and Dunkerton 2001, Czaja and Frankignoul 2002, Merkel and Latif 2002, Scaife et al. 2017). A seasonal mean NAO consequently reflects the combined influence of these different teleconnections, as well as chaotic variability.

Each climate process increases the likelihood of specific conditions at the surface, during the entirety or parts of the winter. For example an easterly QBO, a SSW, El Nino conditions, and a negative tripole SST distribution all lead to an increased chance of negative NAO conditions (Thompson et al. 2002, Baldwin and Dunkerton 2001, Merkel and Latif 2002, Rodwell and Folland 2002). For El Nino, the negative NAO response occurs two-thirds of the time (Toniazzo and Scaife, 2006) and predominantly impacts late winter (Broennimann, 2007). Conversely a westerly QBO, La Nina conditions and positive tripole Atlantic SSTs, increase the chance of a positive phase of the NAO (Thompson et al. 2002, Pozo-Vazquez et al. 2001, Czaja and Frankignoul 2002). Knowledge of the state of these different climate processes ahead of the winter can lead to an improvement in the predictability of European winters (Thompson et al. 2002, Broennimann 2007, Marshall and Scaife 2009, Folland et al. 2012, Hall et al. 2017).

2.6.1 NAO prediction skill

While seasonal prediction systems are skilful in predicting tropical climate, skill in predicting mid-latitude climate has historically been low (National Academy of Sciences, 2010). Climate models have typically shown little atmospheric circulation response to ocean and land surface anomalies. However, recently Scaife et al. (2014b) demonstrated that skilful predictions of the winter NAO from forecasts initialised around the 1st November were possible. A correlation of approximately 0.6 was found between forecast and observed winter mean NAO index between 1993 and

2012 using the GloSea5 prediction system (see Figure 2.10). Scaife et al. (2014b) hypothesised that the skilful predictions of the NAO resulted from the ability of the model to accurately represent the key teleconnections between the ocean and upper atmosphere and the North Atlantic winter climate. The magnitude of the response to given forcings was however found to be much smaller than in observations. Consequently although the ensemble mean correlated well with the observations, its variability was much smaller than observed. Such forecasts are referred to as being 'under-confident' (Eade et al., 2014). Scaife et al. (2014b) demonstrated that a large number of ensemble members was required to give a skilful prediction of the NAO, as this enabled the predictable signal to emerge from the ensemble noise.

Subsequently equivalent winter NAO prediction skill has been found over a longer period (1981-2016) using the same coupled model (Dunstone et al., 2016) and an even higher level of skill has been achieved using a multi-model ensemble (NAO correlation of 0.85, Athanasiadis et al. 2017, Baker et al. 2018). Baker et al. (2018) found that dynamical models from centres other than the Met Office, also gave under-confident NAO predictions and that winters which were successfully forecast in all models were years with a strongly positive or strongly negative observed NAO.

2.6.2 North Atlantic climate prediction skill

Other features of North Atlantic winter climate have been shown to be skilfully predicted. Kirtman et al. (2014) demonstrate skilful predictions of winter SSTs in the North Atlantic to the west of the UK, from a July start date. Riddle et al. (2013), Kang et al. (2014) and Stockdale et al. (2015) demonstrate skill in predicting the interannual variability of the winter Arctic Oscillation (AO) using a range of coupled ensemble prediction systems. Scaife et al. (2014b) showed that both winter storminess and winter wind speed were skilfully forecast over Northern Europe when using direct output from the GloSea5 system. However, winter temperatures were more skilfully forecast when using a statistical prediction based on the model NAO prediction, rather than using the model forecast temperatures. Athanasiadis et al. (2014) found that skilful prediction of the frequency of both instantaneous and multi-day blocking events was possible over the UK using the GloSea5 system.

With the improvement in seasonal predictability of winter climate in the North Atlantic and European region, the ability of such systems to predict societally relevant variability has been assessed. For example, skilful forecasts of sea ice cover (Karpechko et al., 2015), transport delays (Palin et al., 2016) and river flows (Svensson et al., 2015) using the predictability of the NAO have all been demonstrated.

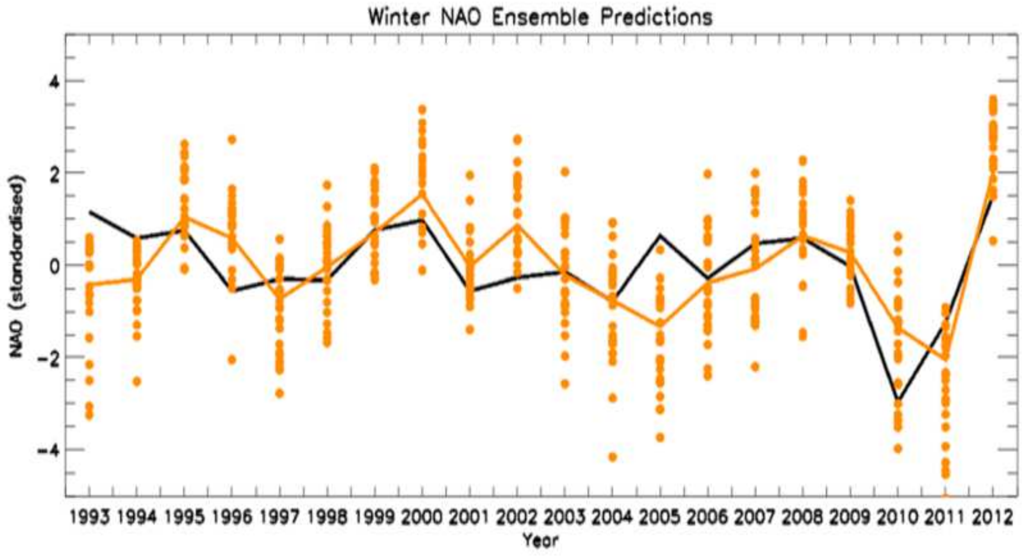

Figure 2.10: GloSea5 prediction of the winter mean NAO index. The NAO in observations (black line), ensemble mean forecasts (orange line), and individual ensemble members (orange dots) in winter hindcasts. Scaife et al. (2014b).

The use of seasonal forecasts by the energy sector is described in section 2.8.5.

2.7 Basics of the UK's energy system

A basic description of the UK energy system in 2017 is given, summarising information available from the latest Digest of UK Energy Statistics (BEIS, 2018). A number of primary fuels are consumed within the UK, including petroleum (48%), natural gas (29%), primary electricity (17%) and coal. Since 2004 the UK has been a net importer of fuel and in 2017 imports accounted for 36% of energy used. Primary energy consumption has been reducing over the last 10 years by approximately 1% per year, from ~235 Million tonnes of oil equivalent (Mtoe) to ~195 Mtoe. Transport and domestic energy use currently account for nearly two-thirds of final consumption. The main indigenous sources of energy include gas from the UK continental shelf (40% of generation), nuclear (21%), renewable generation (20%) and coal (7%). In the last decades the share of energy from fossil fuels has decreased and is currently at a record low of 80%, whilst that from low-carbon sources (nuclear and renewables) has increased to 18%.

2.7.1 International and national policy context

The energy industry is undergoing a large scale transition, from a system based on the burning of fossil fuels to a low-carbon energy system. With the acceptance of anthropogenically caused climate change, nations around the world are increasingly committed to reducing their green-house gas (GHG) emissions. The United Nations Framework Convention on Climate Change (UNFCCC) led to the Kyoto Protocol in 1997 (UNFCCC, 1997) and more recently the Paris Agreement in December 2015 (UNFCCC, 2015). The latter, the first truly global agreement, aims to reduce greenhouse gas emissions and to limit the increase in global average temperature to 1.5°C–2°C above pre-industrial levels.

In 2008 the Climate Change Act was passed, committing the UK Government by law to reduce GHG emissions by at least 80% of 1990 levels by 2050 (UK Government, 2008). This includes an interim target to reduce GHG emissions by at least 34% by 2020. To help achieve these reductions, the 2008 Act introduced carbon budgets, which set legally-binding limits on the total GHG emissions that the UK can emit over a series of 5 year periods. Given the energy sector is the largest contributor to GHG emissions, the Government has set targets to reduce energy sector emissions. For example, the Government has been advised to reduce emissions of carbon dioxide per kWh to 100g or below by 2030, from ~500g in 2008 (Climate Change Committee 2009, 2015). Under the EU's 2009 Renewable Energy Directive, the UK has the target of obtaining 15% of its energy from renewable sources by 2020, from a baseline of 3% in 2009 (European Commission 2009, DECC 2009). This target is further broken down into 30% of electricity, 12% of heat and 10% of transport from renewable sources by 2020.

2.7.2 Gas supply and demand

In 2017 approximately half of all gas supplies came from the UK's North-Sea Gas fields, whilst a similar amount was imported (BEIS, 2018). This contrasts sharply with the year 2000, when all UK gas needs were met by North Sea supplies. Gas supplies are imported from Norway, the Netherlands and Belgium through sea-bed pipelines. Alternatively liquefied natural gas (LNG) is shipped into the UK (predominantly from Qatar). The National Transmission System (NTS) moves the gas from the import hubs to the major demand centres across the country. The distribution network of smaller pipes then delivers the gas to individual homes and offices.

In 2017 approximately 35% of UK gas demand came from the domestic sector for the heating of homes and water (BEIS, 2018). A similar amount was used for the generation of electricity. Industrial usage accounted for only 10% of total gas demand. Gas demand has seen a gradual decline since the early to mid 2000s, such that the demand in 2017 was down by a fifth compared to that of 2000. The reduction in gas demand is primarily associated with a reduction in industrial demand. However, there has also been a reduction in gas demand for both domestic use and for power production over the same period, related to improvements in energy efficiency, such as home insulation.

2.7.3 Electricity supply and demand

In the UK, electricity is traditionally generated using a range of methods and fuels, including coal, gas, nuclear, hydro-power and diesel, with power plants distributed across the country. In addition to indigenous generation, there are four interconnectors with Europe, allowing the trading of electricity (between England - France, England - Netherlands, Northern Ireland - Ireland and Wales - Ireland). Electricity is moved around the country via the high voltage national transmission network and then delivered to homes via the more local, lower voltage distribution network.

For electricity, supply is completely driven by demand, because electricity cannot currently be stored in large amounts. Electricity demand in the UK reached a peak in 2005 and then reduced thereafter. In recent years there has been a shift in the production of electricity away from coal to gas generation, and in the last couple of years a shift from coal to renewable generation. In 2015, the carbon price floor for a tonne of CO_2 doubled from £9 to £18. Carbon emissions from coal are over double those of gas and consequently in 2016 the generation of electricity from burning coal significantly decreased (BEIS, 2018).

There has been a steady increase in generation of electricity from renewable sources since 2000 (see Figure 2.11), driven by national and international incentives, including the Renewable Energy Directive and advice from the UK's Climate Change Committee. In 2017, bio-energy and onshore wind power each account for nearly a third of renewable electricity generation, with offshore wind and solar power accounting for approximately a fifth and a tenth respectively. The percentage of electricity derived from renewable sources has increased from $\sim$4% in 2004 to 28% in 2017, reaching nearly 100TWh (BEIS, 2018). The current distribution and capacity of onshore and offshore wind farms across the UK is shown in Figure 2.12. The growth of renewable electricity generation is expected to continue, with future scenarios predicting an increase in wind and solar power capacity of between 60%–150% and 15%–100% respectively by 2030 (National Grid, 2019). Much of the growth in wind power is expected to come from increased offshore capacity.

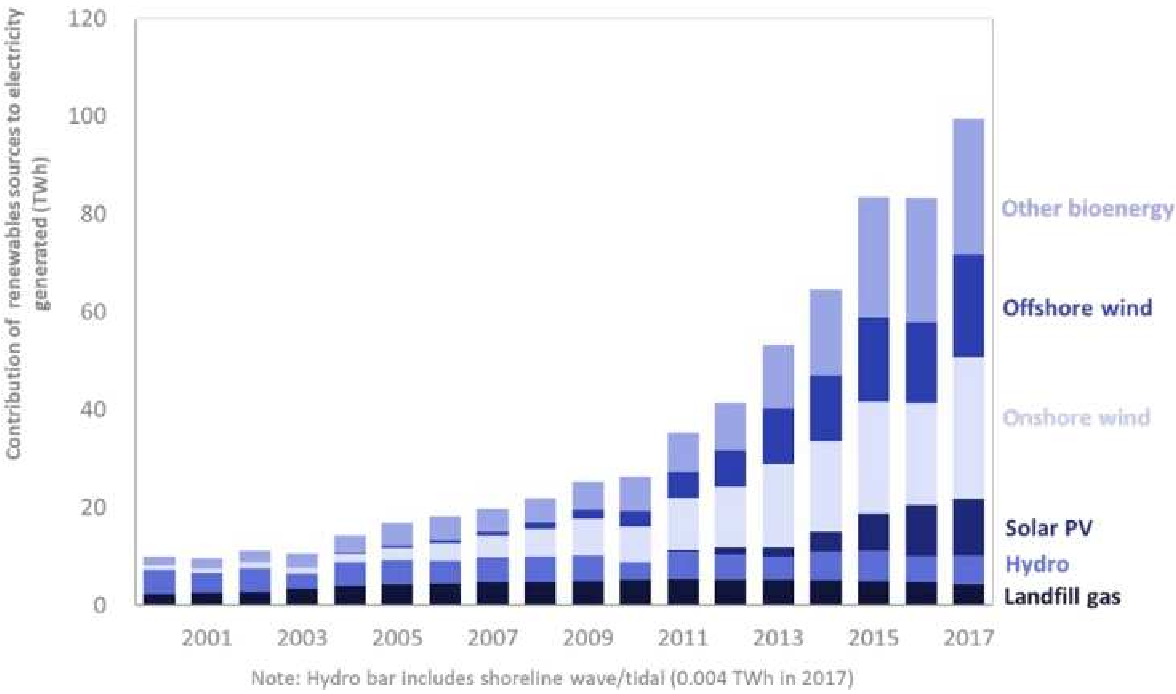

Figure 2.11: The contribution of renewable sources to electricity generated between 2000 and 2017 (TWh), BEIS (2018), chapter 6: Renewable sources of energy.

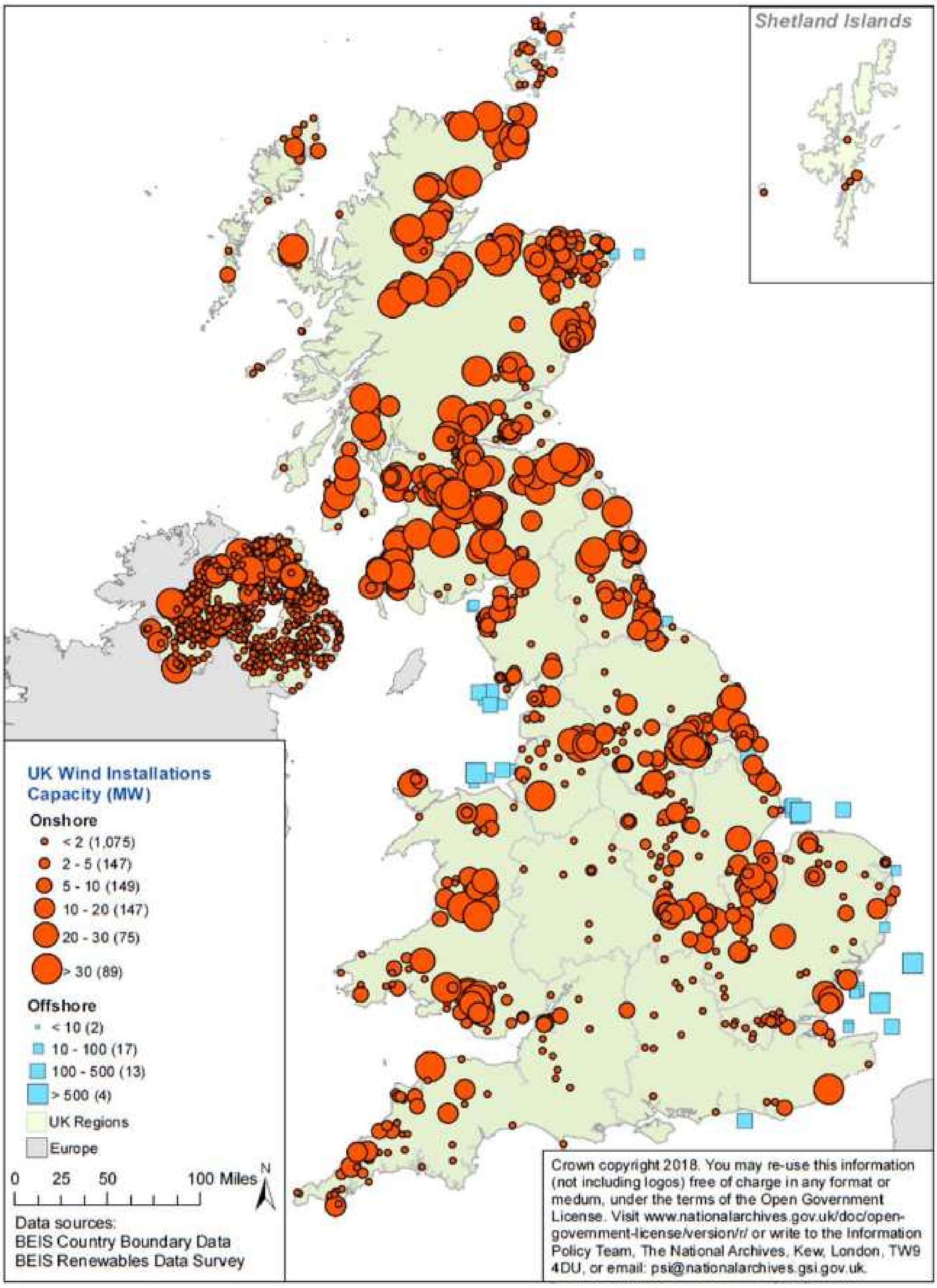

Figure 2.12: Current UK onshore and offshore wind installation capacity, BEIS (2018), chapter 6: Renewable sources of energy.

Considering total energy consumption (transport, heat and electricity), in 2017 over 10% came from renewable sources. Meeting the UK's interim renewable energy targets has been achieved by the rapid increase in renewable electricity generation. However the renewable heat and renewable transport targets are appearing harder to achieve, with less than 8% of overall heat and less than 5% of transport energy use coming from renewable sources (BEIS, 2018).

2.7.4 Management of the energy system

National Grid is the operator of the UK's gas and electricity system and is responsible for ensuring a secure supply of energy. Security of supply can be defined as a system's ability to provide a flow of energy to meet demand in a manner and price that does not disrupt the course of the economy (Grubb et al., 2006). Threats to supply include failure of a primary fuel source, due to import reliance or domestic issues, transmission network problems, generation capacity limitation or operational failures due to inadequate spinning reserve (Mitchell et al., 1996). Demand for energy varies across a range of timescales, including across a year, a week, a day and within an hour (e.g. Mirasgedis et al. 2006, Psiloglou et al. 2009, Summerfield et al. 2015). Ensuring there is sufficient energy supply therefore requires advance warning of likely demand, of available supplies and real-time flexibility to manage unforeseen variations.

A number of tools are currently used by the grid operator to ensure sufficient supplies of energy are available at different times of the year, including the energy market, the capacity market and the balancing services market (Engie, 2016). The energy market describes the basic trading between generators and suppliers and is designed for everyday use. In contrast, the balancing services market and the capacity market are designed to ensure sufficient supplies of energy are available during specific periods. For example, the balancing services market enables the grid operator to buy energy at a pre-agreed price at any time of year to help keep the system in balance. Whilst the capacity market is specifically designed to ensure sufficient supply is available during periods of system stress, such as during peak demand periods. Through a capacity auction, the grid operator will agree to pay a monthly payment throughout the year to a supplier, on the condition that they provide a certain amount of electricity when asked.

Demand forecasting

Knowledge of future demand is critical for management of the energy system, and is at the core of nearly all decisions made in energy markets (Hahn et al., 2009). Forecasting of demand occurs on different timescales, including very short-term forecasts (minutes to an hour ahead), short-term forecasts (an hour to a week ahead), medium-term forecasts (a week to a year ahead) and long-term forecasts (longer than a year ahead), each with a different purpose (Hahn et al. 2009, Apadula et al. 2012). Short and very short-term demand forecasts allow the grid operator and utility companies to estimate energy spot prices and to bid for and schedule energy supply requirements and contributions (Fischer 2010). Such forecasts also enable the safe operation of the energy system, for example by ensuring sufficient gas is held in storage to underpin daily operations of the NTS (National Grid, 2016). A small improvement in the accuracy of demand forecasts can reduce production costs and increase profitability (Cho et al., 2013). Medium-term forecasts of demand are useful for the assessment of security of supply, scheduling of fuel supplies, maintenance operations and negotiation of supply contracts (National Grid 2016, Apadula et al. 2012). Whilst longer-term demand forecasts aide energy trading and new build investment decisions (Szoplik, 2015). For example, National Grid make demand forecasts for the coming 10 years (the 'Ten Year Statement') to better plan the longer term development of the NTS (National Grid, 2016). The modelling of energy demand is discussed in section 2.8.

Winter planning

During winter, cold episodes can lead to peaks in electricity and gas demand. When supplies of energy available are insufficient to meet the high levels of demand, energy prices can rise very quickly. The increase in the energy price can cause additional sources of energy to become available, helping to fill the demand - supply imbalance. If sufficient supplies cannot be sourced, there is the risk of electricity black-outs or gas shortages. To ensure the UK energy sector is as prepared as possible for the coming winter, each October National Grid release a 'Winter Outlook' report (National Grid, 2017). This report details the operator's view on the security of supply of electricity and gas systems for the coming winter period, following consultation with the wider energy industry. For the electricity sector, the outlook includes a forecast of the coming winter's peak transmission system demand, the expected margin between supply and demand, the amount of reserve planned, the assumed interconnector supply and the 'loss of load expectation', which measures the risk across the whole winter of demand exceeding supply under normal operation. For example, for the winter of 2017/2018 the forecast of peak demand was 50.7GW, which included national demand (49.1GW), power station demand (600MW) and base load interconnector exports (1GW). For winter 2017/2018 the expected margin was 6.2GW and the loss of load expectation was 0.01 hours per year (National Grid, 2017).

For gas demand the 'Winter Outlook' report gives a forecast of the coming winter's total demand, the minimum storage requirement, the 1-in-20 year peak day demand, the peak day supply margin and the expected availability of different gas supplies (National Grid, 2017). Demand forecasts are for the whole national transmission system (NTS) which includes residential and industrial demand attached to the local distribution network, industrial plants directly linked to the NTS, gas injected into storage and exports to the European mainland and Ireland. For example, for the 2017/18 winter, total demand was forecast to be 51.4 billion cubic meters (bcm, or approximately 565TWh, using National Grid's recommended conversion of 1mcm to 11GWh). The 1-in-20 year peak day demand forecast was 502 mcm per day (or 5522GWh), where the local distribution zone component was approximately 350 mcm per day (or 3850GWh).

The 'Winter Outlook' forecasts do not consider any weather forecast information for the coming winter, rather it assumes standard winter conditions and then assesses the risks associated with past weather related peak demand events. For example, peak electricity demand estimates are based on seasonal normal weather, where for each week of the year, a 30 year average of relevant weather variables, including temperature, wind speed and solar irradiance is constructed. These averaged values are translated into demand using the climatological linear regression relationship between demand and weather. This PhD therefore helps to address this gap by considering whether skilful prediction of winter energy demand is possible using seasonal predictions of winter climate.

2.8 Influence of weather and climate on the UK's energy system

The UK energy system has been impacted by weather throughout its development. For example during the winter of 1947, six weeks of continuous snow prevented the transportation of coal around the country. The heating of homes and businesses, and the generation of electricity at that time were almost entirely dependent upon coal, and consequently the country's energy supplies were severely affected (Prior and Kendon, 2011). Although today's energy system is designed to cope with the majority of weather conditions experienced in the UK, extreme events can still cause serious impacts. For example, a deep low pressure system on the 12th February, 2014, brought very strong winds and damaged the overhead transmission and distribution network, leaving 100,000 homes without power across the UK (Kendon and McCarthy, 2015). The storm also caused extreme wave heights off the southern coast of Ireland which impacted the operations of the Kinsale gas platform. In contrast, during the cold winter of 2010, heavy snowfall and ice brought down trees and power lines and resulted in 45,000 homes in Scotland having disrupted electricity supplies (Prior and Kendon, 2011).

Both the demand for and generation of energy are significantly impacted by the weather (Bessec and Fouquau 2008, Szoplik 2015). The impacts of weather and climate on electricity and gas demand are described in detail in sections 2.8.1 and 2.8.2 respectively. With the increase in the capacity of renewable electricity, the generation of energy is also increasingly impacted by weather and its variability. For example, wind power, solar power and hydro-power are strongly influenced by the variability of wind speeds, solar irradiation and rainfall accumulation respectively (e.g. Wiser et al. 2011, Arvizu et al. 2011, Kumar et al. 2011). Bio-energy is also weather sensitive, with weather conditions affecting the growth of crops. However, unlike wind and solar power, the climatic sensitivity of bio-energy poses less of an issue for security of supply due to the time-lag between production (i.e. crop growth) and generation of electricity through burning of the biomass. The impacts of weather and climate on wind power resource is described in detail in section 2.8.3.

Most impacts of weather on the energy system are immediate, for example the rapidly changing renewable energy production associated with the passage of weather fronts, or the damage to the network associated with a wind storm. However, some impacts result from extended periods of anomalous weather. For example, heavy rain over a number of days can lead to flooding of ground based assets, or consecutive cold days can lead to dwindling gas supplies, given there is a maximum rate at which gas can be supplied into the network.

2.8.1 The impacts of weather on electricity demand

Due to the utility of demand forecasts, there is a large body of research exploring the drivers and predictability of energy demand. Electricity demand has been shown to be a function of both weather and a variety of socio-economic factors (Psiloglou et al. 2009, Fischer 2010). Temperature is the dominant weather driver of electricity demand in many developed countries, for example in the UK (Henley and Peirson 1997, Taylor and Buizza 2003, Hor et al. 2005, Bessec and Fouquau 2008), in Greece (Mirasgedis et al., 2006), in France (Cho et al., 2013) in Italy (Apadula et al. 2012, De Felice et al. 2013) and in the US (Sailor and Munoz, 1997). Lagged impacts have occasionally been included in demand models (Taylor and Buizza 2003, Mirasgedis et al. 2006, Bloomfield et al. 2016). For example, Mirasgedis et al. (2006) find an improved prediction of demand when the previous two days of temperature are taken into account, which is attributed to human memory and the thermal capacity of buildings.

Bessec and Fouquau (2008) find the shape of the relationship between temperature and electricity demand varies with country. In Northern Europe (for example in Scandinavia), there is a near-linear negative relationship between demand and temperature, with a single peak in winter associated with space heating and lighting. In Southern European countries (for example in Greece, Spain, Italy and Portugal), there is a secondary summer peak associated with cooling demand, which results in a non-linear, U-shaped relationship between temperature and demand (Hekkenberg et al. 2009, Bessec and Fouquau 2008). During the last decade a number of Southern European countries have seen a larger demand peak in summer than in winter, in contrast to earlier decades, which is thought to result from the increasing use of air conditioning (Hekkenberg et al., 2009). In other parts of the world, for example in Bangkok, the single demand peak occurs in summer (Wangpattarapong et al., 2008).

A modest improvement in the predictability of electricity demand has been demonstrated when additional weather variables are included in a demand model, including relative humidity, clearness index, cloudiness, rainfall, solar radiation, wind speed and other derived variables (Psiloglou et al., 2009). Heating and cooling degree day indices have also been widely used to model electricity demand, allowing the separation of the cooling and heating demand relationships (Le Comte and Warren 1981, Hor et al. 2005, Mirasgedis et al. 2006, Apadula et al. 2012). Finally, bio-meteorological indices that combine the influence of different weather variables have also been applied to the modelling of demand. For example, a wind chill index combines the influence of wind speed and temperature effects on demand, whilst the 'heat-index temperature' combines the influence of temperature and humidity on demand (Apadula et al., 2012).

In addition to meteorological drivers, socio-economic factors that affect electricity demand include energy prices, consumer behaviour, income, Gross Domestic Product (GDP), import and export values, manufacturing and population (Henley and Peirson 1997, Psiloglou et al. 2009). To better explore the weather-demand relationships, longer term variations in demand that relate to socio-economic drivers are often removed, using for example linear regression with GDP, non-linear regression with time, or generalised additive models (e.g. Hor et al. 2005, De Felice et al. 2013, Cho et al. 2013 respectively).

The impacts of weather on UK electricity demand

In the UK, temperature and electricity demand have a near-linear negative relationship (Hor et al. 2005, Bessec and Fouquau 2008, Psiloglou et al. 2009, Summerfield et al. 2015). However, above a certain temperature threshold, demand tends to level off. The relationship between monthly mean temperature and electricity demand is shown in Figure 2.13 (Hor et al., 2005). Below ∼14°C demand decreases as temperatures increase, from 14°C - 17°C demand is largely unresponsive to temperature, and above 18°C there is a suggestion of an increase in demand as temperatures increase (Hor et al., 2005). Using daily demand, Hor et al. (2005) found that demand saturated below a given temperature and that demand became unresponsive to temperature at approximately 20°C. The former was attributed to lighting load saturation and a base level of thermal comfort in winter. In addition, heating degree days (HDD) were found to be more closely correlated with demand than temperature, although cooling degree days (CDD) were poorly correlated. Taylor and Buizza (2003) modelled the variation in UK electricity demand due to weather using the effective temperature (an average of current temperature and the previous day's effective temperatures), the cooling power of the wind (a non-linear function of wind speed and average temperature) and effective illumination (a complex function of visibility, number and type of cloud, and amount and type of precipitation).

Clearly defined annual, weekly and sub daily cycles are seen in UK electricity demand (Taylor and Buizza 2003, Hor et al. 2005, Taylor 2010), highlighting for example the winter early evening peak and the steeply increasing demand from 5am to approximately midday. Taylor (2010) show the variation in demand profile with day of the week, highlighting the reduced demand during weekends, Monday mornings and Friday afternoons, compared to other week days (see Figure 2.14). The influence of socio-economic factors, such as day of the week and holiday days have consequently been included in UK demand models, to better reflect the observed variation in demand (e.g. Taylor and Buizza 2003, Bloomfield et al. 2016, Troccoli

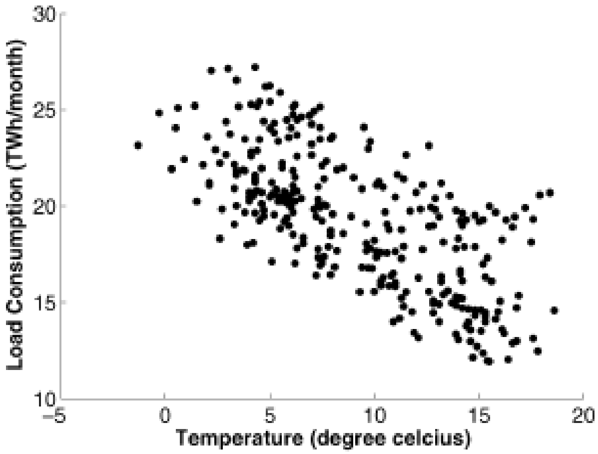

Figure 2.13: Mean monthly demand as a function of monthly Central England Temperature, from 1970 to 1995, Hor et al. (2005).

et al. 2018).

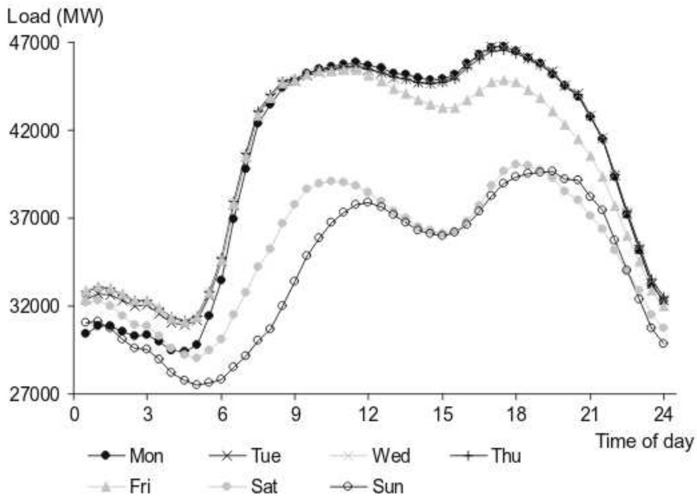

Figure 2.14: Average daily cycle of electricity demand (MW) for Great Britain, for each day of the week, Taylor (2010).

2.8.2 The impacts of weather on gas demand

Across the literature, gas demand is typically modelled using a combination of weather variables (e.g. temperature, HDD, CDD, wind speed, relative humidity, sunshine), socio-economic factors (e.g GDP, population, fuel prices), and building characteristics (e.g. size of building, type of ownership, roof type) (Soldo 2012, Szoplik 2015, National Grid 2016). Residential gas demand has been shown to be very sensitive to temperature, for example in the US the correlation is greater than 0.9, and a 1°C increase in mean monthly temperature leads to an 8% decrease in residential demand (Sailor et al., 1998). In contrast, industrial demand in the US has a very low sensitivity to weather, and is rather influenced by the price of gas and the national income. Longer term trends in gas demand have been seen in the US and Italy, which have been attributed to the strength of the economy (Huntington 2007, Bianco et al. 2014).

The impacts of weather on UK gas demand

There is a surprising lack of UK focussed gas consumption studies in the peer-reviewed literature. van Goor and Scholtens (2014) analyse the daily UK gas consumption record from 2001 to 2011, and find a dominant annual cycle, a lack of any longer-term trend and high daily variability. Summerfield et al. (2015) demonstrates the significant variability of UK gas demand throughout the day, with a peak in demand at either end of the working day (∼7am and 5pm-8pm). The relationship between gas demand and weather in the UK has been most closely analysed by National Grid (National Grid 2016). Gas demand is modelled using a Composite Weather Variable (CWV) which combines the influence of effective temperature, wind chill and seasonal normal effective temperatures (a long term average of effective temperatures, for each day of the year). After optimization, the CWV has a strong, negative, linear relationship with gas demand. (National Grid 2016).

Wilson et al. (2013) explore the co-variability of UK gas and electricity demand and find that gas demand is much more variable than electricity demand. Also, during peak demand periods, there is up to three times as much gas consumed as electricity. Electricity demand variability is found to be more consistent and less subject to seasonal variation compared to that of gas demand. They conclude that even a partial electrification of domestic heating demand would have serious implications for the UK's ageing electrical transmission and distribution networks, due to the increase in magnitude and variability of daily and peak energy flows.

Knowledge gaps

The importance of temperature in UK electricity demand variability has been clearly demonstrated. However, previous studies have investigated this relationship using either lower temporal resolution, but longer length data sets, or shorter data sets of high temporal resolution. For example Hor et al. (2005) and Bessec and Fouquau (2008) consider the relationship over 26 and 15 years respectively but only use monthly data, whilst the daily and sub-daily studies of Psiloglou et al. (2009) and Henley and Peirson (1997) only consider 5 and 1 year of data respectively. In contrast, little is published on the UK temperature - gas demand relationship. In addition, there does not appear to be any literature quantifying the role of climate extremes in energy demand extremes. This PhD therefore aims to address these gaps by robustly assessing the temperature - demand relationships using the longest daily records available, and by using these relationships with historical temperature records to explore the risk of temperature-driven demand extremes.

2.8.3 The impacts of weather on wind power production

Wind power production depends non-linearly on wind speed. The kinetic energy of wind is turned into mechanical energy, through the rotation of the blades of a wind turbine. The turbine shaft is connected to an electrical generator, where mechanical energy is converted to electrical energy by electromagnetic induction (Wiser et al., 2011). The power in the wind is proportional to the cube of the wind speed and hence the amount of electricity produced is also largely dependent on the cube of the wind speed. Figure 2.15 shows the relationship between wind speed, power of the wind and wind power produced, known as the ‘power curve’ (US Department of Energy, 2008). Below the cut-in wind speed (often 3-4m/s), the turbines will not turn and so no power is produced (region I). Above the cut-out wind speed (often 20-25m/s) there is also no power produced as the turbine is stopped from working to avoid damage. Between the cut-in and rated power wind speed (the speed of maximum output, often 11-15m/s), the power produced is proportional to the cube of the wind speed (region II). Above the rated wind speed, a further increase in wind speed does not lead to an increase in wind power, as the maximum generation capacity has been reached (region III). Wind power production is also proportional to the swipe area of the turbine (e.g. see Manwell et al. 2002). As wind speeds typically increase with height, power production has increased as turbines have got progressively larger (Wiser et al., 2011). The power curve of a particular turbine depends on its physical characteristics e.g. height, blade length and design. Wind power production at a particular location is clearly strongly dependent on the local wind field climate and the type of turbines installed.

The impacts of weather on UK wind power production

Due to the UK’s proximity to the Atlantic Ocean and its position at the end of the North Atlantic storm track, the UK has better wind power resource than many

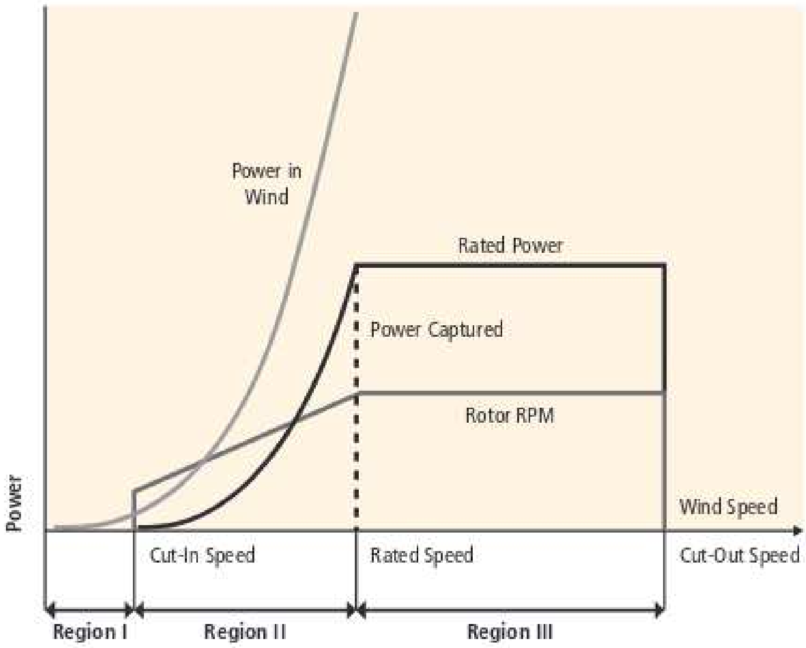

Figure 2.15: Conceptual power curve for a modern variable-speed wind turbine, US Department of Energy (2008).

other countries (see Figure 2.16). The wind climate of the UK is also highly variable, leading to variability of wind power across a range of timescales (Watson 2014, Cannon et al. 2015, Bett and Thornton 2016). Cannon et al. (2015) find that the number of prolonged low or high wind power generation events is well approximated by a Poisson-like random process, with the occurrence rate reducing as the length of the event increases. They also find substantial seasonal variability in the frequency of wind extremes. For example, the number of low wind episodes is found to be greater in summer than in winter, while a higher frequency of ramping events (a rapid change in wind speed) is found to occur in winter because of the greater number of cyclones affecting the UK.

Due to the reduced surface friction over the ocean, wind speeds are usually higher offshore than onshore, leading to higher capacity factors offshore (Drew et al. 2015, Harrison et al. 2015, a capacity factor is the proportion of the maximum electrical energy that a turbine can produce over a given time period). Drew et al. (2015) also find that the planned increase in offshore turbines around the UK would reduce the occurrence of prolonged periods of low generation, increase the occurrence of periods of prolonged high generation and increase the ramping magnitude by a factor of five. Bett and Thornton (2016) show that estimating the annual mean wind speed for England and Wales, requires a very long dataset to sufficiently capture interannual and decadal variability.

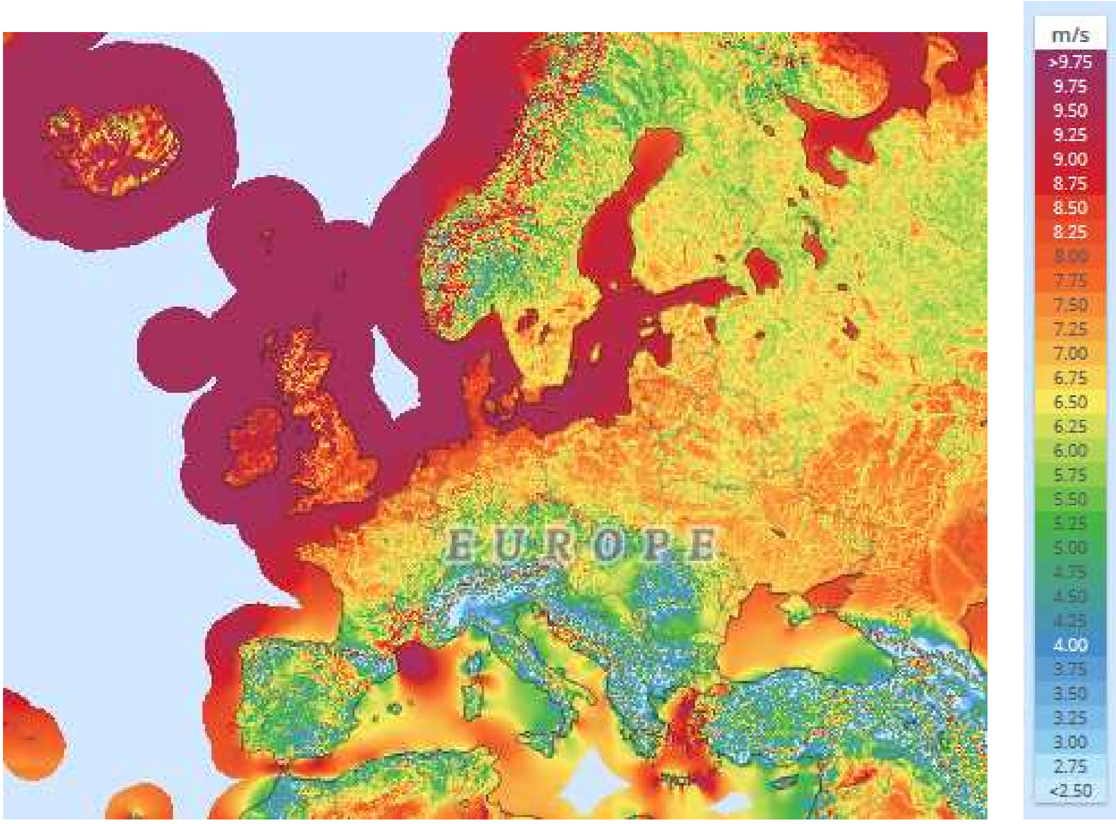

Figure 2.16: Map of annual mean wind speed at a height of 100m from the 'Global Wind Atlas' (m/s) from 2008-2017. This is produced by downscaling ERA5 reanalysis data using the WRF mesoscale and the Danish Technical University (DTU) microscale modelling systems, see DTU (2015).

The impacts of wind power on the energy system

Many studies have investigated the impact of variable wind power generation on the wider energy system. These impacts include the need for extra flexible reserve generation to meet unforeseen changes in generation or demand, increased cycling of flexible power plants due to the impact of greater variability and curtailment of wind power output during periods when supply exceeds demand (Watson, 2014). The more variable and unpredictable the wind speeds and consequent power are, the larger the impact on the energy system and the greater the costs (Watson, 2014). Using a simple representation of the power system, Bloomfield et al. (2016) find that as the amount of wind power increases, the annual amount of power required from baseload plant (such as nuclear) reduces and its interannual variability increases substantially.

To assess the ability of wind power to replace traditional generation sources, the relationship between wind power and electricity demand in the UK has been investigated. Sinden (2007) analysed hourly data between 1996–2003 across all seasons, and found a weak positive relationship between demand and wind power (Pearson correlation of 0.28). During periods of high electricity demand, some studies have found an increased risk of lower wind power supply (Oswald et al. 2008, Zachary and Dent 2012, Harrison et al. 2015), whilst others have found more moderate or higher wind power supply (Sinden 2007, Zachary et al. 2011, Brayshaw et al. 2012). They all emphasize the uncertainty in the relationship due to the shortage of data considered (often less than 10 years).

2.8.4 The influence of atmospheric circulation on the energy system

Over the last decade there has been an increasing interest in the impact of atmospheric circulation patterns on European energy systems. Some studies consider the influence of monthly or seasonal circulation variability (e.g. Brayshaw et al. 2011, Ely et al. 2013, Jerez et al. 2013, Zubiate et al. 2017), whilst others focus on the impact of daily circulation variability (e.g. Oswald et al. 2008, Leahy and McKeogh 2013, Grams et al. 2017).

Monthly-seasonal variability

Reflecting the winter NAO - climate relationships across Europe, a negative NAO index is associated with a decrease in UK wind power, a reduction in hydro-power reservoir levels in Norway and an increase in the combined UK and Scandinavian electricity demand (Brayshaw et al. 2011, Ely et al. 2013). For example Brayshaw et al. (2011) find that at two sites in the UK, a change in phase of the NAO is associated with a 10% change in winter mean wind power production. In contrast, in Spain with a negative NAO phase there is increased wind power, increased hydro-power, and reduced solar power (Jerez et al., 2013). Figure 2.17 demonstrates the North-South dipole in wind speed and consequently wind power across Europe, during different phases of the winter NAO. Zubiate et al. (2017) extend this analysis to investigate the influence of the next two most important atmospheric circulation patterns of regional variability, the East Atlantic (EA) and Scandinavian (SC) patterns. They find that in certain locations, the phase of the EA and SC patterns can modify the NAO - wind speed relationship. For example, when the NAO phase is positive and the EA phase negative, enhanced wind speeds are found over much of north-western Europe (Zubiate et al., 2017), leading to increased wind power capacity factors in Ireland for example (Cradden et al., 2017).

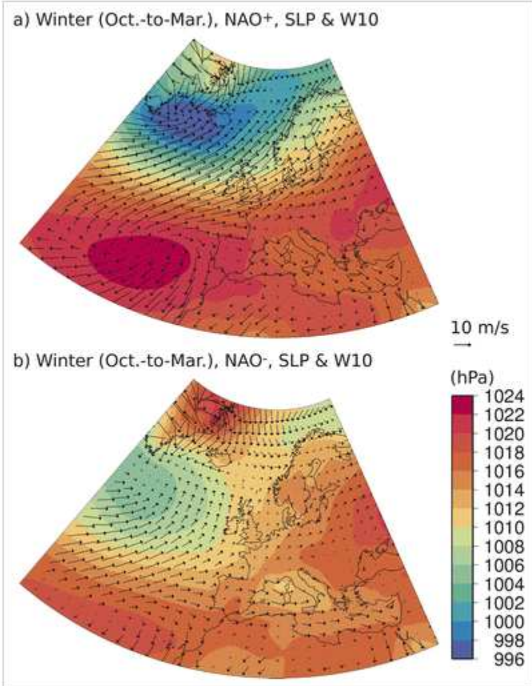

Figure 2.17: Extended winter (October-March) climatology of sea level pressure ('SLP', hPa, colours), and 10m wind fields ('W10') during a) positive and b) negative phases of the NAO, averaged over period 1959-2007, Jerez et al. (2013).

Daily to multi-day variability

With the increasing impact of weather variability on the energy system, interest in the influence of typical daily weather patterns or multi-day regimes has grown. For example, Grams et al. (2017) show that the multi-day fluctuations in Europe's wind power is closely associated with the sequence of Europe-wide weather regimes. Countries adjacent to the North and Baltic Seas (including the UK) have higher than average wind power during cyclonic regimes, but lower than average wind power during blocked regimes. In contrast, south-eastern European countries have the opposite relationship. A number of studies have found that due to the finite size of weather systems, spreading the geographical location of wind farms can help to reduce the variability of their combined output (Sinden 2007, Drake and Hubacek 2007, Oswald et al. 2008, Santos-Alamillos et al. 2014, Grams et al. 2017). Daily wind power in Britain has been found to have a lower correlation with average European wind power when compared to many other European countries, given its more peripheral location (Monforti et al., 2016).

Focussing on the British energy system, Bloomfield et al. (2018) find that the weather conditions that cause the most impact depend on the amount of installed wind power capacity. As wind power capacity increases, the weather pattern that causes highest residual demand (once wind power has been removed) changes from a high pressure system north of the UK to one located directly over the UK. Bloomfield et al. (2018) also find that curtailment of wind power is most likely to be needed when low pressure systems are located to the north of the UK in autumn, as warm, windy conditions, generate high wind power, but moderate demand. Bett and Thornton (2016) find that cyclonic weather types cause a weak anti-correlation between wind speeds and solar irradiance in western Britain. In the east however, where a broader range of weather types influence cloud amount, a weaker relationship between wind speed and irradiance is found.

The influence of weather patterns on the availability of wind power during peak electricity demand periods in the UK, has been discussed in a number of papers. A high pressure system directly over the UK is found by Oswald et al. (2008) and Leahy and Foley (2012) to cause high demand and low wind power availability, during specific case study events. For example, Figure 2.18 shows the low wind power production in Germany, the UK and Ireland, when a high pressure system is located over North-western Europe. The improvement in wind power towards the end of the period is associated with the arrival of a low pressure system. However, Brayshaw et al. (2012) argue that a high pressure system directly over the UK would not generate extreme demand, as temperatures are not sufficiently extreme. Rather they suggest that blocked conditions with northerly or easterly flow over the UK or extended north-south troughs over western Europe, are more likely to give peak UK demand, as these weather patterns drive lower UK temperatures (see Figure 2.19, panels b and c). Brayshaw et al. (2012) also suggest that wind speeds and consequently wind power, would be moderate during such cold weather types.

Knowledge gaps

The uncertainty in both the availability of wind power during extreme demand conditions and in the role of weather patterns in this relationship, therefore deserves further exploration. This PhD aims to clarify this relationship, using a long daily record of electricity demand and a simple model of UK wind power availability. The extent to which the demand - wind power relationship can be explained by meteorology is explored, with a focus on extreme demand periods.

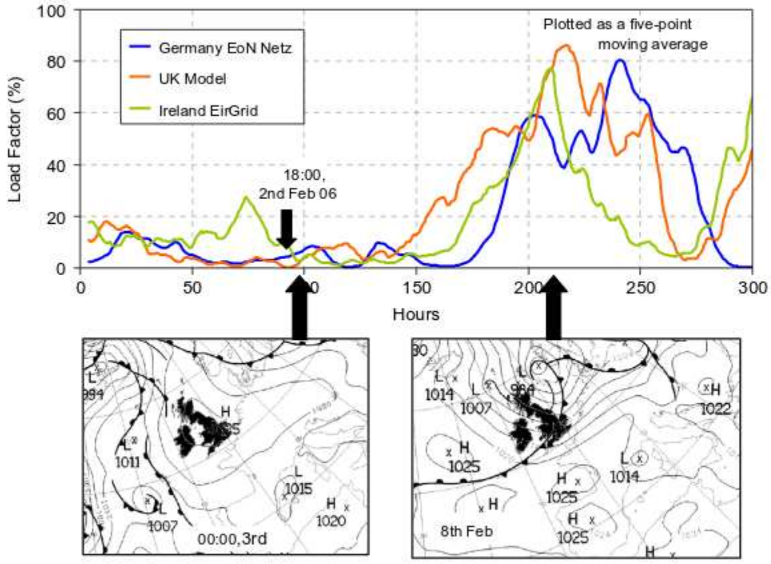

Figure 2.18: North European hourly wind load factors from 30th January to 11th February 2006, with representative mean sea level pressure charts, Oswald et al. (2008).

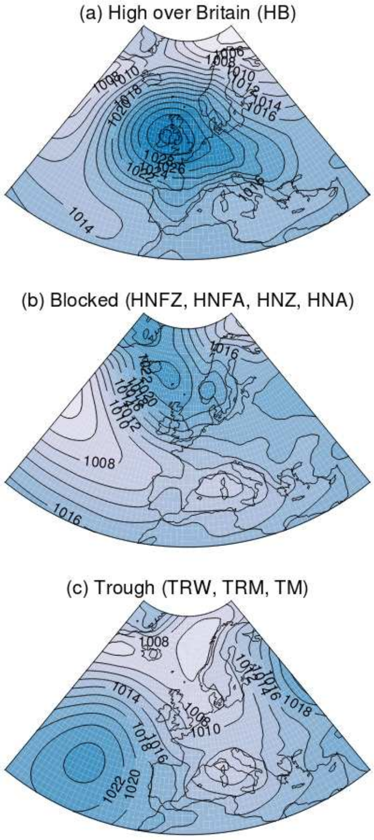

Figure 2.19: Mean sea level pressure patterns that Brayshaw et al. (2012) find are associated with a) moderate GB temperatures and b) and c) very low GB temperatures.

2.8.5 Use of weather and climate forecasts in the energy industry

Short-term weather forecasts are used extensively by the energy sector to improve forecasting of demand and renewable supply (Taylor and Buizza 2003, Foley et al. 2012, De Felice et al. 2013, Lopes et al. 2018). Use of longer-term weather forecasts by the industry is however more limited, due to increasing forecast uncertainty. At the multi-week to monthly lead-time, skilful forecasts of wind power generation are however seen (Lynch et al. 2014, Beerli et al. 2017). The interest in the application of seasonal weather forecasts to energy system management is growing. The potential benefits of their application were first discussed by Troccoli (2010) and Brayshaw et al. (2011), however it is not until recently that the skill of seasonal climate forecasts relevant for the energy industry have been assessed. For example, Bett et al. (2017), Troccoli et al. (2018) and Bett et al. (2018) assess skill in forecasting temperature, wind speed, solar irradiance and rainfall to infer possible predictability of energy demand, wind, solar and hydro power generation respectively. However, there are still very few studies demonstrating the direct application of seasonal climate forecasts for energy management. The two clear examples being the seasonal predictability of electricity demand in Italy using temperature forecasts (De Felice et al., 2015), and the seasonal predictability of wind power and electricity demand in the UK, using predictions of wind speed and the NAO respectively (Clark et al., 2017).

Knowledge gaps

This PhD builds on this work to explore whether seasonal forecasts of climate can help anticipate the UK's winter gas demand. In addition, due to the importance of extreme demand periods for energy system management, an assessment of the skill in predicting the number of high gas demand days over the winter period is also undertaken.

Chapter 3

The role of temperature in the variability and extremes of electricity and gas demand in Great Britain

3.1 Abstract

The daily relationship of electricity and gas demand with temperature in Great Britain is analysed from 1975 – 2013 and 1996 – 2013 respectively. The annual mean and annual cycle amplitude of electricity demand exhibit low frequency variability. This low frequency variability is thought to be predominantly driven by socio-economic changes rather than temperature variation. Once this variability is removed, both daily electricity and gas demand have a strong anti-correlation with temperature (r_{elec} = -0.90 , r_{gas} = -0.94). However these correlations are inflated by the changing demand-temperature relationship during spring and autumn. Once the annual cycles of temperature and demand are removed, the correlations are $r_{elec} = -0.60$ and $r_{gas} = -0.83$. Winter then has the strongest demand-temperature relationship, during which a 1°C reduction in daily temperature typically gives a $\sim$1% increase in daily electricity demand and a 3% – 4% increase in gas demand. Extreme demand periods are assessed using detrended daily temperature observations from 1772. The 1 in 20 year peak day electricity and gas demand estimates are, respectively, 15% (range 14% – 16%) and 46% (range 44% – 49%) above their average winter day demand during the last decade. The risk of demand exceeding

recent extreme events, such as during the winter of 2009/2010, is also quantified.

3.2 Introduction

Predicting electricity and gas demand is important for ensuring there is sufficient supply to meet demand. This is particularly important during extreme demand periods, when the risk of energy shortages and whole sale energy prices rise (National Grid 2014, van Goor and Scholtens 2014).

Energy demand is driven by weather and a variety of socio-economic factors (Psiloglou et al. 2009, Soldo 2012). Temperature is the dominant weather driver of electricity and residential gas demand in many developed countries (Sailor et al. 1998, Mirasgedis et al. 2006, Cho et al. 2013, Timmer and Lamb 2007), where lower temperatures produce heating demand and higher temperatures create air conditioning demand (Hahn et al., 2009). Inclusion of additional weather variables has been shown to modestly improve demand predictability, such as relative humidity, solar radiation, wind-speed and other derived variables (Psiloglou et al. 2009, Soldo 2012, Szoplik 2015). Socio-economic factors affecting electricity and gas demand include energy prices, consumer behaviour, income, Gross Domestic Product (GDP), manufacturing, population and building characteristics (Henley and Peirson 1997, Psiloglou et al. 2009, Szoplik 2015).

Previous studies have found a near-linear, negative relationship between temperature and electricity and gas demand in the UK (Hor et al. 2005, Bessec and Fouquau 2008, Psiloglou et al. 2009, Summerfield et al. 2015). Energy demand is shown to vary across a range of timescales, with clear daily, weekly and annual cycles (Taylor and Buizza 2003, Taylor 2010, van Goor and Scholtens 2014). In addition, UK electricity demand exhibits a long term trend (Hor et al. 2005). However these studies either use high temporal resolution, but short length data sets, or longer data sets of lower temporal resolution. For example Hor et al. (2005) and Bessec and Fouquau (2008) consider the relationship over 26 and 15 years respectively but only use monthly data, whilst the daily and sub-daily studies of Psiloglou et al. (2009) and Henley and Peirson (1997) only consider 5 and 1 year of data respectively.

This study therefore aims to better quantify the relationship between demand and temperature in Great Britain (GB), at a daily timescale, using the longest demand records available (38 years for electricity, 16 years for gas). A comparison of the annual, seasonal and monthly relationships is given. In addition, the risk of demand extremes in GB is quantified for the first time, by creating an artificial extension of the demand data back in time using observed temperature observations and the recent demand-temperature relationships.

3.3 Observed data sets

3.3.1 Demand Data

Daily electricity demand data for GB is available from National Grid[1], for 1971-2013 in giga (10^9) watt hours (GWh). Electricity supply and demand are balanced every second, to maintain the stability of the network's frequency. Consequently, electricity demand is known by measuring how much electricity is generated. National Grid measure the amount of electricity generated across the country that is connected to the transmission network and give a daily total by summing over the day. The demand dataset for GB used here, has been generated by combining two separate demand datasets, one for England and Wales and one for GB (see Sup. Mat., section 3.8.1, for further details). Data is considered from 1975 onwards due to the coal mining strikes and power cuts during the early 1970s. Annual GB electricity demand increased almost monotonically from 1975 until 2006, thereafter a reduction up to the present is apparent (Figure 3.1, upper). A clear annual cycle is visible, with on average a maximum monthly demand in January and a minimum in August, and more clearly seen in Figure 3.2 for one year, 2010-2011.

Daily gas demand data (in GWh) for GB is provided by National Grid for the shorter period 1996–2013. The gas demand represents the total of non-daily metered demand (mainly domestic usage), daily metered demand (for large industrial premises) and shrinkage (gas leaks, theft). It does not include gas consumers directly connected to the national transmission network, such as gas-fired power stations and large industrial units (National Grid 2012a, Wilson et al. 2013). Gas demand is calculated by measuring the flow rate of gas at a variety of different exit points across the network, giving the demand in each local distribution zone and at large industrial sites. Total GB demand is then calculated by summing the demand across the network. Compared to electricity, there is little low frequency variability in gas consumption over this more limited period (Figure 3.1, lower). However there is a clear annual cycle of gas demand with on average a peak in January and minimum in August, as seen in van Goor and Scholtens (2014).

[1] http://www.nationalgrid.com/uk/Electricity/Data

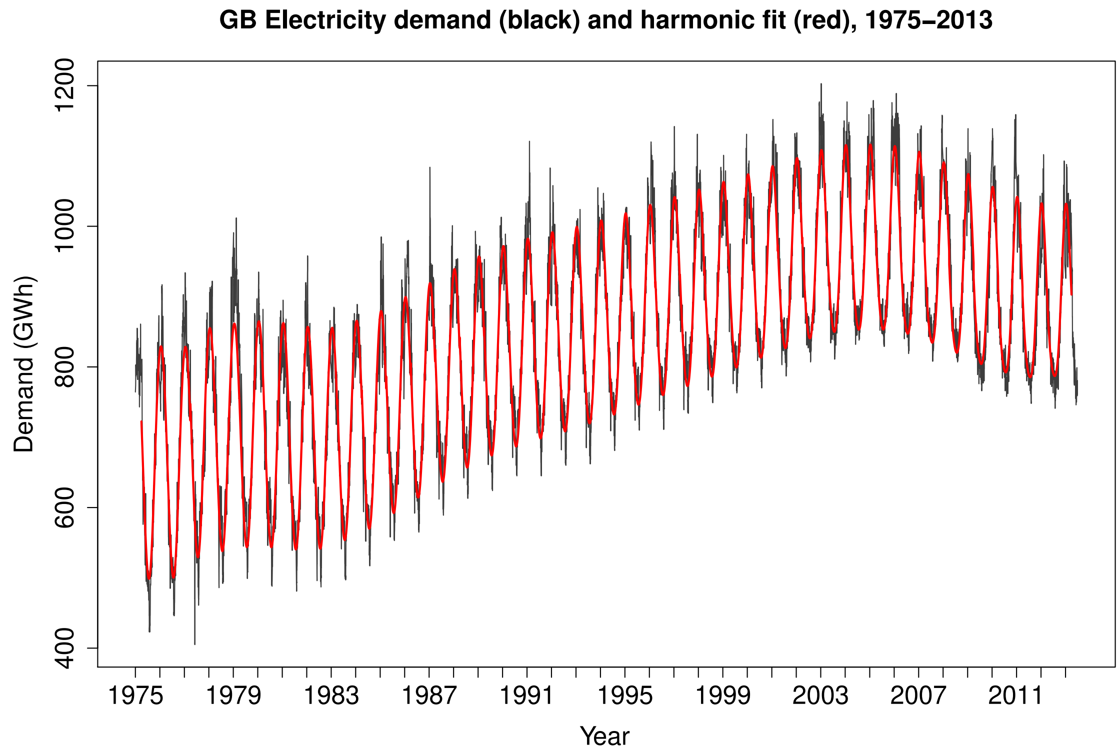

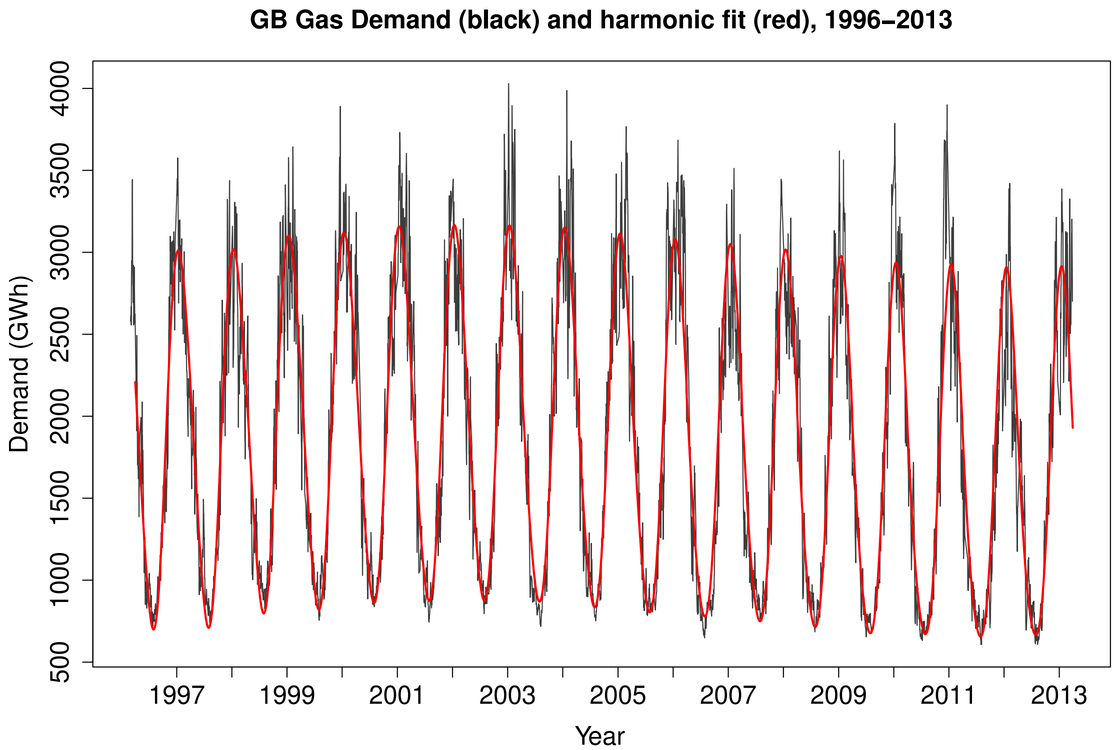

Figure 3.1: Upper: Processed GB electricity demand timeseries (GWh, black) with harmonic fit (red), Jan 1975 - June 2013. Lower: Processed daily GB gas demand (GWh, black) timeseries with harmonic fit (red), March 1996 - March 2013. Demand during weekends and holiday periods has been replaced with linear interpolated values, see text.

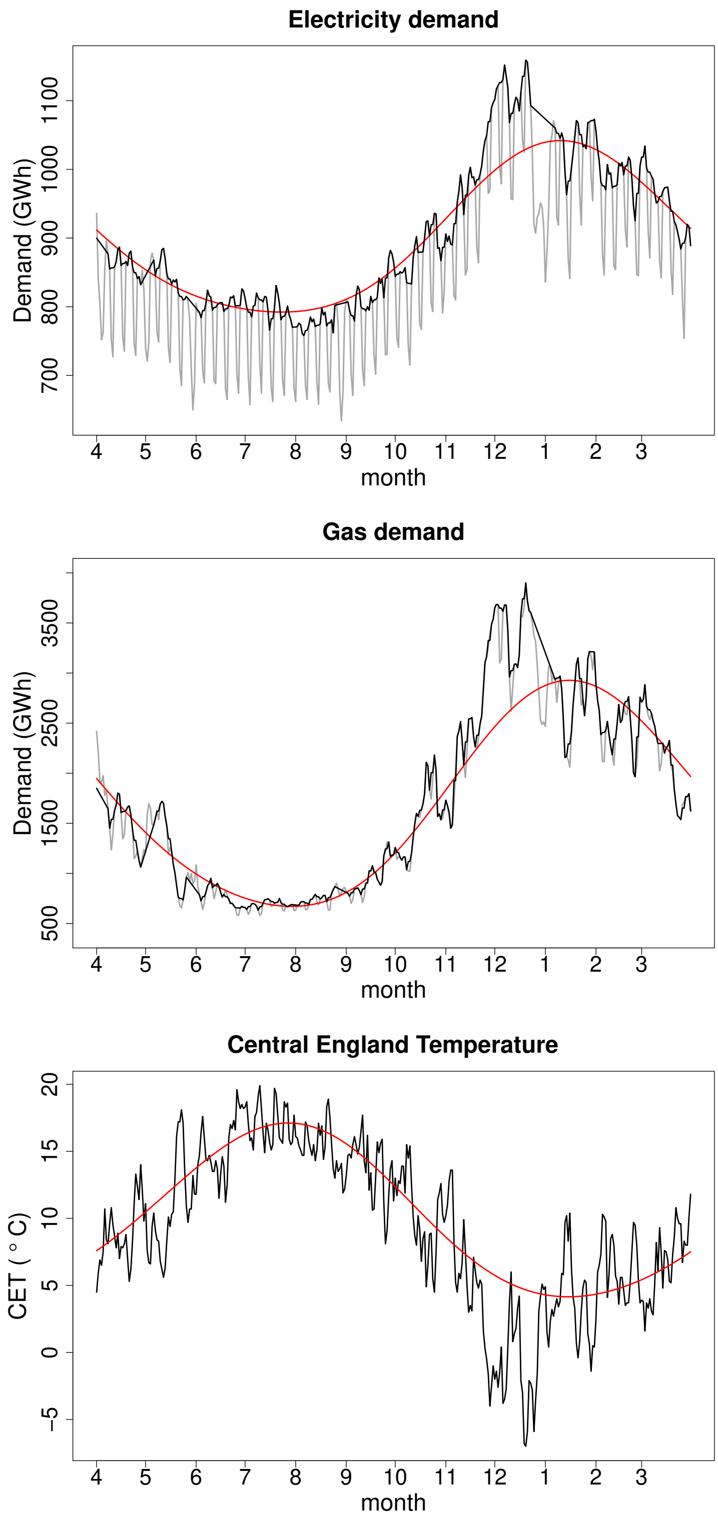

Figure 3.2: GB electricity demand (upper) and GB gas demand (middle) timeseries (grey), equivalent with interpolation over weekends and holidays (black) and harmonic fit (red), April 2010 - March 2011, GWh. Lower: CET timeseries for the same year (°C, black), and harmonic fit (red).

As noted by Taylor and Buizza (2003), a strong weekly cycle in electricity demand is evident, with reduced demand during weekends and holidays (Figure 3.2, grey line). Weekend and holiday days have on average 15% – 20% less electricity demand than week days. Whilst for gas demand a much smaller weekly cycle is seen, with on average only 5% – 10% less demand on non-working days. The difference is consistent with a higher proportion of electricity demand relating to industrial activity, which reduces over the weekend (DECC, 2013).

3.3.2 Temperature Data

To explore the relationship between GB energy demand and temperature, the Central England Temperature record (CET, Parker et al. 1992) is used. This observational dataset gives the average temperature of an area enclosed by Lancashire, London and Bristol and daily data are available from 1772. Shorter datasets covering the whole of GB are available, but as population and demand are weighted to the south of GB, the CET dataset is deemed suitable. In addition the CET record captures the temperature variability seen in other parts of the UK (the daily correlation between CET and the average temperature in Scotland or Wales is very strong, r = 0.93 and r = 0.99, respectively), in agreement with Croxton et al. (2006). The variability in temperature associated with both the annual cycle and daily fluctuations, is much greater than any low frequency variability (Figures 3.2 and 3.3).

As described previously, temperature is the dominant weather driver of electricity demand. However this cannot be the case for the low frequency electricity demand variability seen in Figure 3.1. The steady increase in annual electricity demand up to the mid-2000s would need to be accompanied by a reduction in temperatures over the same period, this is not seen in Figure 3.3. The long term trend in electricity demand leads to a large amount of scatter in the week-day demand-temperature relationship (Figure 3.4, left), which is in contrast to the strong relationship seen in individual years (Figure 3.5). Therefore to better quantify how demand varies with temperature, this low frequency, non-temperature driven demand variability needs to be identified and removed.

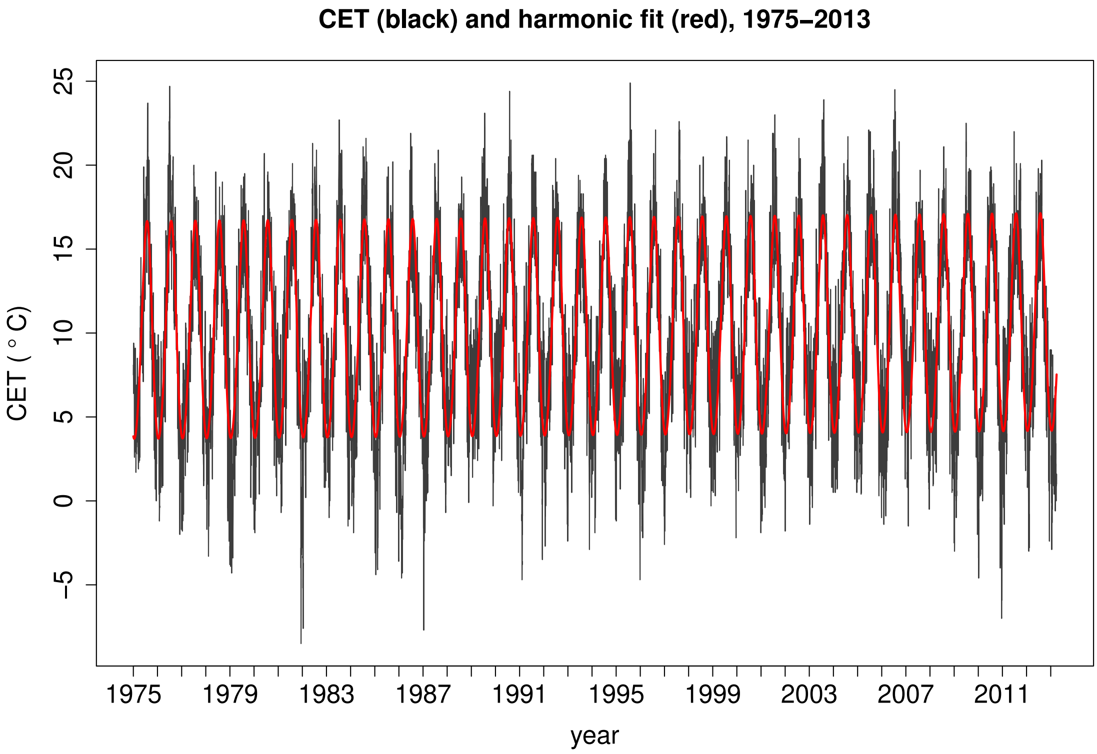

Figure 3.3: CET timeseries (°C, black) with harmonic fit (red), for the period Jan 1975 - March 2013. This is the period for which demand observations are available.

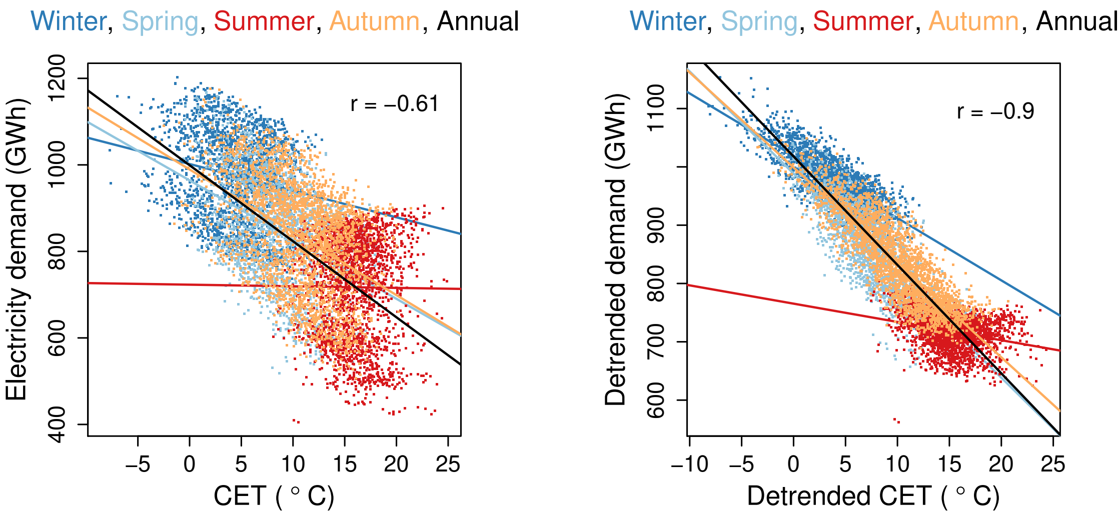

Figure 3.4: Left: Scatter plot of daily temperature (°C) and GB electricity demand (GWh) between January 1975 - March 2013, during week days and non holidays, coloured by season. The Pearson correlation coefficient (r) is given for the annual relationship, with linear fits for each season and annually. Right: as left but detrended GB electricity demand and detrended CET.

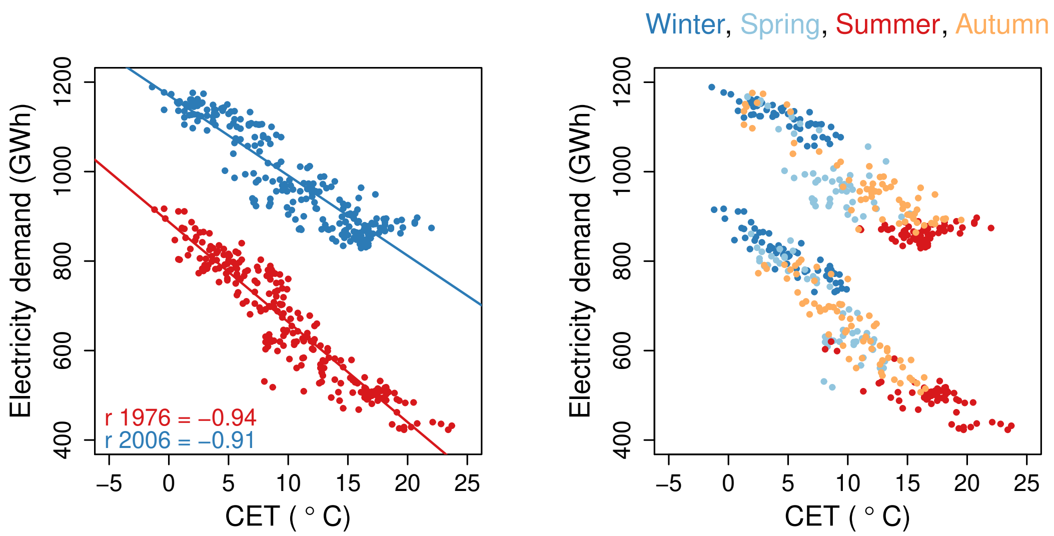

Figure 3.5: Left: The daily relationship between GB Electricity demand (GWh) and CET (°C) for April 1975–March 1976 (red) and for April 2005–March 2006 (blue), with their Pearson correlation coefficient (r). Right: As left, but coloured by season.

3.4 Low frequency demand variability

3.4.1 Identification and drivers

A number of different methods have been used to model or remove long term trends in demand, including using a linear-regression with GDP (Hor et al. 2005, Mirasgedis et al. 2006 and Psiloglou et al. 2009), non-linear regression (De Felice et al. 2013), normalising by population or taking the deviation of demand for a particular day or month relative to the mean for that year (Sailor et al. 1998, Bessec and Fouquau 2008, Hor et al. 2005).

There is a strong positive correlation between GDP and electricity demand prior to 2006 ($r = 0.98$, see Figure 3.6) in agreement with Hor et al. (2005). However from 2007 onwards there is little correlation ($r = 0.07$). The reduction in demand since the mid 2000s is thought to be due to the financial crisis, energy saving measures, an increase in embedded generation (demand that is not seen by the grid operator) and a move away from heavy industry (DECC 2012 and National Grid 2014). The latter three factors would reduce the relationship between GDP and energy demand and may explain the change in relationship seen after 2006. As for electricity, gas demand has a positive but weaker correlation with GDP prior to 2007 ($r = 0.42$) and little correlation after ($r = 0.07$).

The time varying and complex combination of socio-economic drivers of demand suggests that using an individual driver (such as GDP) to model and then remove the long term demand trend is not appropriate. Rather the trend is modelled using a 5 year centred running mean demand. This low frequency demand variability effectively represents the combination of different socio-economic drivers on demand and is subsequently removed prior to comparison with temperature (described in section 3.5.1). A five year centred running mean demand is chosen to be not too long, whilst minimising the impact of an extreme demand season (which could be weather driven) on the yearly demand evolution.

The long term trend and magnitude of the annual cycle of demand are identified using Fourier analysis (see Wilks 2006), benefiting from the quasi-sinusoidal nature of the annual cycle of demand. To construct an evolving background demand ($y(t)$), the demand in any year (April–March) is analysed using a Fourier representation of the form:

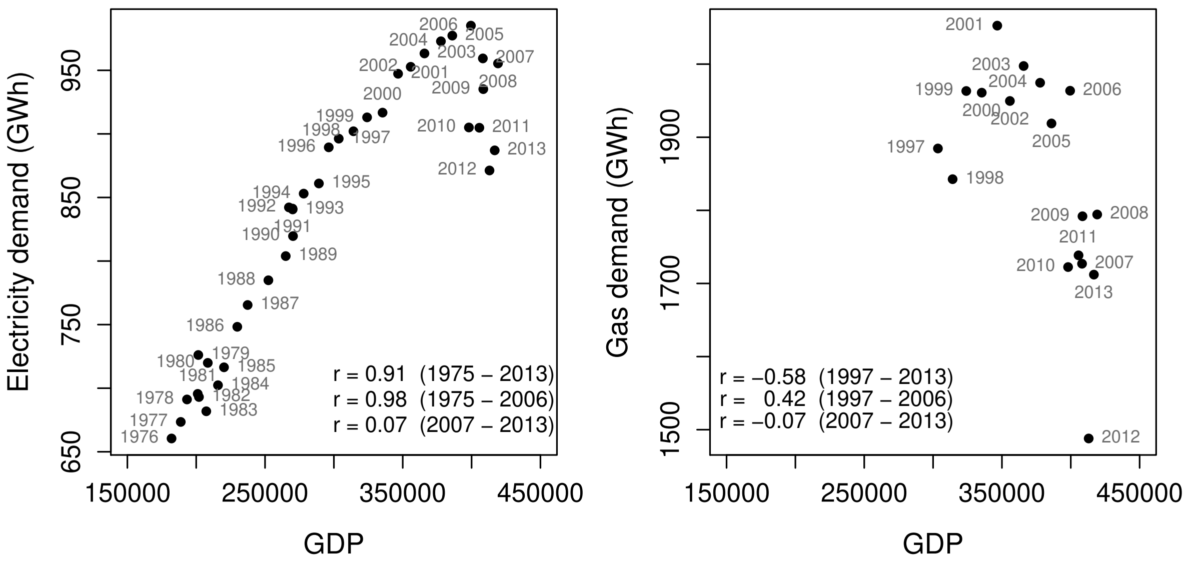

Figure 3.6: The relationship between UK GDP (millions of £s) and annual mean GB electricity demand (left) and GB gas demand (right) in GWh. The Pearson correlation coefficient (r) for different periods is given.

$$y(t) = \overline{y} + A_1 \cos(\omega t) + B_1 \sin(\omega t) + A_2 \cos(2\omega t) + B_2 \sin(2\omega t) \tag{3.1}$$

where, $\frac{2\pi}{\omega} = 365$ days. A second order representation is necessary to capture the asymmetries in the annual cycle of demand. This produces yearly values of each parameter on the right-hand side of equation 3.1. To produce a smoothly evolving background demand, the evolution of each of these parameters is smoothed. A_1, B_1, A_2, and B_2 are smoothed by fitting a linear regression line through the annual values between 1975 and 2013. Yearly mean demand ($\overline{y}$) is smoothed by taking a 5 year running mean due to its non-linear form (red line, Figure 3.7 left), as described earlier. For the two years at either end of the timeseries $\overline{y}$ is represented by a 3 year average. Low frequency variability is therefore defined as variability with a timescale of greater than about 5 years, whilst high-frequency variability is defined as variability on a daily, seasonal and inter-annual timescale.

Here, the focus is on the week-day (Monday - Friday) temperature-demand relationship, and including non-working days would have undesirable effects on the Fourier representation. Consequently, prior to fitting the Fourier expansion, weekend demand is replaced with the average of the adjacent Monday and Friday. Similarly, demand during bank holidays and 3 days either side, is replaced with linearly interpolated values between adjacent non-holiday days. This process maintains the length of the record for the sake of the Fourier analysis. The processed and original demand timeseries are shown in black and grey in Figure 3.2 respectively.

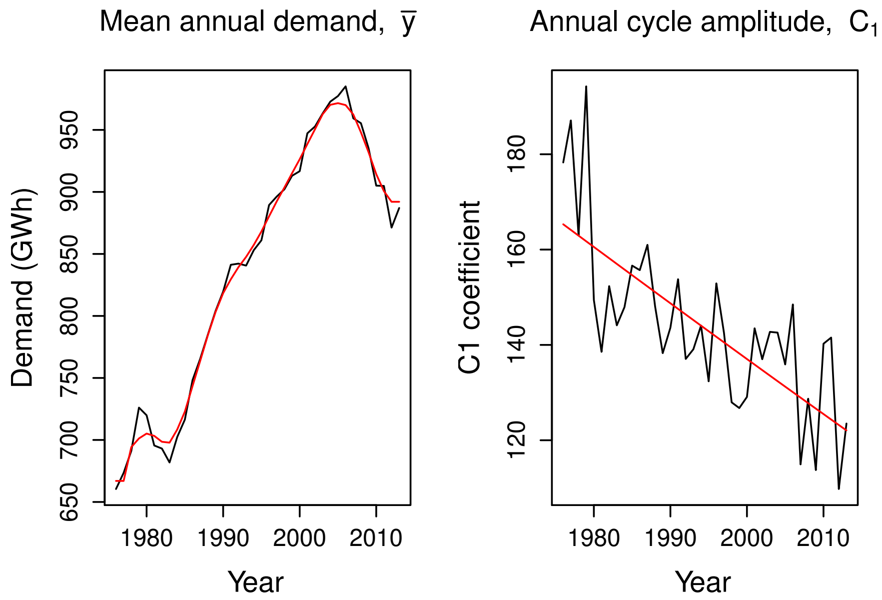

Figure 3.7: Fourier harmonic parameters of Electricity demand analysis. Left: Annual mean demand ($\overline{y}$, black), its 5 year running mean (red). Right: First harmonic wave amplitude (C_1, GWh, black) and its smoothed representation (red). The smoothed C_1 is calculated from the linear representations of A_1 and B_1.

3.4.2 Results

The slowly evolving background electricity and gas demand timeseries, resulting from the Fourier fitting and smoothing, are shown in red in Figure 3.1. The Fourier representation successfully captures both the low frequency demand variability and its changing annual cycle.

The Fourier representation also allows the amplitude of the annual cycles of electricity and gas demand and their evolution to be compared. The first Fourier component (the annual cycle) can alternatively be written as $C_1 \cos(\omega t - \phi_1)$, with amplitude ($C$) and phase shift ($\phi$), where $C_1 = \sqrt{(A_1^2 + B_1^2)}$ and $\tan\phi = \frac{B_1}{A_1}$. Gas demand has a large annual cycle, where its amplitude (C_1) is ∼60% of the long term mean demand and changes little over the recorded period (Figure 3.1 lower and C_1, Figure 3.8). In contrast the annual cycle of electricity demand is considerably smaller and reduces by approximately a third over the last 38 years (Figure 3.7 right, also seen in Figure 3.1 upper). For example, in 2012 the amplitude was only 14%

of the mean demand of that year. In the recent period (2005-2012), approximately two-thirds of residential gas consumption was for space heating compared to less than a quarter for electricity (DECC 2013, see their Table 3.02, Domestic data), explaining the greater sensitivity of gas demand to temperature and its larger annual cycle. The reduction in the amplitude of the annual cycle of electricity demand is associated with summer demand increasing at a faster rate than winter demand, with the difference reducing by on average 1.7GWh/year, or approximately 7% per decade (Figure 3.9). An equivalent reduction in the seasonal cycle of temperature is not seen, rather non-meteorological drivers are likely responsible.

The Fourier analysis also highlights that the annual mean gas demand ($\overline{y}$) increases between 1996 to the early 2000s and then reduces thereafter (left hand panel of Figure 3.8). Over the whole period, negative linear trends in gas demand are seen in spring, summer and autumn, with reductions of 1-2% per year (Figure 3.10).

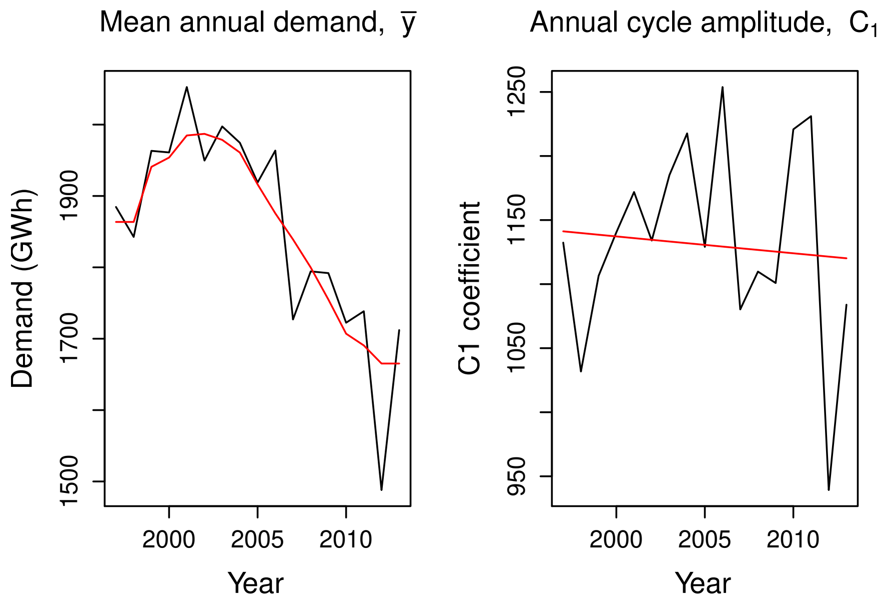

Figure 3.8: Fourier harmonic parameters of GB gas demand analysis. Left: Annual mean demand (GWh, black) and 5 year running mean (red). Right: First harmonic wave amplitude (C_1, GWh, black) and its smoothed representation (red). The smoothed C_1 is calculated from the polynomial representations of A_1 and B_1.

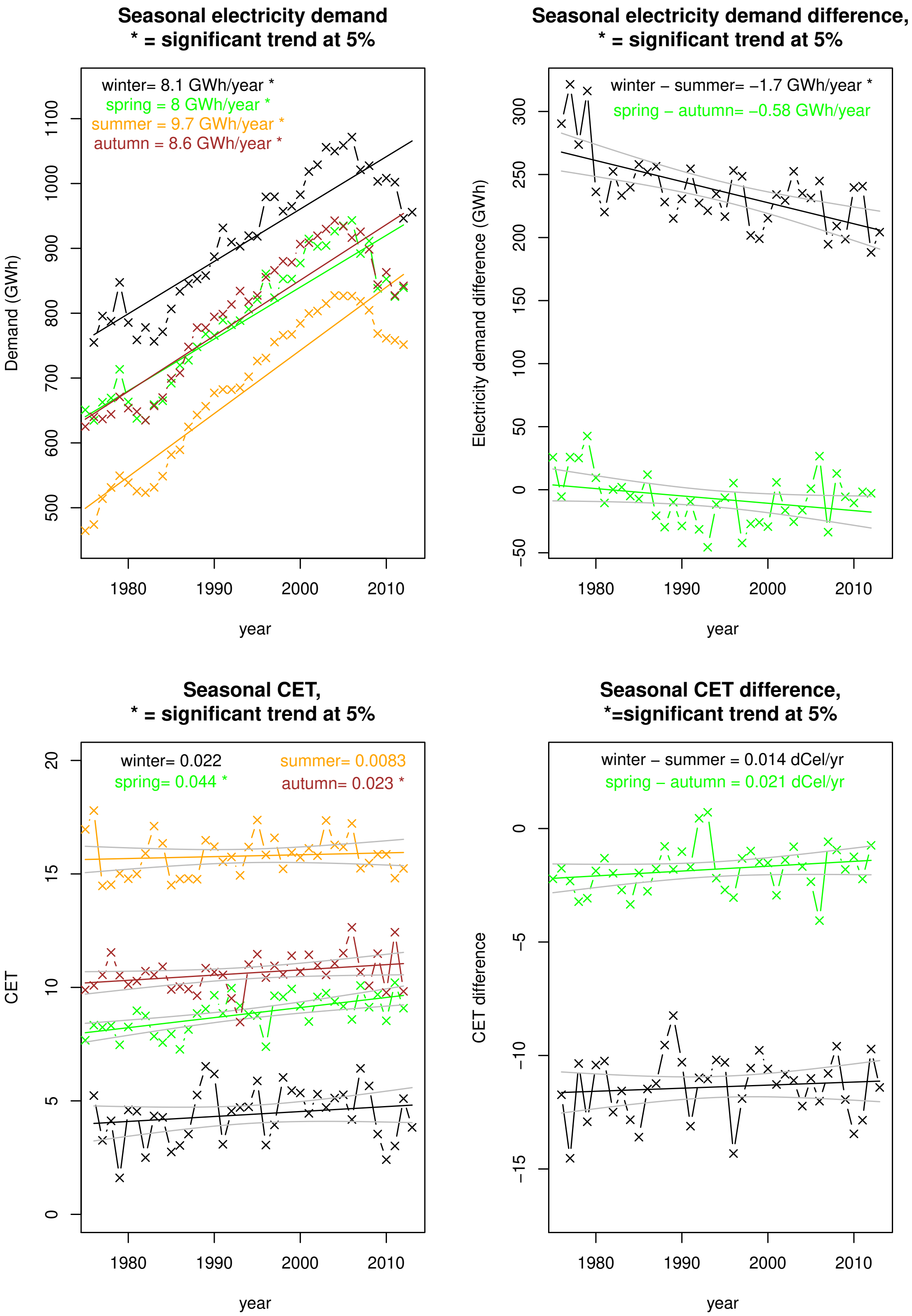

Figure 3.9: Seasonal mean of daily GB electricity demand (GWh) and CET (°C) and linear trends over the period 1975-2012 (left) and winter/summer and spring/autumn differences in these two variables (right). Statistical significance of the trend at the 5% level is indicated by a *.

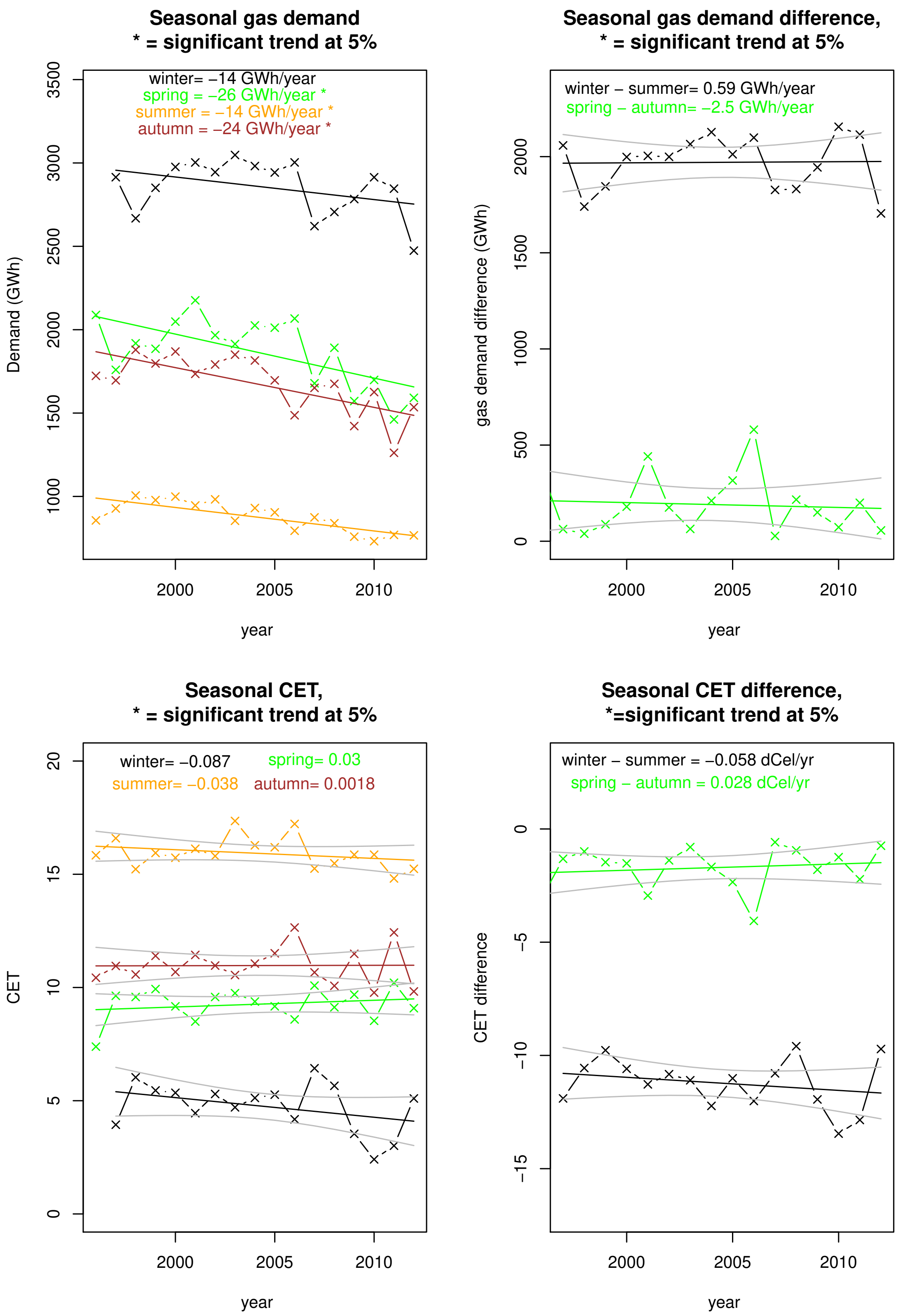

Figure 3.10: Seasonal GB gas and CET trends over the period 1996-2012 (left) and winter/summer and spring/autumn differences (right)

3.5 Demand - temperature relationships

The desire to understand the current risk of demand extremes has determined how the demand-temperature relationship is established.

3.5.1 Methodology

Demand - removing the low frequency variability

Low frequency demand variability, associated with socio-economic changes, weakens the demand-temperature relationship and is therefore removed. This is achieved by replacing the slowly varying background demand field with a constant annual cycle demand background. The two stages undertaken to achieve this are:

$$R = D - B$$
$$D_d = R + B_c$$

where:
D = Demand (black line in Figure 3.1)
B = Slowly varying background demand (red line in Figure 3.1)
R = Residual demand.
B_c = Repeating climatological mean annual demand cycle (red line in Figure 3.11)
D_d = Detrended demand, where the low frequency variability has been removed (black line in Figure 3.11)

The resultant detrended demand (D_d) timeseries is shown in Figure 3.11. This process has effectively retained the high frequency demand variability and the climatological annual cycle, whilst removing the long term variations in both annual mean demand and annual cycle magnitude. For example the demand spike in winter 1986-1987 or the anomalously high demand throughout winter 1978-1979 are still present in this detrended demand timeseries.

Temperature - removing the long term trend

Temperature variability occurs across all timescales, from sub-daily to centennial. Decadal scale variability in atmospheric temperature (as seen in Figure 3.12) is driven by slowly varying climate dynamics, including the Atlantic Multi-decadal oscillation and the El Nino southern oscillation (Knight et al. 2006, Fraedrich and Muller 1992) and external forcings including aerosols and solar variability. Such

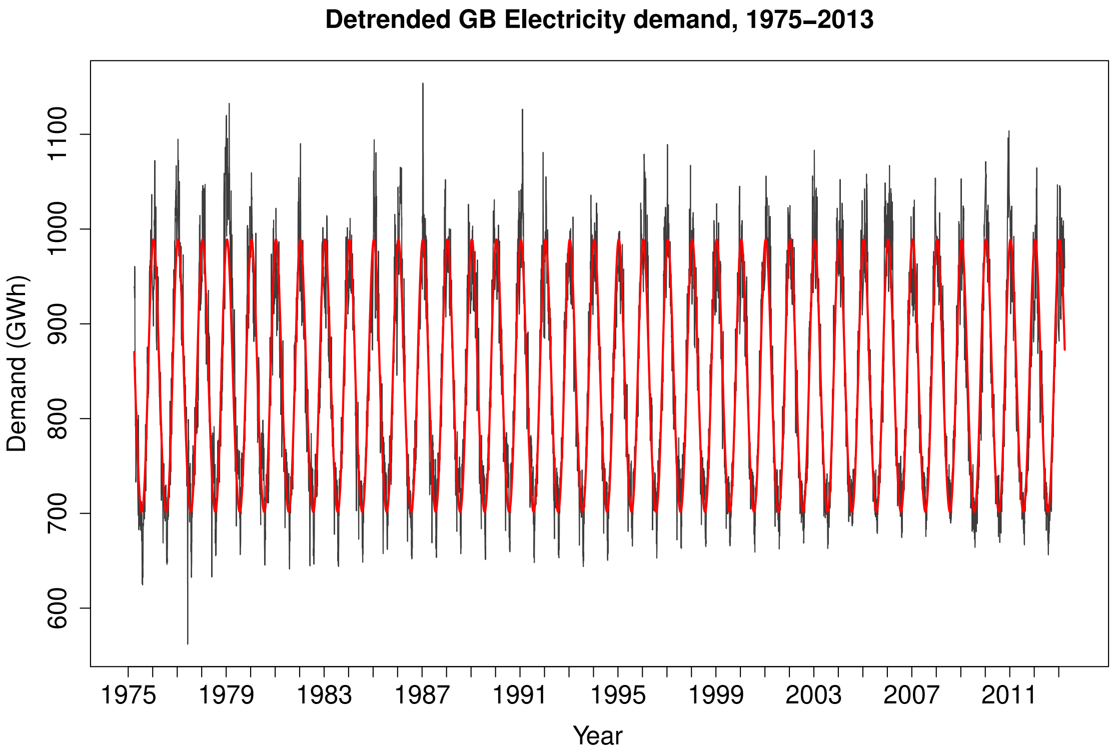

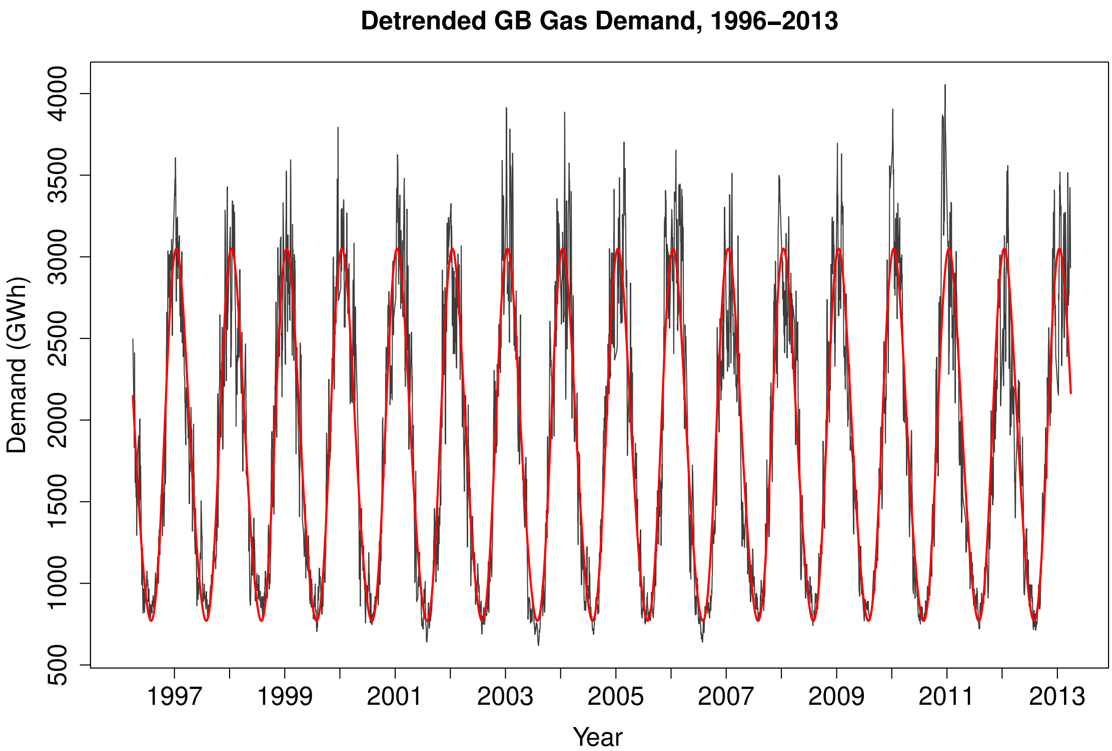

Figure 3.11: Upper: Detrended GB electricity demand timeseries (GWh, black) and climatological annual cycle (red), April 1975 - March 2013. Lower: Detrended GB gas demand timeseries (GWh, black) and climatological annual cycle (red), Jan 1996 - March 2013.

variations in temperature are important to include when calculating the risk of demand extremes. However longer scale temperature variability, which is presumed to be predominantly associated with anthropogenic climate change, makes the likelihood of cold winter days lower today (Brown et al. 2008, Hartmann 2013, Bindoff 2013). To account for this non-stationarity, the long term temperature trend needs to be removed prior to the demand-temperature relationship and risk of extremes being established (as discussed in Coles 2001).

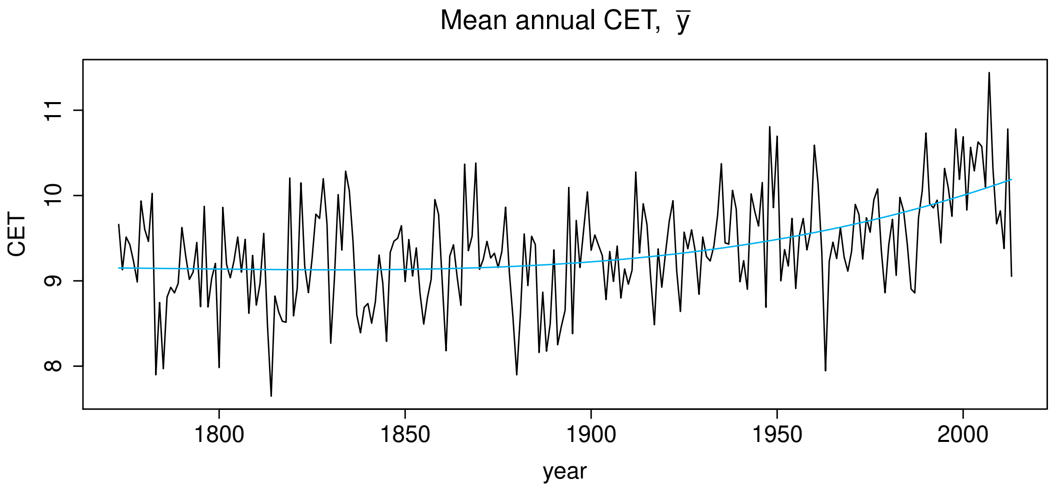

Figure 3.12: Annual mean CET (°C, black) used in the Fourier expansion, and a third order polynomial fit (blue).

A long term trend in CET can also be modelled using a Fourier expansion, as shown in red in Figure 3.3 for the recent period. The detrending approach used is the same as that for demand (see section 3.5.1), with a few important differences. Firstly, the evolution of the annual mean temperature is represented by a third order polynomial (blue line, Figure 3.12), to better capture the long term trend. Secondly, the evolution of A_x and B_x is not modelled, rather climatological average values are used, giving a constant annual cycle in the background timeseries. Consequently, once this background field has been removed, only decadal and higher frequency variability remains in the 'detrended temperature' timeseries, including any changes in the annual cycle (in contrast to detrended demand).

The relationship between detrended demand and detrended temperature can now be established. The relationship is determined using all years of data, this approach therefore assumes the relationship remains constant through the data period. The relationship is only considered over working week-days (excluding weekends, bank holidays and 3 days either side of bank holidays).

3.5.2 Results

Annual relationship

The removal of low frequency demand variability leads to a much stronger week-day relationship between electricity demand and detrended temperature, increasing the correlation from -0.61 to -0.90 (Figure 3.4, right and top row Table 3.1), which is now similar to that seen within individual years. This suggests that the key relationship between demand and temperature has been retained whilst the socio-economic influences on demand have been successfully removed. The strength of the relationship is now comparable to that of raw gas demand and temperature, where $r = -0.94$ (Figure 3.13). Low frequency gas demand variability is small, consequently its removal barely modifies its annual correlation with temperature (Table 3.2). The daily relationships are seen to be slightly non-linear, with the negative relationship levelling off above $\sim$17°C, similar to that found in Psiloglou et al. (2009) and Summerfield et al. (2015).

Seasonal and monthly relationships

The electricity demand-temperature relationships for each season also improve substantially after removal of low frequency demand variability, for example the winter correlation increases from -0.19 to -0.80 (Table 3.1). Modest correlation increases are also seen after detrending the gas demand (Table 3.2). A strong anti-correlation between daily detrended temperature and electricity demand is found in winter, spring and autumn (magnitude ≥ -0.80, Figure 3.14), with a much weaker correlation in summer ($r = -0.28$), in agreement with Psiloglou et al. (2009). Electricity

Data	Raw correlation	Detrended correlation	Deseasonalised, detrended correlation
All days	-0.61	-0.90	-0.60
Winter days	-0.19	-0.80	-0.81
Spring days	-0.40	-0.82	-0.64
Summer days	-0.01	-0.28	-0.12
Autumn days	-0.44	-0.86	-0.62

Table 3.1: Summary of correlations between daily GB electricity demand and daily CET, between 1^{st} January 1975 and 31^{st} March 2013, considering week-day and non-holiday days only (Column 1). Column 2, the same however the correlation is between detrended demand and detrended CET. Column 3, the same as column 2, except the respective annual cycles have been removed.

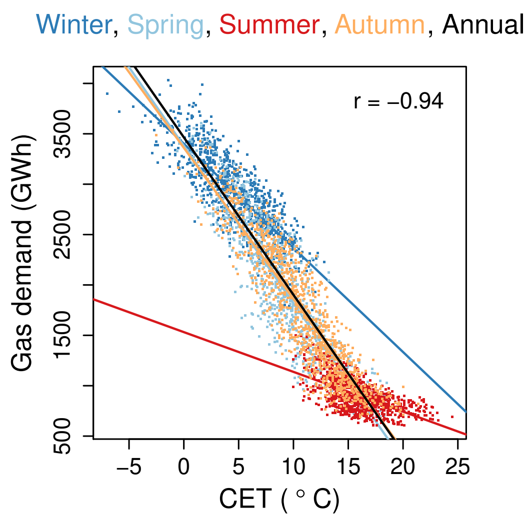

Figure 3.13: Scatter plot of daily temperature and GB gas demand between March 1996 - March 2013, during week days and non holidays, coloured by season. The Pearson correlation coefficient (r) is given for the annual relationship, with linear fits for each season and annually.

Data	Raw correlation	Detrended correlation	Deseasonalised, detrended correlation
All days	-0.94	-0.95	-0.83
Winter days	-0.83	-0.91	-0.90
Spring days	-0.88	-0.91	-0.83
Summer days	-0.60	-0.76	-0.65
Autumn days	-0.91	-0.94	-0.87

Table 3.2: Summary of correlations between daily GB gas demand and daily CET between March 1996 and March 2013. See Table 3.1 for details.

demand saturation at extreme low temperatures, as claimed by Hor et al. (2005), is not seen. Gas demand is strongly related to temperature in each season, with stronger correlations than those of electricity, particularly in summer (Table 3.2 and Figure 3.16, left-hand column).

The strength of the seasonal relationships between detrended demand and either CET or detrended CET is compared and the difference is found to be very small (correlations vary by a maximum of 0.01). This highlights that over the 38 year period of demand observations, the long term trend in temperature is small compared to higher frequency variability, and therefore barely influences the daily demand-temperature relationships.

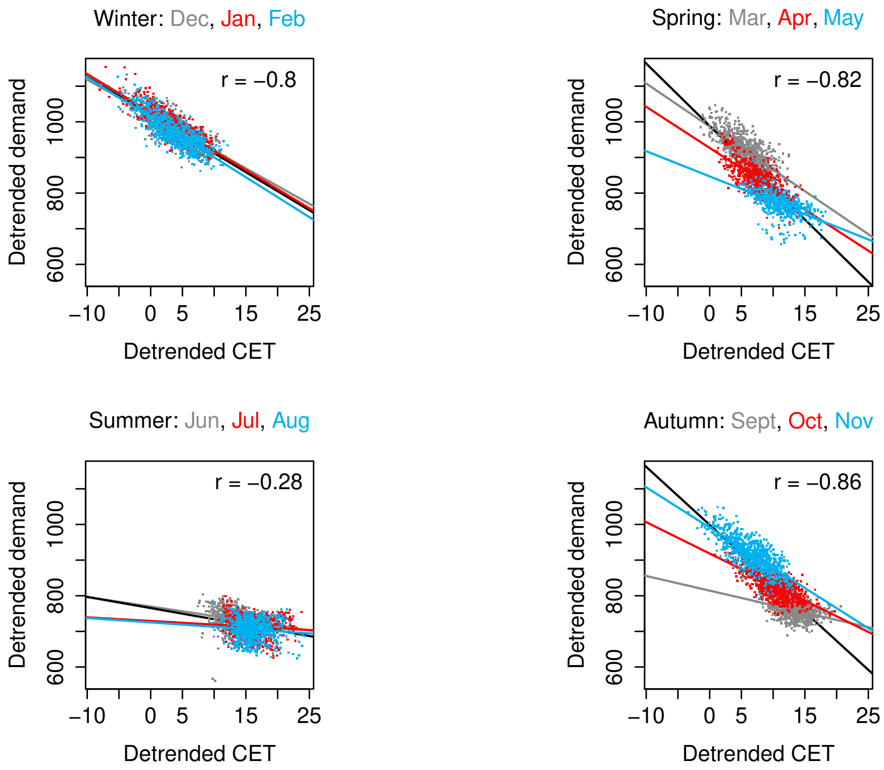

Figure 3.14: Scatter plot of daily detrended temperature (°C) and detrended GB electricity demand (GWh), during week days and non holidays between 1^{st} January 1975 - 31^{st} March 2013, coloured by month. The Pearson correlation coefficient (r) and the linear fit through each month and the whole season (black) are also shown.

For both electricity and gas demand, the all days correlation is higher than that of individual seasons. This reflects the large annual cycle in temperature and the fact that the annual cycle in demand is not fully explained by the annual cycle in temperature. During spring or autumn the relationship between demand and temperature changes (see Figure 3.14). For example, the March relationship is nearer to that seen in winter, whilst the May relationship is more similar to that found in summer. A day with a temperature of 7°C would on average give an electricity demand of ∼900GWh in March, ∼850GWh in April and ∼800GWh in May. However during winter or summer, the monthly relationships are very similar. The change in relationship within a season cannot be caused by temperature. One hypothesis is that during spring and autumn, for the same daily average temperature, a difference in daylight hours could modify the demand for lighting and possibly also for heating.

The strength of the seasonal relationships during spring and autumn is better established using the residual relationships (where the annual cycles have been removed, see Figures 3.15 and 3.16). The all days correlation is now lower or equivalent to that of the individual seasons ($r = -0.60$ for electricity and $r = -0.83$ for gas, see last column in Tables 3.1 and 3.2). Winter now has the strongest relationships, with approximately two-thirds of the variability in electricity demand being linearly accounted for by temperature variability ($r = -0.81$) and over four-fifths of gas demand variability ($r = -0.90$). Temperature sensitivity in winter is now similar or higher than that seen in spring and autumn, contrary to that seen when the annual cycle is present. Over the data period, a 1°C decrease in daily temperature during winter months will typically give rise to a 10–12GWh increase in daily electricity demand (∼1% increase, established using the monthly linear fits in Figure 3.14) and a 105–115GWh increase in daily gas demand (3%–4% increase). Temperature sensitivity is at a minimum in summer (1–3GWh increase in demand/°C of cooling), whilst demand increases by 7–13GWh in spring and 4–12GWh in autumn, per degree of cooling. Unlike more southern European countries, GB has limited air-conditioning within residential properties, explaining the weak sensitivity of demand to temperature in summer.

A similar picture is seen for gas demand, where temperature sensitivity is highest in winter and lowest in summer. A 1°C decrease in daily temperature during winter months will typically give rise to a 105–115GWh increase in daily gas demand (3%–4% increase), and a 20–50GWh increase in demand in summer. Demand increases by 90–135GWh in Spring and 60–120GWh in Autumn, per degree of cooling.

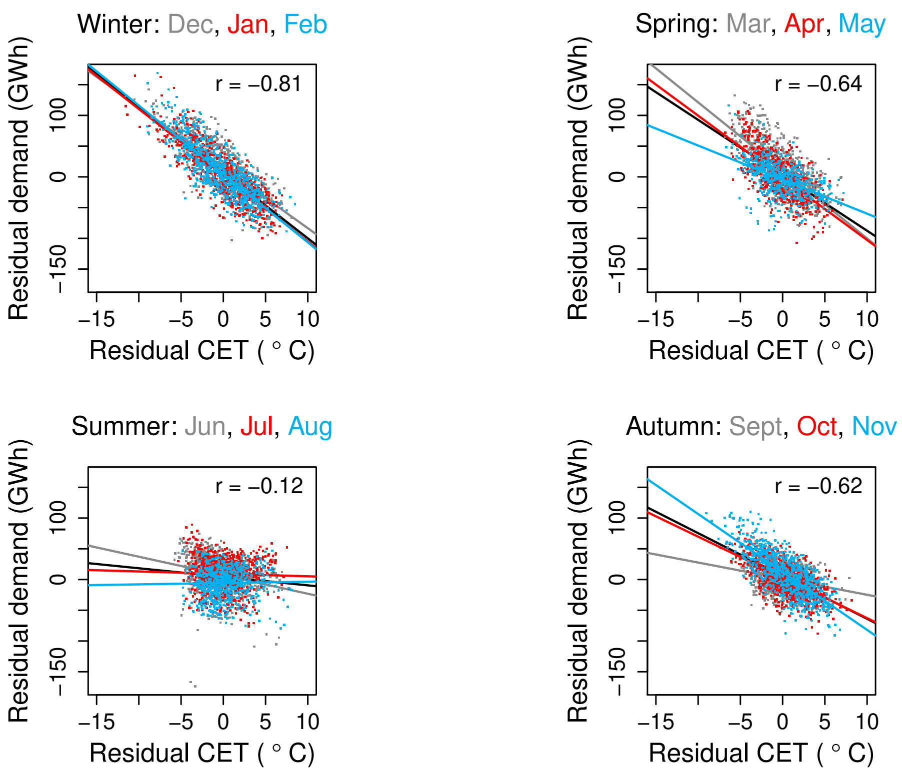

Figure 3.15: Scatter plot of daily detrended temperature residual (°C) and detrended GB electricity demand residual (GWh), during week days and non holidays between 1^{st} January 1975 - 31^{st} March 2013, coloured by month. The Pearson correlation coefficient (r) and the linear fit through the whole season are also shown (black)

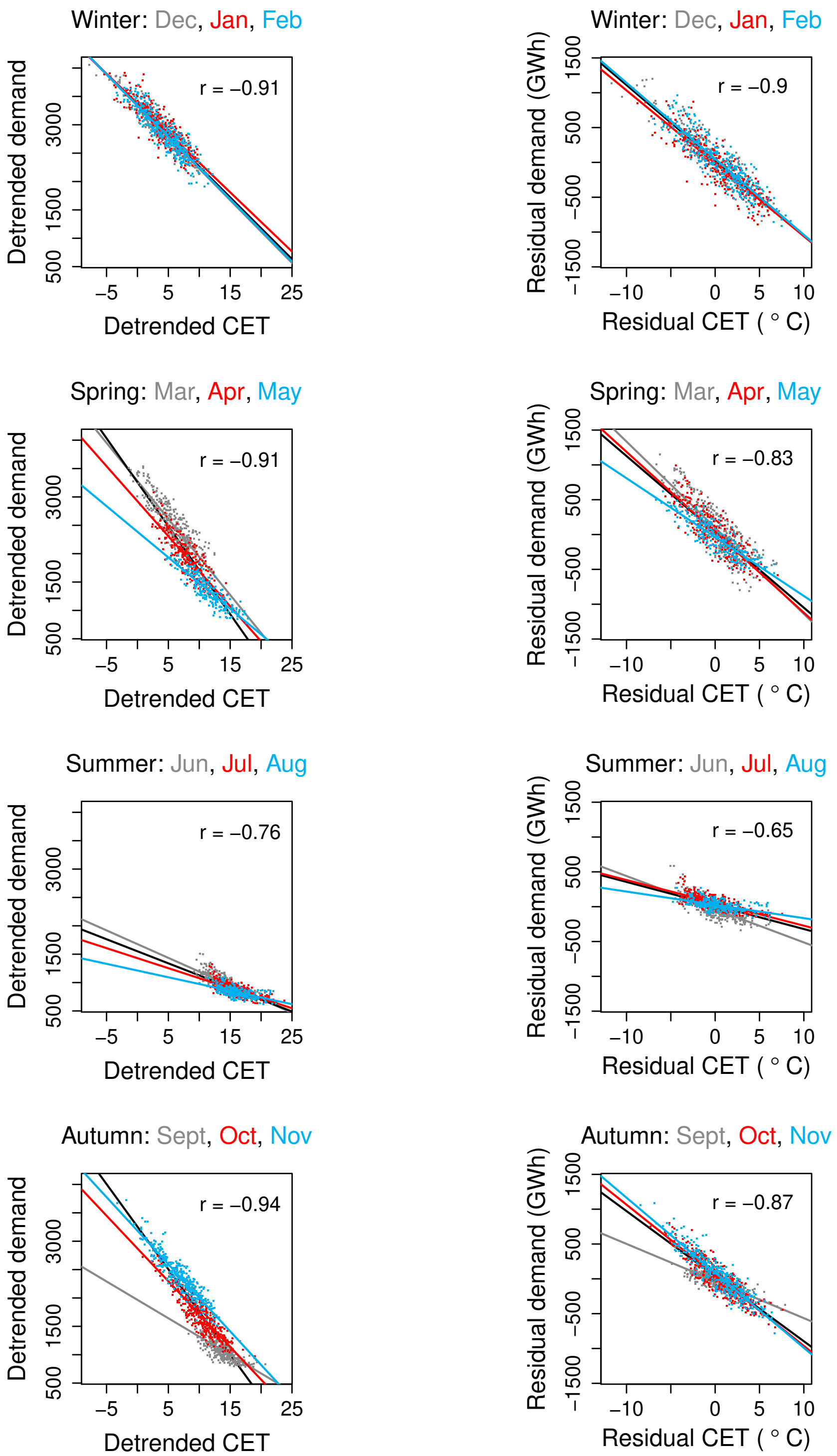

Figure 3.16: Left column: Scatter plot of daily detrended temperature (°C) and detrended GB Gas demand (GWh), during week days and non holidays between 1st March 1996 - 31st March 2013, coloured by month. The Pearson correlation coefficient (r) and the linear fit through each month and the whole season (black) are also shown. Right column: as left but with residual demand and residual temperature.

3.6 Extreme demand periods

In preparation for each winter, National Grid estimates both the magnitude of extreme electricity and gas demand conditions and total generation capacity, to ensure sufficient supply. For electricity demand, they estimate the 1 in 20 year peak demand, where peak demand is defined as the maximum instantaneous demand (in GW) during a financial year. They also estimate the average cold spell peak demand, which is defined as the peak demand within a year which has a 50% chance of being exceeded as a result of weather variation alone (National Grid 2012b). As part of the gas winter security assessment, the 1 in 20 year and 1 in 50 year peak daily, weekly, monthly and seasonal mean demand are estimated (National Grid 2014).

3.6.1 Methodology

The longer a demand timeseries the better the quantification of its extremes. The observations of electricity and gas demand cover 38 years and 16 years respectively. However a much longer artificial demand timeseries can be generated using the entire detrended CET record (1772 – 2013) and the modern detrended temperature–demand regression relationships (as described in Section 3.5.2). These artificial daily demand estimates, give the demand that would have occurred given historical temperatures, but are consistent with demand from a modern energy system. The winter mean relationship is chosen because of the interest in high demand extremes. The risk of recent extreme demand periods is assessed by counting the number of artificial events since 1772 where demand equals or exceeds the recent event of interest.

The mean absolute error between regression predicted and actual demand over the observed period is small. Bootstrap sampling is employed to quantify uncertainty in the demand estimates, resulting from uncertainty in the regression model and the limited sample size. For further details on the mean error and bootstrap sampling see Sup. Mat (section 3.8.2). All extreme demand estimates are presented as a percentage difference from the average winter day demand over the last decade (Dec 2003–Feb 2013, hereafter referred to as ‘climatology’), as calculated by the regression model. The climatological electricity and gas demand are 980GWh and 2951GWh respectively.

3.6.2 Results

Daily extremes

Over the 241 years, the top 1% of electricity demand days in winter have a demand estimate which is at least 10.8% (10.4% – 11.1%) above climatology (Figure 3.17 and table 3.3). The 1 in 20 year peak day electricity demand estimate is 15% (14% – 16%) above climatology, whilst the average cold spell demand estimate is 10.2% (9.8% – 10.6%) above climatology. The coldest day in the record occurred on the 20th January 1838, with a detrended temperature of -11.7°C, giving an electricity demand estimate 17% (12% – 21%) above climatology. It is not possible to compare the 1 in 20 year peak demand estimate with that forecast by National Grid because the latter is instantaneous demand in GW rather than daily demand in GWh.

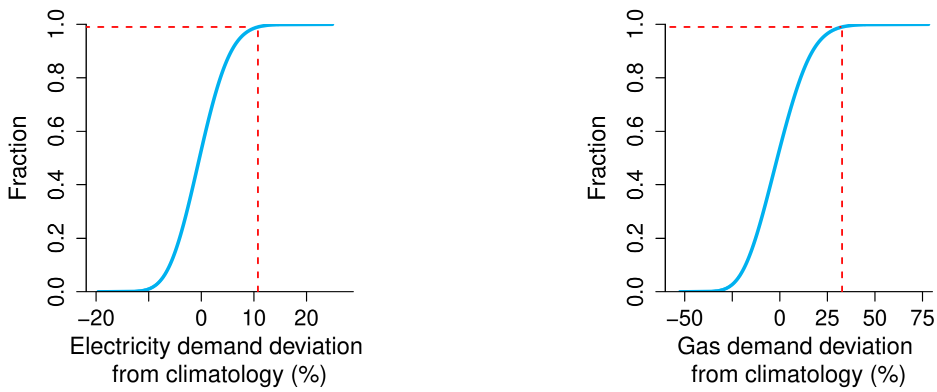

Figure 3.17: Left: The cumulative frequency distribution of the deviation of winter daily GB electricity demand for 1772 – 2013, from the average winter day's demand (December 2003–February 2013, 'climatology'). The results presented are from the regression bootstrap. The red lines indicate the top 1% of winter demand days. Right: as left but GB gas demand.

Equivalent statistics are given in Table 3.3 and Figure 3.17 for gas demand. The deviations from climatology are greater for gas than electricity, which is consistent with gas demand being more sensitivity to temperature change. The 1 in 20 year peak day gas demand estimate is 46% (44% – 49%) above climatology, whilst the 1 in 50 year demand estimate is 50 % (47% – 54%) higher. Based on the climatological demand from 2003-2013, the 1 in 20 year peak day gas demand value is 4308GWh or 392mcm, which is higher than the 2017/2018 forecast value of approximately 350mcm. This difference may reflect the reducing demand for gas over recent years, as the equivalent forecast for winter 2013/14 was 388-402mcm (National Grid, 2013), which is similar to that calculated here.

Averaging period	Elect. demand Top 1%	Elect. demand Max	Gas demand Top 1%	Gas demand Max	Date of Max
Winter Day	10.8% (10.4–11.1)	16.6% (12.2–20.7)	33% (31–34)	57% (47–66)	20/01/1838
Month	5.6% (5.0–6.3)	7.2% (6.4–7.9)	19% (18–21)	24% (22–26)	Jan 1795
Winter	3.2% (2.7–4.0)	4.6% (4.2–5.1)	11% (9–13)	16% (15–17)	1962/1963

Table 3.3: The minimum percentage increase of average daily demand during the top 1% of winter days, months and winters between 1772 and 2013, relative to the recent decade's daily winter mean demand value of 980GWh for electricity and 2951GWh for gas. The dates of maximum gas and electricity agree. The 5 – 95 percent uncertainty range from bootstrap sampling is given in brackets (see section 3.8.2 in Sup. Mat.).

Monthly and seasonal extremes

December 2010 is a recent, extremely cold month (Maidens et al. 2013). The detrended temperature was on average -1.5°C, giving temperature driven electricity and gas demand estimates of, respectively, 5.7% (4.9% – 6.4%) and 19% (18% – 21%) above climatology. Over the 241 year period, a month with at least as much electricity or gas demand as December 2010 is estimated to occur on average once every $\sim$34 years (20 – 60 years). Months with greater demand would have occurred in the past given the temperatures experienced. For example January 1795 was the coldest month since 1772, with a detrended average temperature of -2.9°C. Such conditions would give a monthly average electricity and gas demand estimate 7.2% (6.4% – 7.9%) and 24% (22% – 26%) above climatology respectively.

Winter 2009/2010 is a recent extreme winter (Cattiaux et al. 2010, Fereday et al. 2012), when the average daily detrended temperature was 1.6°C. Estimates of winter mean temperature driven electricity and gas demand are, respectively, 2.3% (1.8% – 2.7%) and 8% (7% – 9%) above climatology. Over the 241 year period, a winter with at least as much electricity or gas demand as 2009/2010 is estimated to occur on average once every $\sim$18 years (12 - 27 years). Winter 1962/1963 was the coldest winter since 1772, with an average detrended temperature of -0.6°C. Under such conditions, winter average electricity and gas demand is estimated to be, respectively, 4.6% (4.2% – 5.1%) and 16% (15% – 17%) above climatology.

The 1 in 50 year peak gas demand week, month and season are estimated to be 35% (33% – 37%), 20% (18% – 22%) and 9% (8% – 11%) above climatology respectively. It is of interest to note that due to the long term trend in temperature, the risk of a December 2010 or a winter 2009/2010 demand has approximately halved.

Decadal variability of European surface climate is strongly linked with decadal variability of the NAO (Hurrell, 1995). For example, during the 1960s, winters were much colder in Northern Europe compared to those of the 1990s, reflecting the shift from negative to positive NAO conditions over the period. Colder UK winters have also been found to occur more often during periods of low solar activity (Lockwood et al., 2010). Given the artificial demand extremes presented here are driven purely by observed temperature variability, equivalent decadal variability in the demand extremes would be expected.

3.7 Conclusions

Observed daily electricity and gas demand in GB have been analysed between 1975-2013 and 1996-2013 respectively. The daily relationships between week-day energy demand and temperature have been established and their variation with month and season investigated. Low frequency, non-temperature related demand variability is represented by a slowly evolving truncated Fourier expansion, and is removed prior to establishing the relationship with temperature. Artificial estimates of daily demand are made back to 1772 using detrended temperature observations and the modern detrended demand–temperature regression relationships. The current risk and magnitude of extreme demand events has then been quantified. The main conclusions are given below:

- From 1975 – 2006 annual electricity demand increases almost monotonically, after which a reduction is seen. Over the same period the annual cycle amplitude of electricity demand reduces by a third, which is associated with summer demand increasing at a faster rate than winter demand.

- Both daily electricity and gas demand are strongly anti-correlated with daily mean temperature ($r_{elec} = -0.90$, $r_{gas} = -0.94$), once low frequency non-temperature related variability in demand has been removed. However these correlations are inflated by the demand-temperature relationships changing throughout spring and autumn. Once the annual cycles of temperature and demand are removed, the correlations drop to $r_{elec} = -0.60$ and $r_{gas} = -0.83$.

- Winter has the strongest demand-temperature relationship (r_{elec} = -0.81 , r_{gas} = -0.90), and high temperature sensitivity. Over the data period, a 1°C reduction in daily temperature in winter typically gives a ∼1% increase in daily electricity demand and a 3% – 4% increase in gas demand.

- A higher proportion of gas demand is consumed for domestic heating compared to electricity, which is consistent with its stronger anti-correlation with temperature, its larger relative annual cycle, its weaker weekly cycle and its greater sensitivity to temperature change.
- The 1 in 20 year peak day electricity demand estimate is 15% (14% – 16%) above the average winter day demand. The 1 in 20 and 1 in 50 year peak day gas demand estimates are 46% (44% – 49%) and 50% (47% – 54%) above the average winter day respectively. Today the risk of a month having at least as much electricity or gas demand as December 2010 is estimated to be one in ∼34 years (20 – 60 years). The risk of a winter having at least as much electricity or gas demand as the 2009/2010 winter is estimated to be one in ∼18 years (12 – 27 years). The long term trend in temperature means the risk of a December 2010 or a winter 2009/2010 demand has approximately halved.

This improved understanding of the demand-temperature relationships and the risk of extremes should aid operational management and longer term planning of Great Britain's energy system.

3.8 Supplementary Material

3.8.1 Electricity demand data

Two different electricity demand datasets have been combined to give a total GB daily demand record between 1971 and 2013. A daily England and Wales (E&W) electricity demand dataset is available from April 1971 to December 2009. A half hourly GB total electricity demand dataset is available from January 2001 to March 2013. A daily average conversion factor from E&W to GB total demand is calculated over the overlap period (January 2001 to December 2009), where on average E&W makes up 90% of GB demand. Using this conversion factor and the E&W demand data, a daily GB demand record prior to 2001 is created and combined with the later GB data to give a full record. This follows the methodology used within National Grid (personal communication). The electricity demand data are published INDO (Initial Demand Outturn) and are based on National Grid operational generation metering. The demand excludes station load, pump storage pumping and interconnector exports.

3.8.2 Regression uncertainty and bootstrap sampling

Prior to using the regression relationships to make out of sample predictions, their robustness has been explored. The mean absolute error of the electricity and gas demand estimates (the difference between the predicted and actual demand) over the observed period is calculated using cross validation. This means that for a prediction of demand on a given day, the regression relationship between observed demand and temperature is calculated using all observations except for those 10 days either side of the day in question (see e.g. Wilks 2006). For electricity the mean absolute error is 21GWh, equivalent to approximately half the standard deviation of winter demand. For gas demand, the mean absolute error is 130GWh, or approximately a third of the winter standard deviation. The cross-validation correlation between predicted and actual electricity demand is 0.80, whilst for gas demand is 0.93.

Bootstrap sampling is employed to quantify uncertainty in the demand estimates, resulting from uncertainty in the regression model and the limited sample size. For each daily temperature, 1000 demand estimates are created assuming a normal distribution of regression residuals, sampling the uncertainty in the regression relationship. The central demand estimates presented give the average across this bootstrap. In addition a 5-95 percent bootstrap range is given in brackets, which additionally includes sample uncertainty. For each bootstrap timeseries, a different selection of 241 years is chosen and to maintain decadal variability, 10 year blocks are chosen at random with replacement.

Chapter 4

The relationship between wind power, electricity demand and winter weather patterns in Great Britain

4.1 Abstract

Wind power generation in Great Britain has increased markedly in recent years. However due to its intermittency its ability to provide power during periods of high electricity demand has been questioned. Here we characterise the winter relationship between electricity demand and the availability of wind power. Although a wide range of wind power capacity factors is seen for a given demand, the average capacity factor reduces by a third between low and high demand. However, during the highest demand average wind power increases again, due to strengthening easterly winds. The nature of the weather patterns affecting Great Britain are responsible for this relationship. High demand is driven by a range of high pressure weather types, each giving cold conditions, but variable wind power availability. Offshore wind power is sustained at higher levels and offers a more secure supply compared to that onshore. However, during high demand periods in Great Britain neighbouring countries may struggle to provide additional capacity due to concurrent low temperatures and low wind power availability.

4.2 Introduction

The British Government is committed to reducing greenhouses gas emissions whilst maintaining a resilient and affordable energy supply. Britain has an ambitious target to achieve 15% of its energy consumption (electricity, heat and transport) from renewable sources by 2020 (EU, 2009). Policy measures have led to an increase in the percentage of energy consumption generated from renewables, from 3% in 2009 to 8% in 2015. Wind power accounted for approximately half of the renewable electricity generated in 2015 and it is therefore already playing an important role in the British energy system (DECC, 2016). Offshore wind capacity is expected to grow significantly over the next decades (DECC, 2013, 2016), in part to help meet the increase in electricity demand expected with the electrification of heating and transportation.

Operational managers ensure electricity supply and demand are balanced second by second. To achieve this, forecasts of demand and supply are made in the months, days and hours prior to real time. Peak demand is a primary concern, and the grid operator must ensure ahead of each winter that sufficient supply is available. This is of growing importance due to an increased security of supply risk in Britain in recent years, associated with closing of older coal and gas plants (Royal Academy of Engineering, 2013; Ofgem, 2015). The intermittent nature of wind power means that estimating its availability in advance is challenging. A better knowledge of the relationship between electricity demand and wind power supply is therefore advantageous, especially during peak demand. The availability of interconnection supply from neighbouring countries during peak British demand is also of growing interest, due to increasing interconnector capacity and the participation of interconnectors in the Capacity Market (a system developed to ensure security of supply, DECC 2016).

The influence of weather on the demand–supply balance is increasing, due to the high temperature sensitivity of demand (Bessec and Fouquau, 2008; Thornton et al., 2016) and increasing renewable generation. Consequently, interest in this issue is growing (Sinden, 2007; Oswald et al., 2008; Zachary et al., 2011; Brayshaw et al., 2011; Zachary and Dent, 2012; Ely et al., 2013; Harrison et al., 2015). A weak positive relationship is found between electricity demand and wind power supply across the year in Britain (Sinden, 2007), with the reverse found in winter (Zachary and Dent, 2012; Harrison et al., 2015). However during very high demand conditions, some studies suggest the risk of lower wind power supply (Oswald et al., 2008; Zachary and Dent, 2012; Harrison et al., 2015), whilst others suggest more moderate or higher supply (Sinden, 2007; Zachary et al., 2011; Brayshaw et al., 2012). They all emphasize the uncertainty in the relationship due to the short data lengths considered (often less than 10 years). Large scale weather patterns have been shown to influence electricity demand and renewable supply over Northern Europe, including the North Atlantic Oscillation (NAO, a measure of the large scale north–south atmospheric pressure difference), and high pressure systems (Brayshaw et al., 2011; Ely et al., 2013). The influence of high pressure on wind power supply and demand is however under debate (Oswald et al., 2008; Brayshaw et al., 2012; Leahy and Foley, 2012).

The aim of the paper is to quantify the winter relationship between daily electricity demand and wind power supply across Great Britain (GB) over an extended period (34 years). The role of weather patterns on this relationship is explored, with a particular focus on high demand conditions. The wider European context is then considered, by assessing temperature and wind power conditions across Europe during periods of high GB demand.

4.3 Data and methodology

4.3.1 Electricity demand data

An observed electricity demand dataset was provided by National Grid, the grid operator, for the period January 1975 to March 2013. This dataset gives the total electricity demand across GB for each day in giga watt hours (GWh). Annual electricity demand is shown to steadily increase from 1975 until 2006 and then reduce (Thornton et al., 2016). The magnitude of the annual cycle in demand is also found to reduce over the whole period. These long term changes in demand cannot be explained by temperature changes, rather are thought to be predominantly driven by socio-economic factors (Thornton et al., 2016).

To better quantify the relationship between weather driven electricity demand and wind power, these long term changes in demand are firstly removed. This is achieved by representing the evolution of the annual mean demand and annual cycle by a slowly evolving second order Fourier expansion. This slowly evolving background is then removed from the full demand time-series and is replaced by a repeating long term mean annual demand cycle (Thornton et al., 2016). This process effectively retains the demand variability on a daily, seasonal and interannual timescale, whilst removing variability on timescales greater than 5 years. Full details of the detrending methodology are given in Chapter 3, where the original and detrended electricity demand time-series are shown (Figures 3.1 and 3.11 respectively).

4.3.2 Wind power model

Wind power availability is modelled using reanalysis wind speeds and an idealised wind power model. In the latter, a uniform distribution of turbines across GB is assumed, including both onshore and coastal offshore regions (see Figure 4.1). Regions under consideration for siting of future offshore turbines have also been included, for example in the North Sea. The uniform distribution approach does not attempt to accurately represent current-day generation, but rather it aims to capture the general variation in available wind power across GB and through time. This approach has the additional benefit of giving information on possible future generation sites.

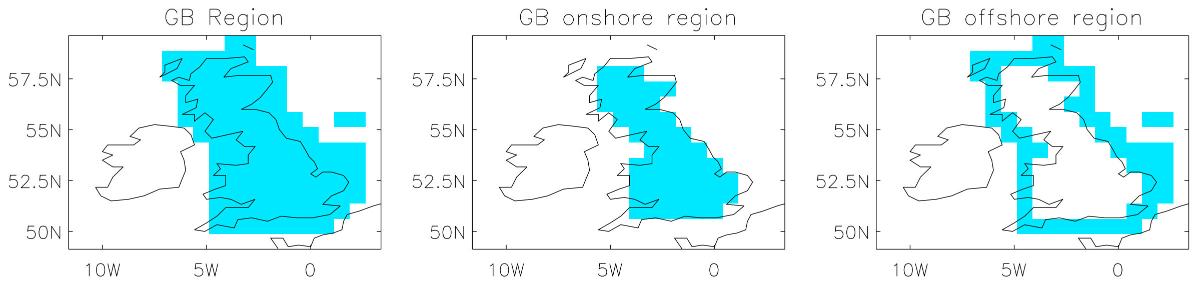

Figure 4.1: The regions over which the wind power availability is considered: the full GB region (left), the onshore region (middle) and the offshore region (right).

A daily wind power estimate is calculated using 6-hourly, 60m height wind speeds and air density, which are available from the ERA-Interim dataset. ERA-Interim is a gridded global reanalysis dataset, with a resolution of approximately 80km by 80km and is available from January 1979 to the present. A reanalysis dataset is created by rerunning a global weather model over a long period, whilst ingesting all available observations. It provides a multivariate, spatially complete and coherent record of atmospheric circulation (Dee et al., 2011).

The wind speed at each ERA-Interim grid-point is fed through a typical power curve, the Vestas V90 1.8-2MW turbine[1] is chosen with a cut in, cut out and rated wind speed (U_r) of $4m/s$, $25m/s$ and $12m/s$ respectively. A wind power capacity factor is then calculated as follows:

$$Capacity factor = \frac{\rho U^3}{\rho_c U_r^3}$$

where U represents the wind speed after it has been modified by the power curve characteristics, ρ is the air density and $\rho_c = 1.225kg/m^3$, a typical density. The capacity factor therefore takes both wind speed and air density changes into account.

The wind power capacity factor is calculated at each grid point, every 6-hours and then averaged to give a daily mean, for all days between 1979 and 2013. In addition a regional mean capacity factor is calculated for each day, from the daily mean values. By presenting the wind power as a capacity factor, the importance of the choice of turbine is limited. The resultant wind power capacity factors should however be considered as indicative, rather than numerically exact, given the idealised wind power model used. Even with these simplifications, the modelled GB average capacity factor in winter ($\sim$0.5) is found to compare favourably with a study where the wind farm distribution and capacity are more realistically represented (Harrison et al., 2015). Given the idealised wind power model used, we consider the electricity demand and wind power separately, rather than combining to give a proportion of demand met by wind power.

4.4 Electricity demand, wind power relationship

The electricity demand – wind power relationship is calculated over the period for which both datasets are available (January 1979 to March 2013). The relationship is only calculated over week days (Monday – Friday) during non–holiday periods. Weekends, bank–holidays and 3 days either side of bank holidays are excluded from the analysis due to the different demand profiles seen over these non-working days (Thornton et al., 2016). The data considered therefore represents 62% of the full data set and consists of 7804 days.

To put the winter relationship between electricity demand and wind power in context, we start by showing the relationship across the year and in each season. A

[1] `http://www.vestas.com/en/products_and_services/turbines`

clear seasonal cycle in demand is seen, with lowest demand in summer and highest demand in winter (Figure 4.2, upper left). A wide range of wind power conditions exist for a given electricity demand, and the range is smallest in summer and largest in winter.

During the lower three-quarters of demand days, there is the seemingly helpful relationship that as demand increases so does average wind power, as found by Sinden (2007) (black line Figure 4.2, upper–middle). This reflects the variation in temperatures and wind speeds with season, with calmer, warmer conditions in summer and cooler, windier conditions in late autumn and early spring. However above the 75$^{\text{th}}$ percentile of demand, average wind power reduces, which occurs predominantly in winter and autumn. Understanding this downturn in wind power provides the motivation for this paper. Given our interest in high demand days, which predominantly occur in winter (Figure 4.2, upper right), only winter days are considered.

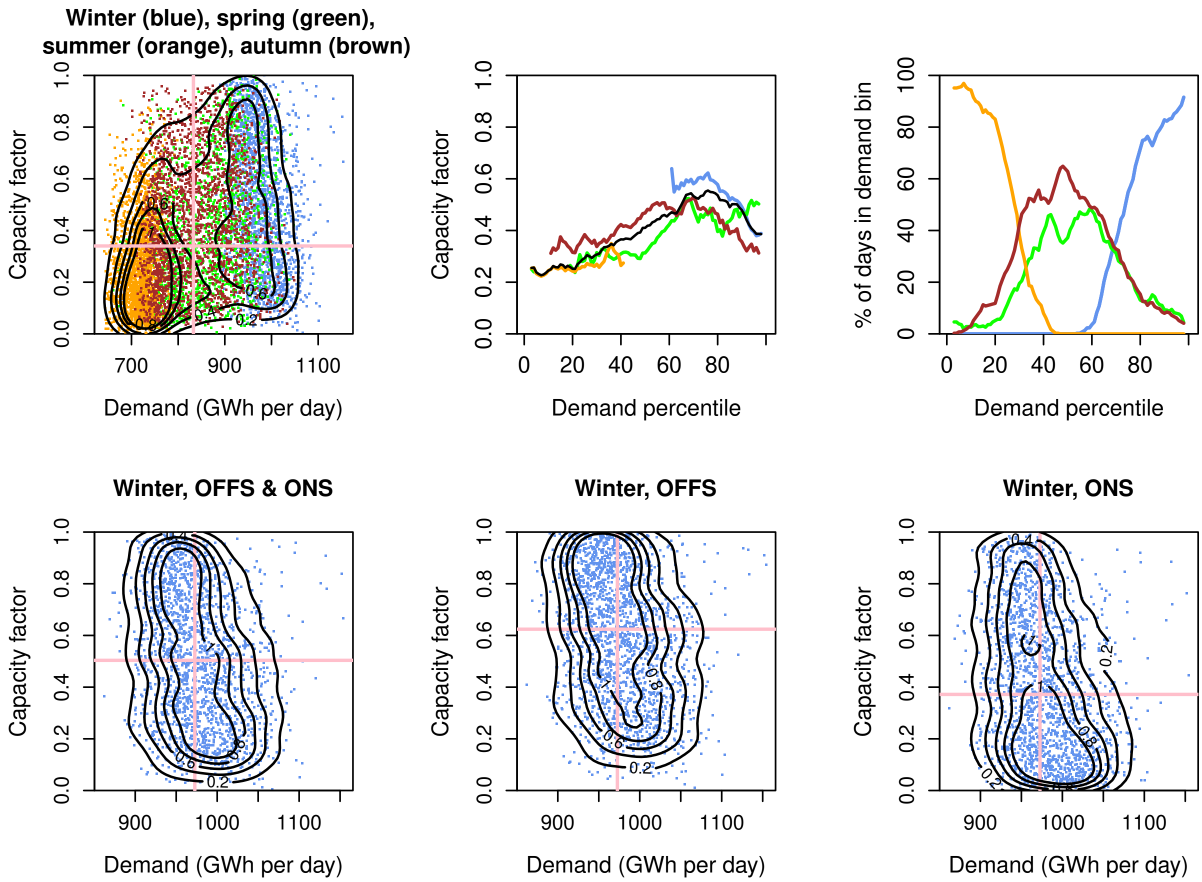

Figure 4.2: Upper left: Scatter plot of daily GB electricity demand and GB mean wind power capacity factor in winter (blue), spring (green), summer (orange) and autumn (brown). Density contour interval is 0.02%. Pink lines show the median demand and capacity factor across all days. Upper middle: Variation in GB average wind power capacity factor with percentile of electricity demand, averaged over a 5% demand bin, for each season (colours) and all days in year (black). A minimum of 18 values (1% of that seasons' days) are required to make a mean capacity factor. Upper right: For a given level of demand, the percentage of days in each season. Lower: Scatter plot of winter daily electricity demand and wind power when averaged across GB (left), offshore region (middle) and onshore region (right).

4.5 Winter relationship

The tendency for lower wind power during higher winter demand is shown by the tilt of the density contours of the daily distribution (Figure 4.2, lower left). It is also clearly seen when averaged across days of similar demand (Figure 4.3, left). Average wind power reduces by a third between lower and higher winter demand, from approximately 60% to 40% of rated power. Around the 85^{th} percentile of winter demand, average wind power is at a minimum, however above this, wind power begins to increase again. Although this upturn appears small, in percentage terms it is larger than the respective increase in demand (Figure 4.3, right). On average, therefore, wind power can satisfy a larger proportion of the highest demand than it can at the 85^{th} percentile of demand. For comparison with previous studies, the relationship between wind power and demand is also shown with respect to the average cold spell demand (see section 4.5.2).

The same relationship is seen when wind power is averaged across both onshore and offshore regions separately and across different regions of GB (North-west, North-east, South-west and South-east), see Figures 4.4 and 4.5. The demand–wind power relationship is therefore largely insensitive to the spatial distribution of turbines across GB. Across all demand conditions, average offshore wind has a capacity factor 15–25 percentage points higher than onshore wind, because of higher wind speeds offshore (Drew et al., 2015) (Figure 4.4). Although the reduction in capacity factor with increasing demand is similar for onshore and offshore regions (reducing by $\sim$0.2), the percentage decline is smaller offshore than onshore, due to the greater magnitude of offshore wind power. For example, onshore wind power nearly halves whilst offshore wind power reduces by less than a third. In addition to wind power being lower onshore, during higher demand conditions, it is more frequently lower (Figure 4.2, lower row).

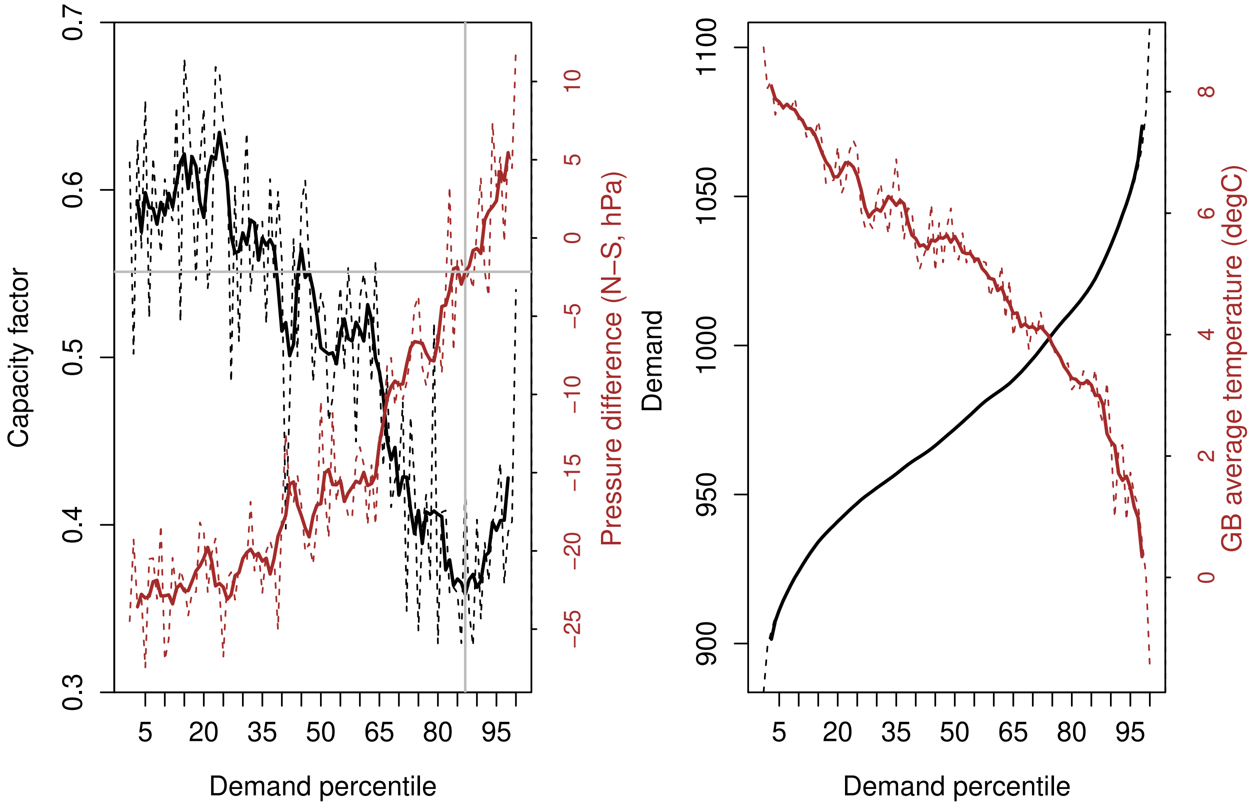

Figure 4.3: Left: Variation in GB average wind power capacity factor (black) and meridional pressure difference between two regions north and south of GB (hPa, red) with winter percentile of GB electricity demand, averaging over 1% bins (dashed) and 5% bins (solid). The pressure difference during the minimum wind power is highlighted by the grey lines. This pressure difference is used as a proxy to represent the larger scale pressure field over the North Atlantic (see section 4.5.3 for details). Right: Variation in electricity demand (GWh, black) and GB average temperature (°C, red) with percentile of winter electricity demand.

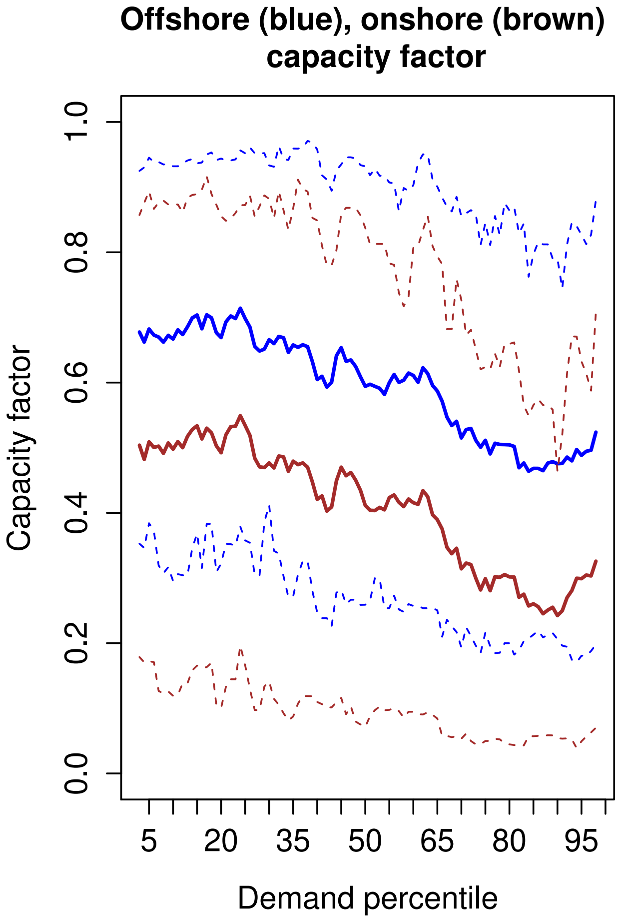

Figure 4.4: Variation in average GB onshore (brown) and offshore (blue) wind power capacity factor with winter percentile of GB electricity demand. Capacity factors are presented as rolling 5% demand bin means. The 10^{th} and 90^{th} percentile capacity factors for each demand bin and each region are given (dashed).

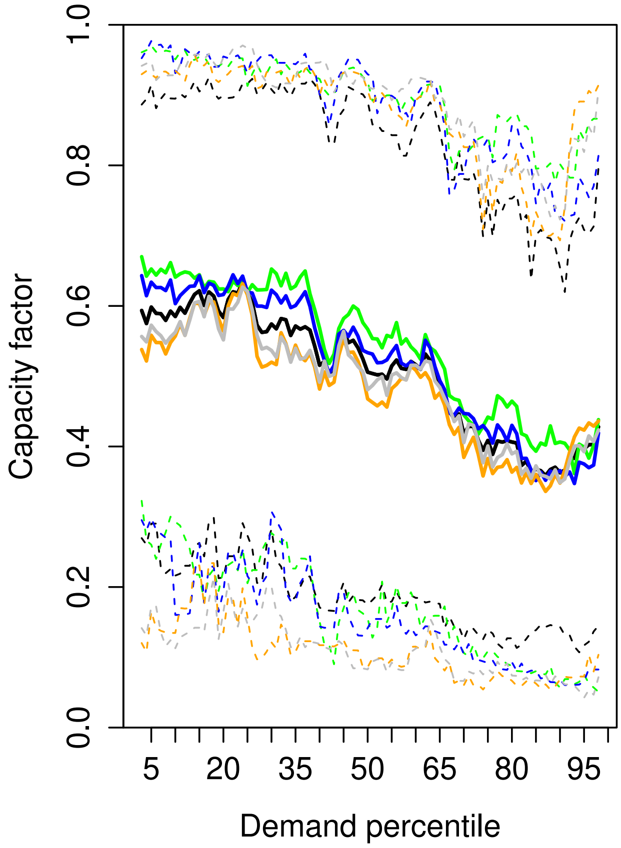

Figure 4.5: Variation in wind power capacity factor with winter percentile of GB electricity demand, when averaged over both onshore and offshore regions of GB (black) and individual regions: North-west (green), North-east (blue), South-west (orange), South-east (grey). Capacity factors are presented as rolling 5% demand bin means. The 10^{th} and 90^{th} percentile capacity factors for each demand bin and each region are given (dashed).

4.5.1 Observational comparison

Reanalysis datasets are often used in place of observations due to their consistent, gridded representation of weather and climate. However the reanalysis fields can be biased with respect to the raw observations. To test the validity of the ERA-Interim generated wind power capacity factors, equivalent factors have been established using observed wind speeds. The HadISD dataset (Dunn et al., 2012) gives quality controlled sub-daily, 10m wind speed measurements at various locations across GB (Figure 4.6). To compare the wind power generated using either observed or reanalysis wind speeds, ERA-Interim equivalents of the observations are made. Wind power is calculated using 10m ERA-Interim wind speeds, at the nearest ERA-Interim land grid point to each wind speed observation. A minimum of four wind power values are required to make a daily mean at any location and then a minimum of 4 values per region to make a regional daily mean. The relationship between wind power and demand is similar when using either ERA-Interim or observed wind speeds (Figure 4.6). ERA-Interim wind speeds can therefore be considered sufficiently representative to assess the countrywide demand – wind power relationship.

4.5.2 Wind power – demand relationship, using average cold spell demand

Previous studies investigating the demand – wind power relationship, present demand as a percentage of the average cold spell (ACS) demand (Zachary et al., 2011; Brayshaw et al., 2011; Zachary and Dent, 2012; Harrison et al., 2015). ACS demand is defined as the peak demand within a year which has a 50% chance of being exceeded as a result of weather variation alone (National Grid, 2012b). Peak demand in this context is defined as the maximum daily demand during a financial year.

The reduction in wind power with increasing electricity demand (seen in Figure 4.3) is also seen when using this alternative representation (Figure 4.7, left), in agreement with previous studies (Zachary and Dent, 2012; Harrison et al., 2015). The upturn in wind power during high and extreme electricity demand is however much stronger using this ACS representation, with wind power capacity factors above 0.6 when demand is greater than 105% of ACS demand. This upper tail reflects the strong easterly winds associated with cluster 1.

Although this form of the relationship gives the average wind power during the very highest demand conditions, it is based on very few extreme demand days (see red line). This representation does not require the same number of observations

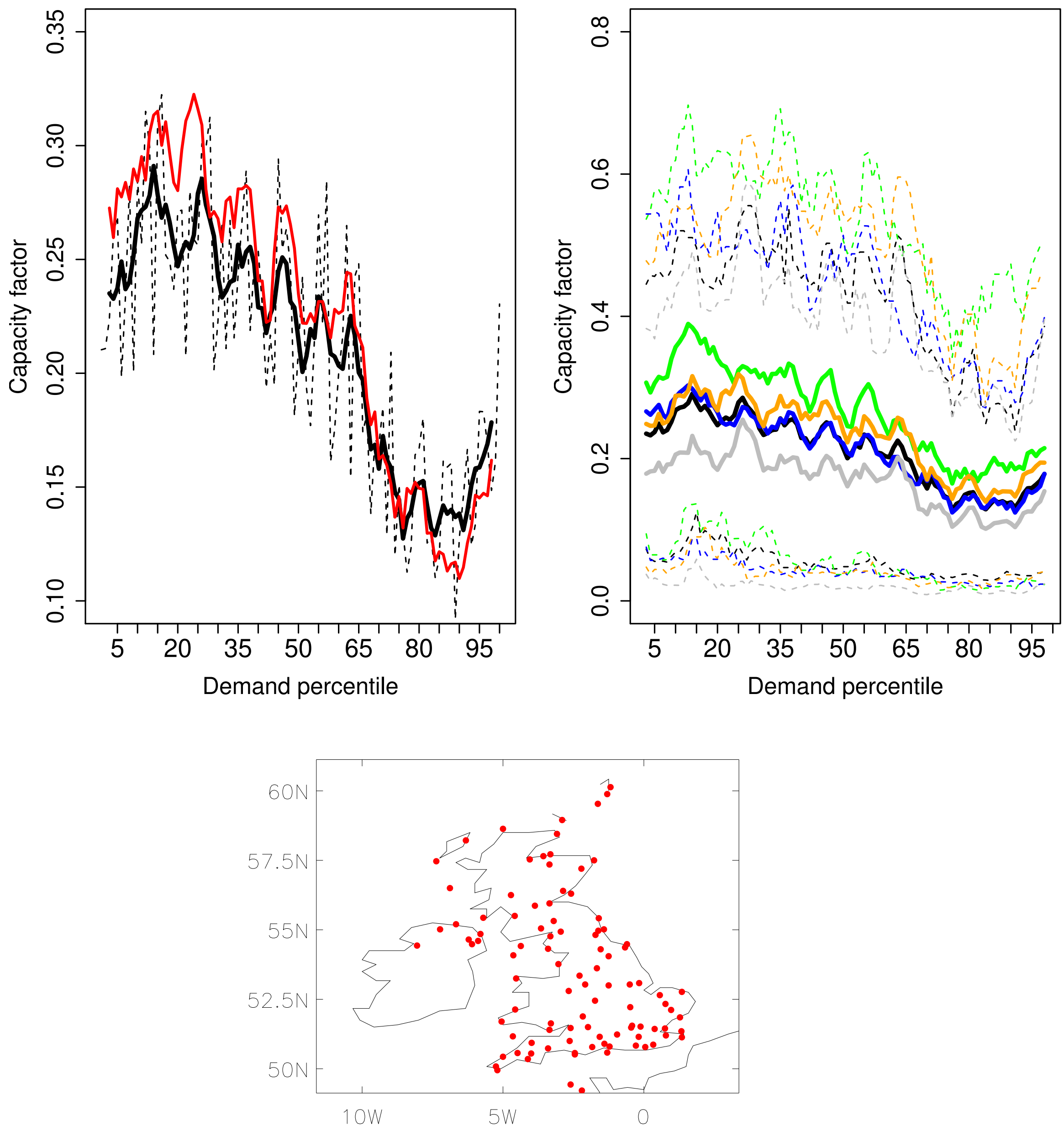

Figure 4.6: **Top left**: Variation in GB average wind power capacity factor with winter percentile of the GB daily electricity demand, based on HadISD 10m observed wind speeds (black) and ERA-Interim 10m wind speeds nearest to the observation locations (red), when averaged over 1% (dashed) and 5% (solid) demand bins. Wind capacity factors have been calculated with constant density ($1.225 km/m^3$) and assuming the same power curve characteristics as for 60m winds. **Top right**: Observed (HadISD) 10m wind power capacity factor when averaged over GB (black, solid), and regional means: North-west (green), North-east (blue), South-west (orange), South-east (grey). The 10^{th} and 90^{th} percentile capacity factors for each demand bin and each region are given (dashed). Capacity factors are presented as rolling 5% demand bin means. **Bottom**: location of HadISD observations.

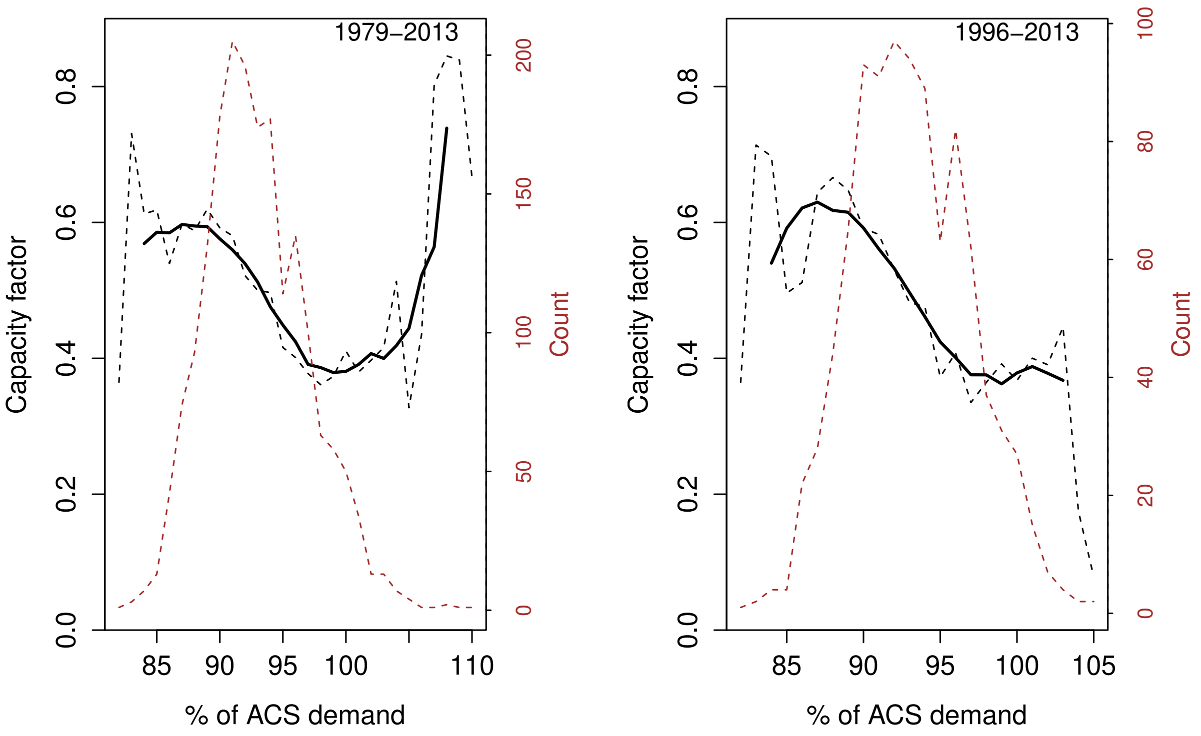

Figure 4.7: Variation in GB average wind power capacity factor (black) and bin count (red) with percentile of average cold spell electricity demand, averaging over 1% bins (dashed) and 5% bins (solid). Left: full period (1979 – 2013), right: second half of period (1996 – 2013).

per bin unlike when using percentiles of demand, consequently the number of observations greatly reduces as the event becomes more rare. The uncertainty in the average wind power availability during peak demand is highlighted by looking at the relationship over a shorter period. If only the most recent half of the data period is considered (1996–2013), the upturn is barely seen and very low wind power occurs at the highest demand, as seen previously (Zachary and Dent, 2012; Harrison et al., 2015). In this more recent period, peak demand is more frequently driven by the Greenland high weather type, explaining the lower average wind power availability seen. An assessment of the frequency of the high demand weather types using longer historical sea level pressure records would allow a better representation of this upper tail when using the ACS representation.

4.5.3 The role of weather patterns

In the extra-tropics, large scale weather patterns in the lower atmosphere play a dominant role in shaping the weather experienced at the surface. The important weather features, such as low and high pressure systems, can be identified from a surface pressure field adjusted for the height of any topography. This is referred to as mean sea level pressure (MSLP). We therefore compare the average MSLP field during different demand conditions. Two demand categories are defined: low and high demand, representing the lower and upper 5% of winter demand days respectively, each containing 90 days. On average, a low or high demand day would be expected to occur two to three times per winter (only considering work days).

During low demand in winter, high pressure is centred over France and Spain, with low pressure centred over Iceland on average (Figure 4.8). This stronger than average pressure difference across the North Atlantic, resembles the positive phase of the NAO. Associated with this pattern are generally stronger westerly winds (winds from west to east) and higher temperatures (Hurrell, 1995). The air temperature across GB is over 3°C higher than normal and wind power is often >20% above normal, with capacity factors ∼0.5 onshore, and >0.7 in many offshore regions.

In contrast, during high electricity demand, high pressure extends from Russia and Scandinavia across GB on average, with anomalously high pressure in northern Europe and anomalously low pressure in southern Europe (Figure 4.8). These negative NAO type conditions typically produce colder, calmer conditions in northern Europe (Hurrell, 1995). Cold easterly winds (winds from east to west) cause GB temperatures to fall below freezing and wind power is lower than average across all of GB (onshore capacity factors are typically <0.4, whilst offshore >0.5). Greatest reductions in wind power are seen over Scotland (>30% lower than average). The third column in Figure 4.8 will be discussed in section 4.8.

The reduction in wind power with increasing demand in winter can therefore be explained by variations in the atmospheric pressure pattern over north-western Europe. A proxy for this field is the north-south (meridional) pressure difference over GB (red line, Figure 4.3 left). This is calculated by averaging the mean sea level pressure over the two regions shown in Figure 4.8, upper left (northern region : 27°W–21°E, 57°N–70°N, southern region: same longitudes, 38°N–51°N) and then subtracting the southern pressure from the northern pressure. A positive difference implies generally easterly winds, and a negative difference westerly winds. The greater the magnitude of the pressure difference, the stronger the resultant winds. The reduction in wind power with increasing winter demand seen in Figure 4.3 is consequently associated with a weakening of both the meridional pressure difference and the westerly winds. Minimum average wind power occurs when there is little pressure difference (grey lines, Figure 4.3), associated with high pressure sat directly

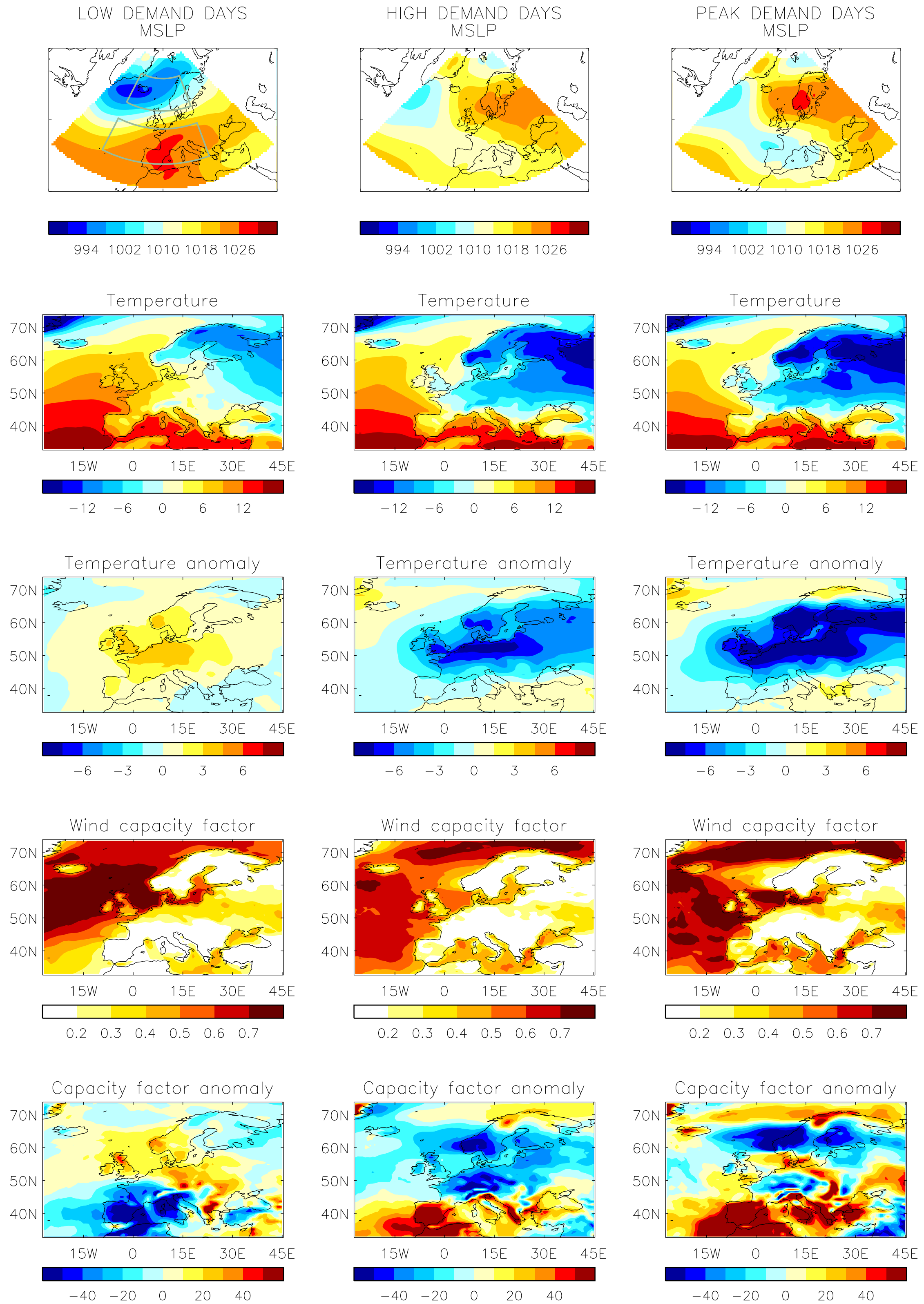

Figure 4.8: Mean of MSLP, (mb, top), 2m temperature (°C, 2nd row), temperature anomaly (°C, 3rd row), wind power capacity factor (%, fourth row) and wind power capacity factor anomaly (% difference from climatology, bottom) during low (left column), high (middle column) and peak (right column) GB electricity demand, 01/01/1979 – 31/03/2013. Anomalies are relative to the winter climatology. Gray boxes in upper left panel show the regions over which the pressure is averaged prior to calculating the pressure difference.

over GB (Brayshaw et al., 2012). The upturn in wind power during higher demand is associated with a reversed and strengthening meridional pressure difference, and strengthening easterly winds.

Average air density over GB increases as demand in winter increases, due to a reduction in temperature and an increase in pressure. However the impact of density changes on the wind power – demand relationship is minimal. Using constant density would only over-estimate the reduction in wind power between higher and lower demand in winter by approximately 3%.

4.6 High electricity demand

To better understand the spatial and temporal variation of wind power during high demand days, we determine the dominant weather patterns during high demand and their respective wind power availability. K-means clustering (Wilks, 2006) is applied to the mean sea level pressure fields of all high demand days. Four clusters are found to adequately represent the daily variability in the pressure field and are shown in the left-hand column of Figure 4.9. These clusters highlight the typical pressure patterns seen during a high demand day.

4.6.1 Clustering methodology

K-means clustering is a non-hierarchical clustering technique that requires the number of clusters to be specified in advance. The minimum number of clusters found to minimise the pattern correlation ratio (Huth, 1996) was four, when averaged over 100 repetitions (Figure 4.10). The k-means clustering algorithm systemically assigns each daily MSLP field to the cluster most similar to itself, by choosing the cluster which minimises the absolute difference between the sample and the cluster centroid (the average of the fields within that cluster). An area weighting (cosine of latitude) is applied to this difference to account for the bunching of grid points towards the polar regions. The cluster centroids are updated after every reassignment, progressively moving the centroids away from their original random number fields. The assignment of each day is repeated a number of times to minimize the variability within each cluster and maximize the variability between clusters.

The whole clustering process is repeated 100 times, allowing the most robust cluster set to be established. Across the cluster bootstrap, the cluster origins change and the ordering of the high demand days is also jumbled to ensure the cluster set is not dominated by the order of the first few high demand days. To determine

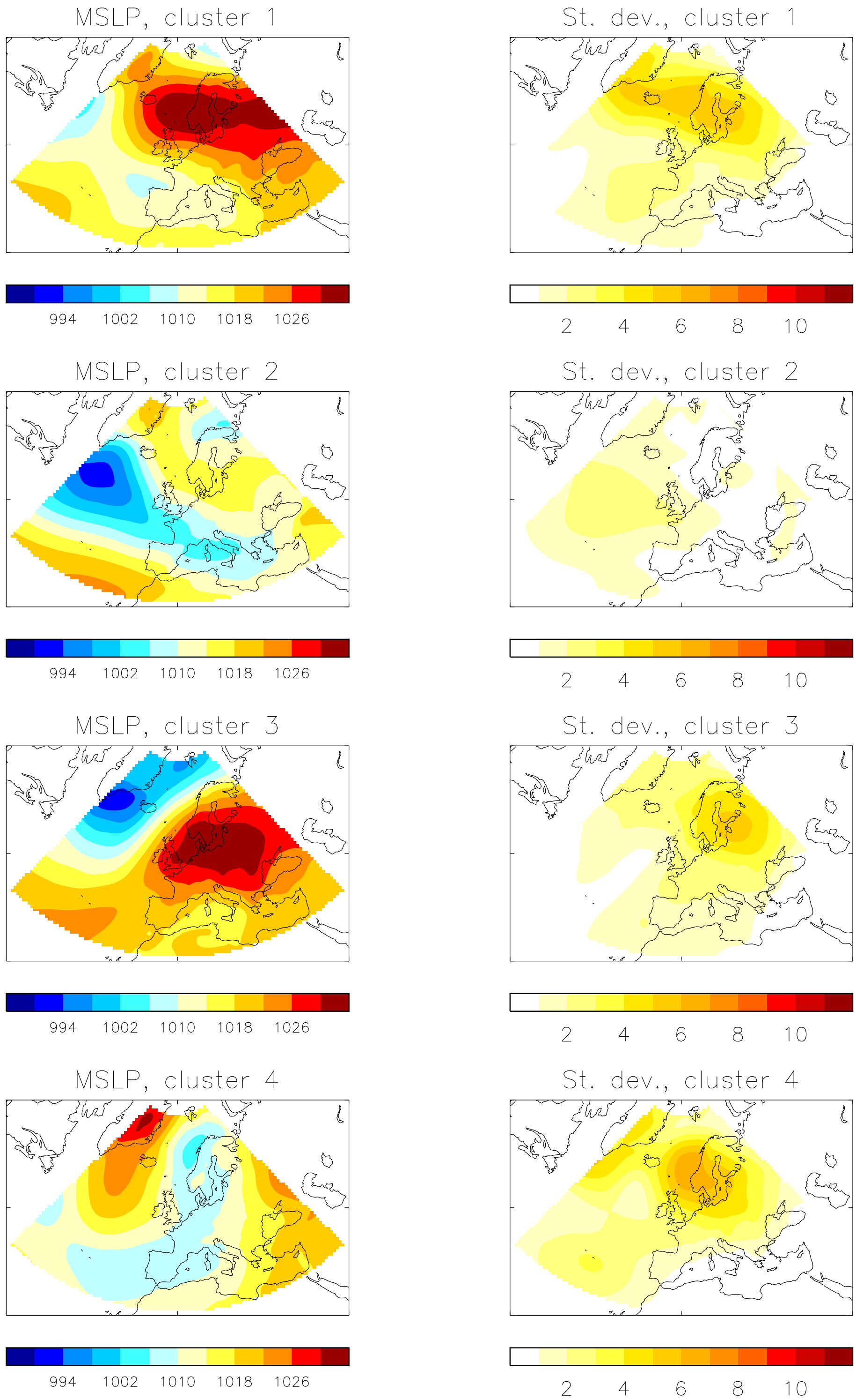

Figure 4.9: The cluster centroids over high demand days (MSLP, hPa, left column) and the standard deviation of each cluster across the bootstrap (hPa, right column).

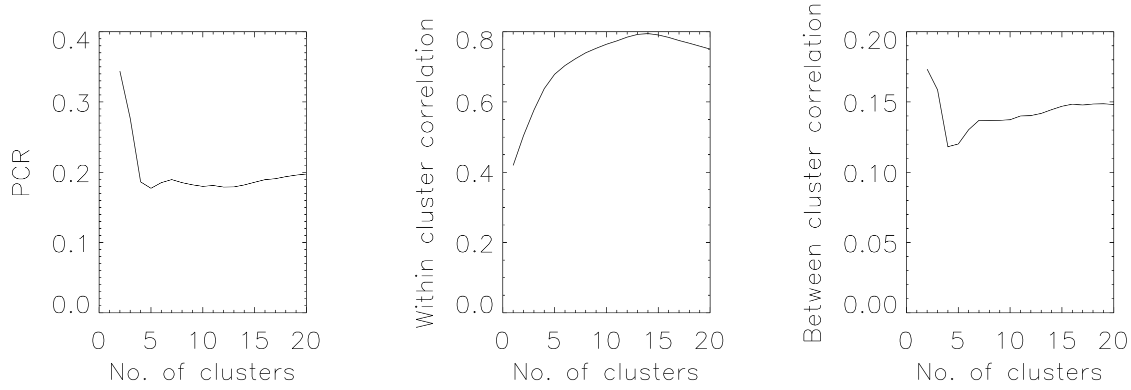

Figure 4.10: The variation in the pattern correlation ratio (PCR, left), the within cluster correlation (middle) and the between cluster correlation (right) with number of clusters chosen. The PCR is the between cluster correlation divided by the within cluster correlation.

the most representative cluster set across the bootstrap, the following two step procedure is undertaken. Firstly the clusters within each cluster set are ordered to best match the order of the first set. This is done by choosing the cluster order that maximises the sum of the cluster by cluster pattern correlation. Secondly, the average pattern correlation between one set and another is calculated, by taking the average correlation of the ordered cluster pairs. The set with the highest average pattern correlation with all other sets is chosen as the most representative. The cluster centroids are robust, as the variability in pressure across the bootstrap is small compared to the strength of the pattern (see right hand column of Figure 4.9).

4.6.2 High demand weather types

The four high demand weather patterns show that high pressure in the region plays an important role in generating high electricity demand in GB, in agreement with Brayshaw et al. (2012). Each cluster has a similar occurrence frequency (ranging from 19% – 32% of high demand days, see Figure 4.11). High pressure is found over Scandinavia/Scotland (clusters 1 and 2), over central and northern Europe (cluster 3) and over Greenland and the North Atlantic (cluster 4), causing the advection of cold air over GB by easterly, south-easterly or northerly winds respectively.

During each high demand weather type, anomalously low temperatures are

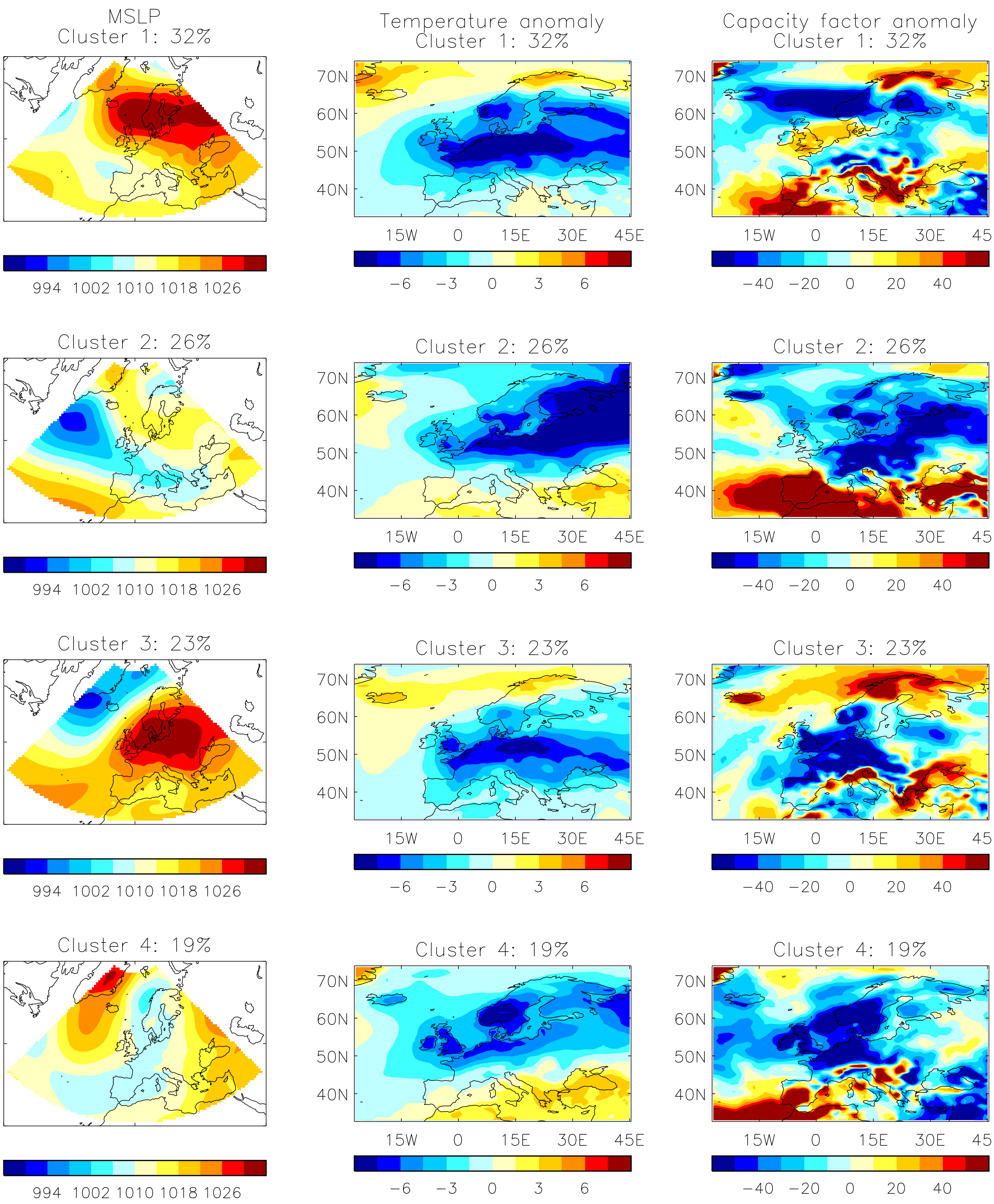

Figure 4.11: The cluster centroids over high demand days (MSLP, hPa, left column). The average 2m temperature anomaly (°C, middle column) and wind power capacity factor anomaly (% difference from climatology, right column) when averaged across all days in each cluster. Anomalies are relative to the winter climatology from 01/01/1979 – 31/03/2013. This cluster set is the set most representative of the bootstrap, see section 4.6.1 for details.

found across GB, with daily average temperatures often below freezing (Figure 4.11, and Figure 4.12). This is expected, given the strong anti–correlation between electricity demand and temperature in winter (Thornton et al., 2016). However, spatial wind power availability differs across the weather types. For example, the strong north-south pressure difference over GB in cluster 1, gives wind power 20% higher than normal over most of England and Wales (capacity factor >0.4 onshore and >0.7 offshore). In contrast, a high pressure over Greenland and weak pressure over GB (cluster 4), gives wind power at least 40% below normal (capacity factors of <0.3 on land and <0.5 offshore).

GB average wind power can vary across days with the same weather type (Figure 4.13, left), reflecting the daily variation in both the pattern and its magnitude. Even with this variation it is clear that high demand days with wind power above the winter average are predominantly generated by the Scandinavian high and Atlantic low pressure patterns (clusters 1 and 2 respectively, see dots above the red line). In contrast, the central European and Greenland high pressure patterns predominantly give daily capacity factors below the winter average (clusters 3 and 4 respectively).

In Chapter 5, to explore seasonal prediction skill, a method is developed to identify whether a given day can be classified as a high demand day based on the similarity of its pressure field to one of the identified high demand weather types. The Spearman rank correlation between the number of high demand days per winter and the number of identified high demand weather type days per winter is 0.57. This highlights that it is possible to have a day with a similar large-scale pressure field to one of the high demand weather types, but without high demand actually occurring and vice versa. This reflects the fact that the weather patterns describe the large-scale pressure pattern across North-western Europe, rather than the localised flow direction over GB which is critical for determining demand. However, even with this caveat, the number of high demand weather type days per winter is found to be a skilful predictor of winter demand (see Chapter 5).

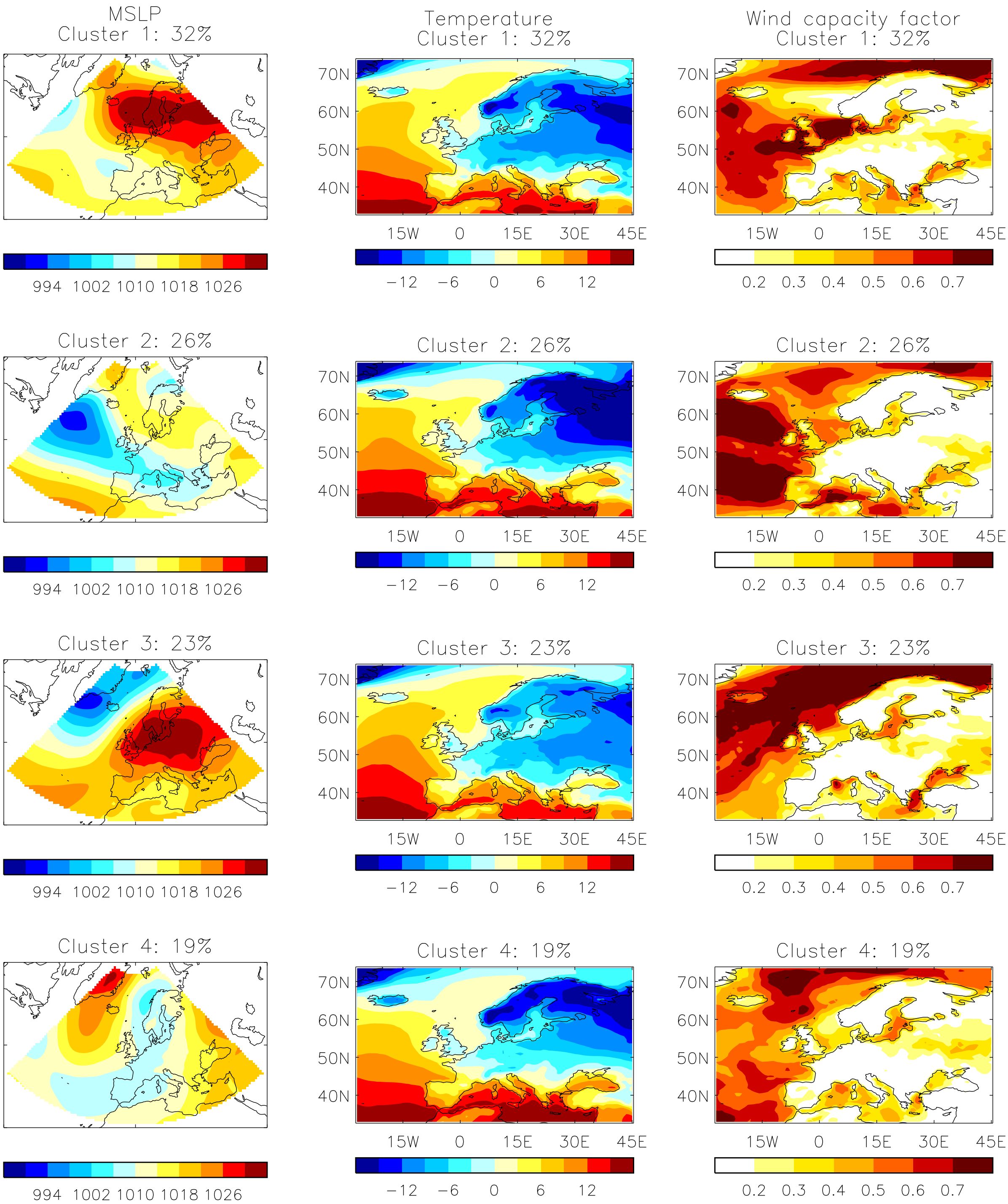

Figure 4.12: The cluster centroids over high demand days (MSLP, hPa, left column). The average 2m temperature (°C, middle) and wind power capacity factor (%, right) when averaged across all days in each cluster. The cluster set is the set most representative of the bootstrap, see section 4.6.1 for details.

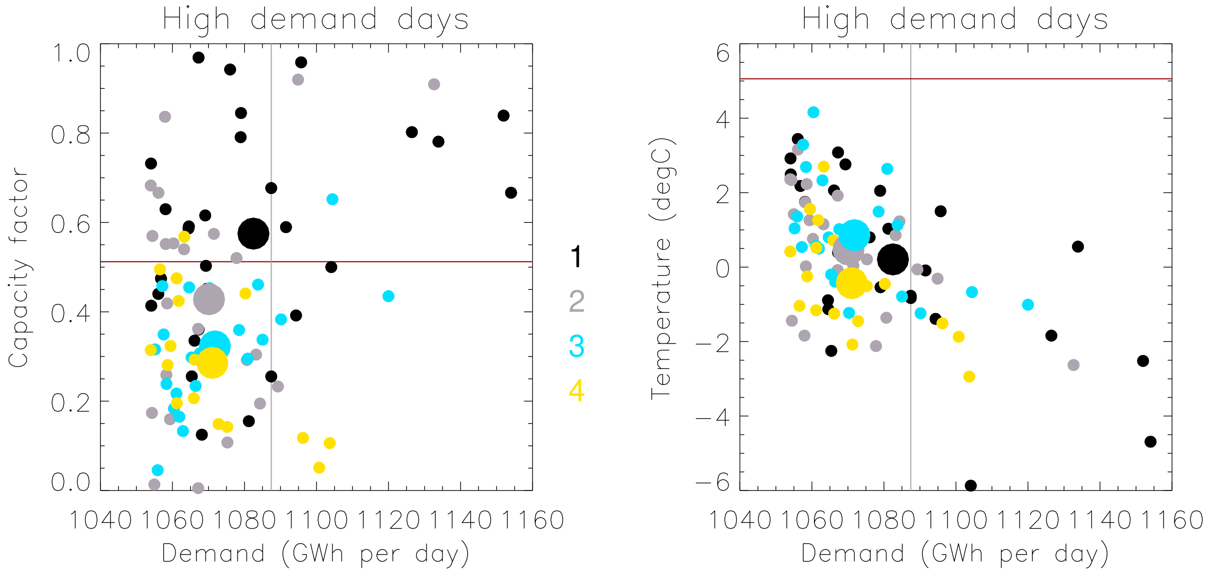

Figure 4.13: Daily electricity demand and GB mean wind power capacity factor (left) and mean 2m temperature (right) during high demand days. Each day is coloured by its MSLP cluster number (see figure 4.11). The mean properties for each cluster are indicated by a large circle. The vertical grey line defines the lower boundary of the peak demand days and the horizontal red lines mark the winter average wind power capacity factor (left) and temperature (right).

4.7 The wider European picture

The weather patterns that bring low temperatures and high demand to GB, also cause anomalously low temperatures across many parts of Europe, both on average, and during individual types (Figures 4.8 and 4.11 respectively). This is particularly true for the northern half of Europe where temperatures can be 6°C below the winter average. Given the strong relationship between electricity demand and temperature in many European countries (Bessec and Fouquau, 2008), high energy demand is therefore likely in neighbouring countries during high GB demand.

The majority of Europe also experiences below average wind power during high GB demand on average (Figure 4.8, middle column, bottom row). Many countries have onshore wind power capacity factors <0.2, 20% or more lower than normal. Spain and Portugal are the exception, with much higher wind power than normal (>40% higher), although capacity factors are still only ∼0.2 onshore and ∼0.4 offshore. The anti-correlation between the wind field of GB and Iberia (Monforti et al., 2016) reflects the shift in the location of the storm track between the two phases of the NAO (Hurrell and Deser, 2009).

Considering individual weather types, during windy, high demand days in GB, the North Sea, northern Germany and Denmark also have above average wind power, as these regions also sit between the two pressure centres (cluster 1, Figure 4.11). However when GB has below average wind power (clusters 2–4), the majority of mainland Europe also has below average wind power (capacity factors <0.2). The main exception is the Iberian Peninsula during cluster 2, where capacity factors >0.3 (Figure 4.12).

4.8 Peak electricity demand

Peak demand days are of great interest to the energy industry. By their nature they are rare. Here we define peak demand as the top 1% of winter GB demand days, representing 18 days over the 34 year period. With this definition, a peak demand day would be expected to occur on average once every other winter (only considering work days). It is recognised that the sample size is small, but it is worthy of consideration for analysis because of the importance of days with the very highest demand.

The average MSLP pattern associated with peak electricity demand in GB is similar to that during high demand, but more intense (Figure 4.8, right column). The reversed pressure difference is stronger (Figure 4.3), resulting from higher pressure over Scandinavia and deeper pressure over south-western Europe. Strengthened easterly winds give rise to temperatures below -3°C across GB and near average wind power.

The full range of high demand weather types are also seen during peak demand (Figure 4.13), giving a wide range of average GB wind power, from very low (cluster 4, capacity factor of $\sim$0.1) to very high (cluster 1, capacity factor of $\sim$0.8). In this limited sample, half of the peak demand days have wind power above the winter average. The spike in wind power during peak demand seen in Figure 4.3, is therefore explained by the higher percentage of cluster 1 type days. Interestingly, over this period the very highest demand appears to occur when temperatures are very low and wind power is very high, associated with strong easterly winds (cluster 1, Figure 4.13). This suggests that either the higher wind speed directly increases demand, or the higher wind speeds are needed to bring larger quantities of cold air over GB, causing the very low temperatures and consequent very high demand. The former would support the use of a wind chill factor in peak electricity demand estimation, as used by National Grid (Taylor and Buizza, 2003).

Of particular concern is low wind power availability during peak demand. Cluster 4 is therefore of interest as the Arctic air flow can generate very low temperatures and very low wind power. During the 18 peak demand events investigated here, only 3 days have this weather type, all of which occurred during December 2010 (3 yellow points, Fig 4.13). During these days, wind power availability was very low both onshore and offshore (capacity factors <0.2). The relatively small number of years considered here limits our estimation of the likelihood of such peak demand events. An improved estimation could be made by assessing the likelihood of such weather types in a longer historical record or using large ensembles of model simulations.

4.9 Discussion

The availability of wind power during different electricity demand conditions in Britain is analysed between 1979 and 2013. We use daily observations of total GB demand and estimate wind power availability using reanalysis wind speeds and an idealised wind power model.

For the majority of the year, as demand increases, average available wind power also increases. However in winter, average wind power reduces by a third between lower and higher demand. This winter relationship is shown to be driven by the large scale weather patterns affecting Northern Europe. The change from predominantly strong, warm, westerly winds, to colder, calmer, easterly winds explains the reduction in wind power supply as demand increases. However, contrary to what is often believed, during high demand we find a modest recovery in average wind power, which is associated with a reversed north-south pressure gradient and the building of high pressure to the north of GB.

These average relationships hide considerable daily variability, where for a given demand, a wide range of wind power availability is possible. We find that during high and peak demand, a range of high pressure weather types generate similarly cold conditions over GB, but varying wind power supply. Approximately one-third of high demand days have wind power above the winter average, and two-thirds below. However, in our limited sample of peak demand days, although days do exist with very little onshore and offshore wind power, half of days have above average wind power, due to more days with strong easterly winds.

The characterisation of the relationship between electricity demand and wind power supply in Britain, should help both in the short term management of the energy system and in longer term planning. Wind power and demand are currently estimated using short term weather forecasts and demand and supply models. Uncertainty in the forecast of the proportion of demand met by wind power relates to both the accuracy of the weather forecast and the validity of the demand and generation models. Our analysis helps to explain the varying contribution of wind power and should help operational managers better interpret forecast information. For example, the range in possible wind power availability for a given demand can be reduced if the weather type is known.

Here we show that wind power can contribute to the supply mix during high and peak demand. The relationship is complex such that certain weather types provide good wind power, whilst others limit availability. The spatial distribution of wind power availability varies across these weather types, indicating that a spread of wind turbines across GB would maximise the average availability of wind power during high demand. In addition, the percentage reduction in wind power supply with increasing demand is lower offshore than onshore, suggesting offshore wind power is better placed to aid security of supply. This analysis highlights the risk of wide-scale high electricity demand and low wind power days across many parts of Europe, associated with large scale high pressure systems. Neighbouring countries may therefore struggle to provide additional capacity to GB when its demand is high and its wind power low.

Having identified the weather types important for the security of electricity supply in GB, such a classification will allow an assessment of their predictability on a range of timescales and also of possible changes in a changing climate.

Chapter 5

Skilful seasonal prediction of winter gas demand

5.1 Abstract

In Britain, residential properties are predominantly heated using gas central heating systems. Ensuring a reliable supply of gas is therefore vital in protecting vulnerable sections of society from the adverse effects of cold weather. Ahead of the winter, the grid operator makes a prediction of gas demand to better anticipate possible conditions. Seasonal weather forecasts are not currently used to inform this demand prediction. Here we assess whether seasonal weather forecasts can skilfully predict the weather-driven component of both winter mean gas demand and the number of extreme gas demand days over the winter period. We find that both the mean and the number of extreme days are predicted with some skill from early November using seasonal forecasts of the large-scale atmospheric circulation ($r > 0.5$). Although temperature is most strongly correlated with gas demand, the more skilful prediction of the atmospheric circulation means it is a better predictor of demand. If seasonal weather forecasts are incorporated into pre-winter gas demand planning, they could help improve the security of gas supplies and reduce the impacts associated with extreme demand events.

5.2 Introduction

Gas demand in Britain is dominated by demand for residential and commercial heating (National Grid, 2017). Consequently gas demand is highly anti-correlated with temperature (Pearson correlation, $r = -0.90$, Thornton et al. 2016), with demand increasing as temperatures fall. Ensuring a reliable supply of gas is therefore critical to protect more vulnerable sectors of society from cold-related illnesses. The energy supply system is under most pressure during winter, when cold snaps drive peak demand (Thornton et al. 2016, 2017), competition for gas supplies and high energy prices, as for example occurred in early March 2018 (National Grid, 2018). To ensure security of supply the energy system operator assesses the energy situation ahead of the winter. They predict total winter demand, possible extreme gas demand conditions, necessary storage requirements and likely available supplies (National Grid, 2017). Current predictions of winter demand do not consider any seasonal weather forecast information. Instead, average winter conditions are assumed and then risks associated with historical weather related peak demand events are assessed (National Grid, 2017). Seasonal forecast information, if skilful, offers the potential to improve the estimates of winter gas demand and improve security of supply.

Seasonal forecasting of winter climate in North-western Europe and the Atlantic has improved over the last decade (Scaife et al., 2014b; Athanasiadis et al., 2017). The North Atlantic Oscillation (NAO) is the dominant mode of winter variability in this region and its phase dictates the general characteristics of the winter period, including average temperature, wind speed and storminess over much of the European continent (Hurrell, 1995). Skilful forecasts of the winter NAO are now possible (Scaife et al., 2014b; Athanasiadis et al., 2014; Dunstone et al., 2016) and this has been shown to be useful for predicting impacts on society, such as sea ice cover (Karpechko et al., 2015), transport delays (Palin et al., 2016) and river flows (Svensson et al., 2015).

The use of seasonal forecast information by the energy industry is in its infancy with only a few studies demonstrating their potential benefits (De Felice et al. 2015; Clark et al. 2017; Torralba et al. 2017; Bett et al. 2017; Troccoli et al. 2018), and to date none have addressed gas demand forecasting. Clark et al. (2017) have shown that skilful forecasts of winter mean wind power density and electricity demand in the UK are possible using forecasts of wind speed and the NAO respectively. This result combined with the fact that gas demand is more strongly anti-correlated with temperature than electricity demand (Thornton et al. 2016; DECC 2013) suggests that seasonal weather forecasts may also allow skilful gas demand forecasts. In addition, the energy industry's desire for tailored seasonal forecast information is high, as demonstrated by the positive feedback following a recent Met Office winter trial, where seasonal weather forecast briefings were provided.

The aim of this paper is to assess the skill in forecasting the weather-driven component of both winter mean gas demand and the number of high gas demand days over winter, using seasonal forecasts of climate. Winter is defined as the months of December, January and February and the skill of the 3-monthly average forecast from early November is assessed, giving a lead time of one to three months.

5.3 Data and methodology

5.3.1 Gas demand data

A dataset of the daily total gas demand of Great Britain (GB) covering the period April 1996 to March 2018, in giga (10^9) Watt hours (GWh), was provided by National Grid. The gas demand value represents the total demand from residential and large industrial premises (non daily-metered and daily-metered demand respectively) and includes shrinkage (gas leaks and theft). It does not include gas consumers directly connected to the national transmission network, such as gas-fired power stations and large industrial units (National Grid, 2012a). The variation in daily demand over the 22 year period is shown in black in the upper panel of figure 5.1, where a clear annual cycle is evident, with higher demand during the colder winter months and lower demand during the warmer summer months.

The variation in winter mean demand is shown in figure 5.2 (dotted black line) and highlights a general reduction over the 22 year period. The demand variability is only weakly anti-correlated with winter mean temperature variability ($r = -0.39$), much lower than might be anticipated given the known drivers of gas demand. Thornton et al. (2016) demonstrated that low-frequency variability in both electricity and gas demand over a similar period was not driven by temperature, but was rather thought to relate to socio-economic changes over the period. Possible reasons for the reduction in gas demand over the period include more efficient gas boilers, better home insulation with more double glazing, increasing gas prices and a continued shift away from heavy industry (BEIS, 2017).

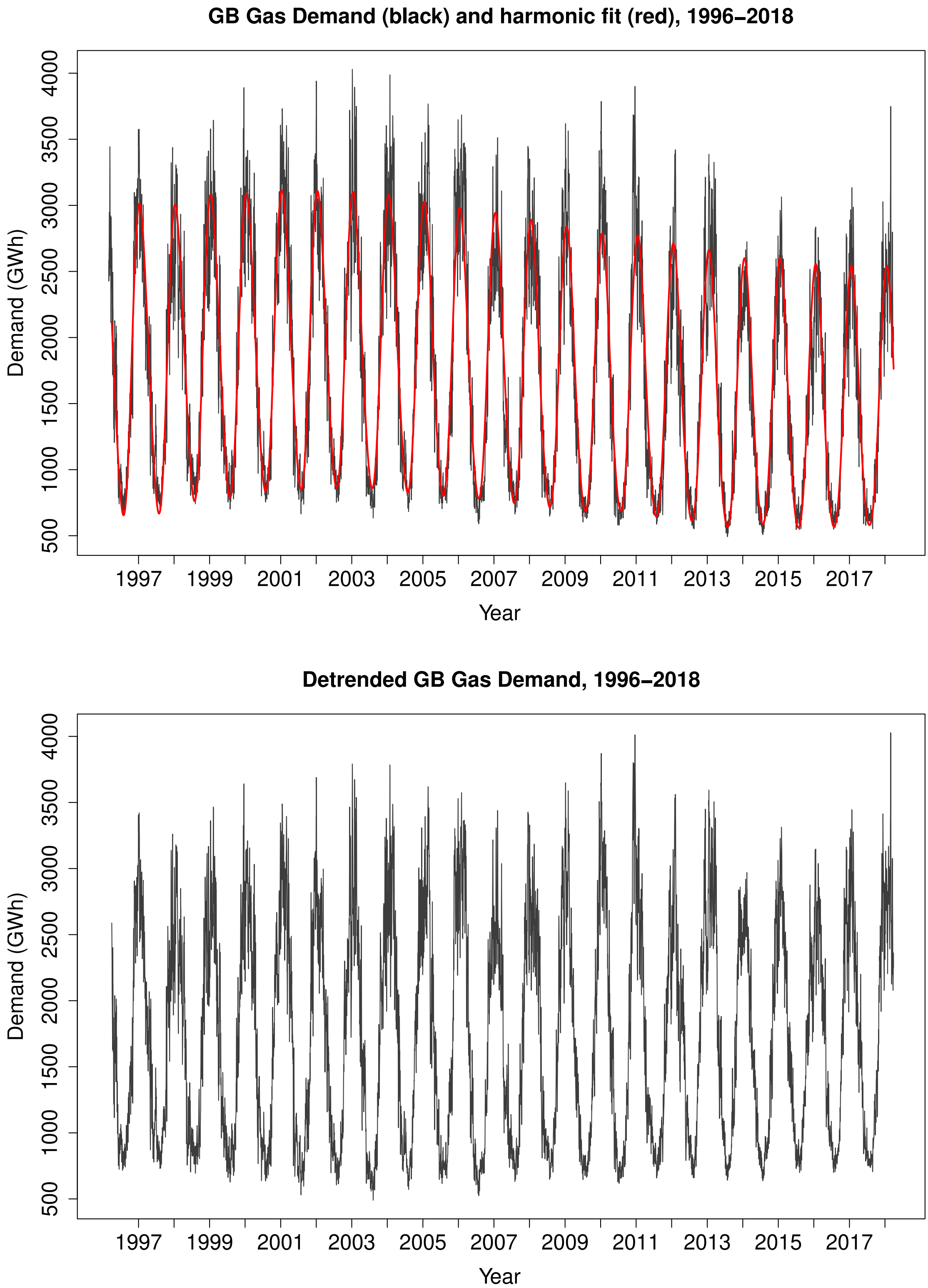

Figure 5.1: Upper: Daily GB gas demand timeseries (black) and harmonic fit (red), April 1996–March 2018. Lower: Daily GB gas demand timeseries where low-frequency variability has been removed. N.B. These plots are an extension of those in Figures 3.1 and 3.7

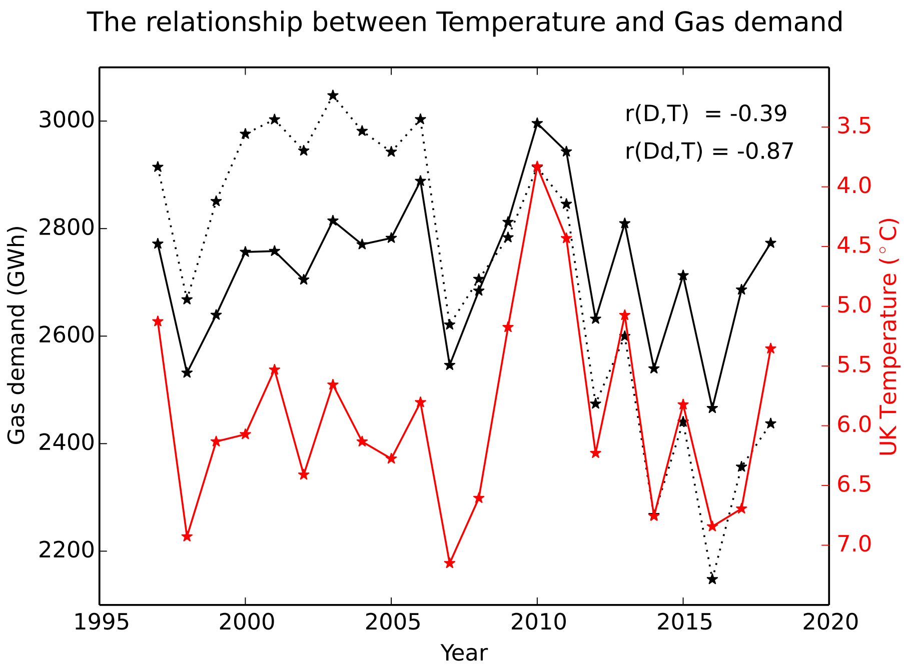

Figure 5.2: The winter mean of GB gas demand (‘D’, black dotted), demand time-series where low-frequency variability has been removed (‘Dd’, solid black) and UK mean temperature (‘T’, red). Pearson correlation coefficients (r) are also given highlighting the much closer relationship between demand and temperature once low-frequency demand variability has been removed. The winter year is labelled according to the January and February of the winter.

To accurately assess the weather-driven component of gas demand and its predictability, much of the demand variability that is not driven by the weather needs firstly to be removed. Thornton et al. (2016) developed a methodology to remove demand variability on timescales greater than 5 years (referred to as low-frequency variability), whilst retaining demand variability on a daily, seasonal and inter-annual timescale. This approach is used here and the first step involves identifying the slowly evolving background demand. This is achieved by fitting a smoothly evolving second order Fourier expansion to the daily demand data and is shown in red in figure 5.1. A gradual reduction in both the annual mean gas demand and magnitude of the annual gas demand cycle is seen over the data period. This background demand is then removed from the daily demand timeseries and replaced with a climatological-mean annual demand cycle. The resultant demand timeseries, where low-frequency variability has been removed, is used in the subsequent analysis and is shown in black in the lower panel of figure 5.1. The highest daily demand over the data period can be seen to shift from the winter of 2003 to 2018 (compare upper and lower panels). Full details of the methodology to remove low-frequency demand variability are given in Thornton et al. (2016).

Following the removal of low-frequency demand variability, the strength of the correlation between winter mean temperature and demand increases from -0.39 to -0.87, better reflecting the known relationship (Thornton et al. 2016, see figure 5.2). The low-frequency variability in observed winter temperature over the 22 year period is small. Consequently, when the 5-year running mean temperature trend is removed, its correlation with demand barely changes ($r = -0.85$).

The predictability of two characteristics of the winter gas demand are investigated, the winter mean gas demand and the number of high demand days per winter.

5.3.2 Seasonal forecast data

The Met Office's global environment model (HadGEM3-GC2, Williams et al. 2015) consists of global models of the atmosphere, the land surface (Best et al., 2011), the ocean (Madec, 2008) and sea-ice (Hunke and Lipscomb, 2010). Both the operational seasonal forecast system, GloSea5 (MacLachlan et al., 2015), and the decadal prediction system, DePreSys3 (Dunstone et al., 2016), are built around this same model. The atmosphere component has a resolution of 0.83° longitude and 0.55° latitude (about 60km at mid-latitudes), with 85 vertical levels and an upper boundary at 85km. The ocean model's resolution is 0.25° in both latitude and longitude, with 75 vertical levels.

In GloSea5 a set of retrospective forecasts, called a 'hindcast' set, is available for winters 1993–2016. Ten ensemble hindcast members are available from each calendar week. The three nearest weeks of hindcasts centred around the desired start time are collected together. For example, for a winter forecast of Dec–Jan–Feb with a one-month lead time, we use the hindcast start dates of 25th October, 1st November and 9th November, giving a total of 30 ensemble members per winter. The DePreSys3 hindcast set is available for winters 1981–2018 and includes 40 ensemble members initialised on the 1st November. In both systems, ensemble member differences are created using a stochastic physics scheme (MacLachlan et al., 2015).

Although small differences in initialisation exist between the GloSea5 and DePreSys3 hindcast sets, the two ensembles are considered to be directly comparable (Scaife et al., 2014b; Dunstone et al., 2016), giving a combined ensemble set of 70 members for winters 1997 to 2016. This large size is beneficial as the prediction skill of a system typically improves with ensemble size, because the noise between ensemble members is reduced, leaving a clearer ensemble mean forecast signal (Scaife et al., 2014b; Eade et al., 2014; Siegert et al., 2016; Scaife and Smith, 2018).

5.3.3 Climate Predictors

Various climate indices are considered as possible predictors of winter gas demand based on atmospheric temperature or the large scale pressure field. These climate indicators are calculated for both observations and forecasts. As a proxy for observations, the gridded 6-hourly instantaneous data sets of the 'Interim' version of the ECMWF Reanalysis (ERAI, Dee et al. 2011) are used. The data has a resolution of 0.75° longitude by 0.75° latitude and is available over the gas demand data period. Three variables are used, 2m temperature, mean sea level pressure (MSLP) and the geopotential height of the 500hPa pressure level (Z500). The 6–hourly data is firstly averaged to a daily mean value and then the following indices are calculated:

- Winter mean UK temperature : temperature is averaged over the region of 10°W–5°E and from 50–60°N to give a UK mean temperature.
- Winter mean NAO: The MSLP is averaged over the regions of Iceland (63–70°N, 25–16°W) and the Azores (36–40°N, 28–20°W) (Dunstone et al., 2016). For each region the winter pressure anomaly from the long term climatology is established and then the difference in these anomalies (Azores − Iceland) is

determined. The same diagnostic of the geopotential height field on the 500hPa pressure level is used to give a mid–troposphere NAO index (NAO_{Z500}).

- Winter mean UK North-South pressure difference (ΔP): Thornton et al. (2017) found that the winter variation in GB daily electricity demand was strongly influenced by the regional pressure field to the north and south of the UK. An index was defined as the difference in pressure between a northern box (27°W–21°E, 57–70°N) and a southern box (same longitudes, 38–51°N), for regions see figure 4 in Thornton et al. (2017). This is effectively a measure of the average westerly winds over the UK. This more UK centred pressure difference index is used here and a mid-tropospheric version is again calculated using the difference in the geopotential height field of the 500hPa pressure level (ΔZ).

- Number of high demand weather type days per winter (N_{WT}): Thornton et al. (2017) found that four large-scale high pressure weather patterns drive low temperatures and high electricity demand in the UK (see figure 4.11, Chapter 4). The weather types were identified by applying K-means clustering to the daily MSLP fields of the wider region. Here we explore whether predictions of the number of such days per winter is a good predictor of winter gas demand. A day is defined as a high demand weather type day if it is sufficiently similar to one of the previously identified cluster centroids. To test the similarity two distance measures are used. A day must have both a higher pattern correlation with a cluster centroid and a smaller absolute pressure difference from that centroid, than the member within the original cluster which is most dissimilar to its centroid.

The same climate indices are also calculated using the forecast data. An index is calculated for each ensemble member individually and then these are averaged to give an ensemble mean index. Due to the significant signal to noise issue when predicting the climate in the mid-latitudes (Scaife et al., 2014b; Eade et al., 2014; Scaife and Smith, 2018), the ensemble mean climate index is used as the climate predictor, rather than the individual ensemble member values. From here onwards, 'climate index' refers to the combined ensemble mean of the climate index.

5.3.4 Methods for assessing forecast skill

For a climate index to be a skilful predictor of gas demand, it must have both a strong observed relationship with gas demand and be well predicted by the climate forecast system itself. Both are assessed using correlation coefficients: the Pearson correlation (r_P) when the variables are continuous (e.g. winter mean gas demand, temperature) and the Spearman rank correlation (r_S) if either of the variables is discrete (e.g. the number of high demand days per winter).

Skill in predicting gas demand is established by assessing the relationship strength between the forecast climate index and the observed gas demand variable, following the approach of Bett et al. (2017). The ability of the climate index to predict above median, above upper tercile or the correct tercile of winter demand is assessed using the Heidke skill score (HSS).

To assess probabilistic forecast skill, a linear regression model is made between observed winter mean demand and the forecast climate index. The skill of probabilistic forecasts for the demand categories above can then be assessed, using the Brier and Rank Probability Skill Scores (BSS and RPSS respectively), employing leave-one-out cross validation. A preliminary assessment of the reliability of the probabilistic forecasts is also given. For a comprehensive description of the different statistical measures see Wilks (2006).

5.4 Results

5.4.1 Using temperature as a predictor of winter mean gas demand

Figure 5.3 summarises the prediction skill of winter mean gas demand using temperature as the predictor. As discussed previously, observed winter mean temperature is strongly anti-correlated with GB winter mean gas demand ($r_P = -0.87$, see figure 5.3a, this is a repeat of figure 5.2, and is included to allow comparison with the predictions). The skill in forecasting winter mean temperature across North-western Europe and the Atlantic is shown in figure 5.4. Temperatures are skilfully forecast over many areas of the North Atlantic and over Scandinavia. In contrast there is little skill over continental Europe. Much of the skill over the ocean is however related to the low-frequency warming trend, such that when the 5 year running-mean winter-mean temperature trend is removed the prediction skill is negligible over most of the North Atlantic (not shown). There is significant skill in predicting the average temperature over the UK region, but the correlation magnitude is still relatively small ($r_P = 0.38$, see Table 5.1 and figure 5.3b). A similar skill level is found when a 5 year running-mean temperature trend is removed.

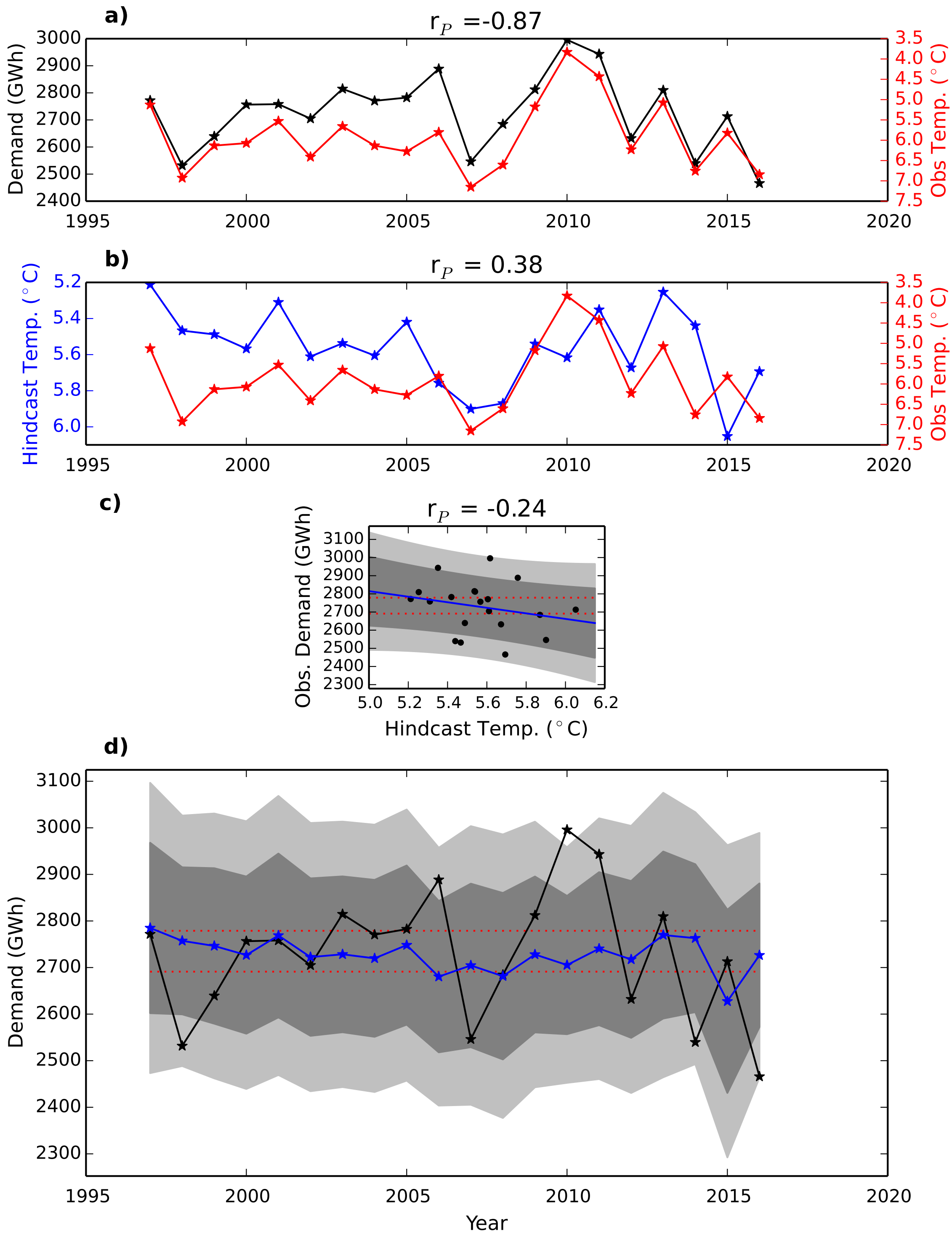

Figure 5.3: Using temperature to predict winter mean gas demand. **a)** Timeseries of the winter mean GB gas demand and winter mean temperature. **b)** Timeseries of winter mean temperature and winter mean hindcast temperature. **c)** Regression relationship between hindcast temperature and observed demand (blue), the prediction interval (central 95% - light grey, central 75% - dark grey), and the observed terciles of gas demand are shown (red dashed lines). **d)** Timeseries of winter mean gas demand (black) and central regression prediction (blue) and prediction interval (grey). The Pearson correlation coefficients (r_P) are given for a) - c). Note, the temperature axes are inverted in a) and b) to allow easier comparison with gas demand.

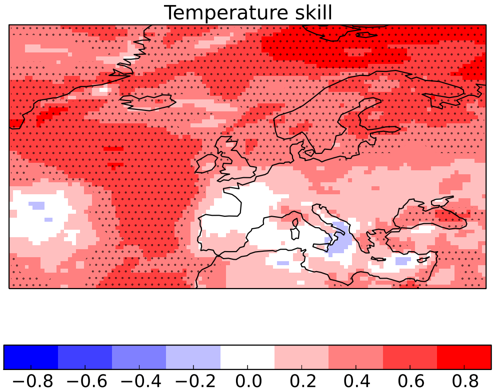

Figure 5.4: Map of the winter mean temperature forecast skill: the Pearson correlation coefficient between hindcast and observed temperature. Statistically significant skill at the 5% level is shown by stippling using a 1-sided Fisher Z test.

A forecast of UK average winter mean temperature is not found to be a good predictor of winter mean gas demand. Although the Pearson correlation coefficient between the hindcast temperature and observed demand has the correct sign (negative), its low magnitude ($|r_P| = 0.24$) means it is not statistically significant at the 5% level. A large spread in the relationship can be seen in figure 5.3c, leading to little variation in the probabilistic prediction of winter mean demand from year to year (figure 5.3d). Although the deterministic HSSs are positive for above median and above upper tercile demand, the equivalent probabilistic skill scores are worse or similar to those of a climatological forecast (e.g. $\text{RPSS}_{ter} = 0.03$, see Table 5.2). In summary, although temperature variability drives a significant proportion of demand variability, forecast temperature is not a good predictor of winter mean gas demand due to the limited skill in predicting UK temperatures.

Climate Index (C)	Obs relationship r_P (D_{obs}, C_{obs})	Climate Index skill, r_P (C_{obs}, C_{hc})	Gas demand skill, $\|r_P\|$ (D_{obs}, C_{hc})
Temperature	**-0.87**	**0.38**	0.24
NAO	**-0.62**	**0.63**	**0.40**
NAO$_{\mathbf{Z500}}$	**-0.66**	**0.63**	**0.55**
ΔP	**0.70**	**0.60**	**0.49**
ΔZ	**0.71**	**0.58**	**0.57**
N$_{\mathbf{WT}}$	**0.66**	**0.56**	**0.57**

Table 5.1: Column 1: Pearson correlation coefficient (r_P) between winter mean gas demand (D_{obs}) and observed winter mean climate index (C_{obs}). Column 2: The hindcast skill in predicting the climate index (correlation of observed and hindcast climate index). Column 3: The hindcast skill in predicting winter mean gas demand (magnitude of correlation between D_{obs} and C_{hc}). All data considers winters 1997–2016. Bold values indicate the correlation is significant at the 5% level using a 1-sided Fisher Z test.

Climate Index	HSS$_{\mathbf{med}}$	BSS$_{\mathbf{med}}$	HSS$_{\mathbf{upper}}$	BSS$_{\mathbf{upper}}$	HSS$_{\mathbf{ter}}$	RPSS$_{\mathbf{ter}}$
Temperature	*0.40*	**0.09**	0.12	-0.13	**0.25**	0.03
NAO	*0.40*	**0.18**	**0.56**	**0.12**	**0.32**	**0.18**
NAO$_{Z500}$	*0.40*	**0.26**	**0.78**	**0.41**	**0.40**	**0.33**
ΔP	**0.60**	**0.19**	**0.56**	**0.18**	**0.32**	**0.26**
ΔZ	*0.40*	**0.28**	**0.56**	**0.30**	**0.47**	**0.32**
N$_{\mathbf{WT}}$	**0.60**	**0.33**	**0.78**	**0.30**	**0.62**	**0.34**

Table 5.2: A summary of verification skill scores for predicting winter mean gas demand when using the different climate predictors. The Heidke skill Score (HSS), the Brier Skill Score (BSS) and the Ranked Probability Skill Score (RPSS), for above median demand (med), above upper tercile demand (upper) and considering all terciles (ter). Scores greater than zero indicate the forecast is better than random chance (in the case of the HSS) and better than a climatological forecast for the BSS and RPSS, following Wilks (2006). Bold (Italics) signifies the score is significant at the 5% (10%) level. Significance is assessed using a 1000 member bootstrap, where the skill score is calculated between the observed demand timeseries and a randomly sampled (without replacement) hindcast timeseries. A value is significant if it is greater or equal to the 95th (90th) percentile of the bootstrap distribution.

5.4.2 Using the atmospheric circulation as a predictor of winter mean gas demand

All circulation-based indices (NAO, NAO$_{Z500}$, ΔP, ΔZ and N$_{WT}$) have a strong observed relationship with winter mean gas demand (r_P of $\sim$ 0.6–0.7, see Table 5.1, column 1). The UK centred circulation indices (ΔP, ΔZ) have a marginally stronger relationship with gas demand than the NAO indices, which likely reflects their better representation of flow direction and strength over the UK. However none of the circulation indices have as strong a relationship with demand as winter mean UK temperature.

The skill in predicting the winter MSLP across North-western Europe and the wider North Atlantic is shown in the left panel of figure 5.5. Skill is found at both high (60°–70°N) and low (30°–40°N) latitudes. In contrast, over the mid-latitudes (40°–60°N) including over the UK there is not significant prediction skill. A similar picture is seen for the Z500 field (figure 5.5, right). Nevertheless, skilful predictions of the winter mean circulation indices are possible ($r_P \sim 0.6$, see Table 5.1, column 2), as the indices measure the difference in pressure between the skilfully predicted low and high latitude regions. This skill is important because it is the gradient in pressure which drives surface weather conditions. The total number of high demand weather type days per winter is also skilfully predicted at the 5% level ($r_P = 0.56$). This weather type skill effectively demonstrates skill in predicting the frequency of days where high pressure influences the UK in winter and is consistent with previous studies (Athanasiadis et al., 2014).

Winter mean gas demand is skilfully predicted when using any of the circulation indices as the predictor, with correlations between hindcast index and observed demand ranging from approximately 0.4 to 0.6 (see Table 5.1, column 3). Predictions of winter mean demand greater than the median or upper tercile are skilful, showing improvements over using a random or climatological forecast (scores often exceeding 0.25, see Table 5.2). For below lower tercile demand all predictors give positive HSSs ($\sim$ 0.3–0.6), however only NAO$_{Z500}$, ΔP and ΔZ give skilful probabilistic forecasts (BSSs of 0.05–0.12). This suggests a possible asymmetry, with better forecast skill for higher demand winters than lower demand winters, which could be beneficial given their larger impact.

Figure 5.6 demonstrates the skill in predicting winter mean gas demand using ΔZ as the climate predictor. The strong observed relationship between ΔZ and demand is shown in figure 5.6a, and the prediction skill of ΔZ is shown in figure 5.6b.

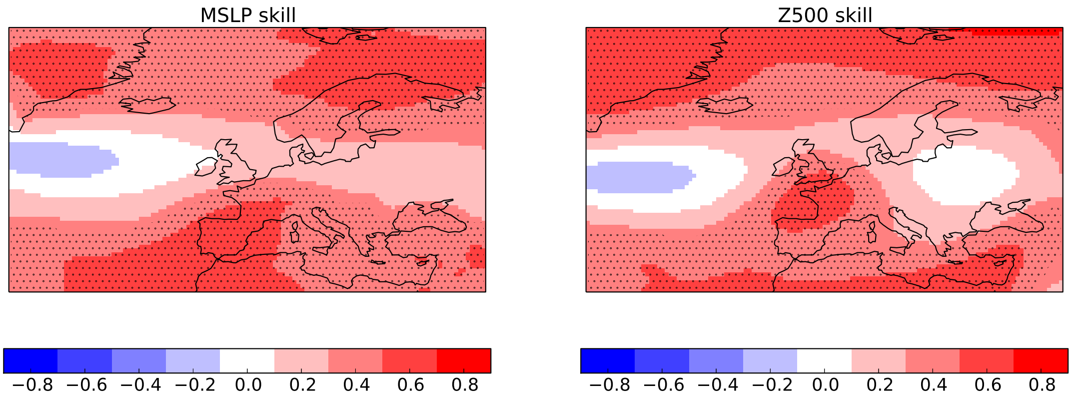

Figure 5.5: Map of the winter mean forecast skill for MSLP (left) and 500hPa geopotential height (right): the Pearson correlation coefficient between the hindcast and observed fields from 1994-2016. Statistically significant skill at the 5% level is shown by stippling using a 1-sided Fisher Z test.

A significant linear relationship exists between observed demand and hindcast ΔZ ($r = 0.57$, see figure 5.6c), leading to a variation in the forecast of gas demand from year to year (figure 5.6d). The probability of above median demand, above upper tercile demand, and the correct tercile category is skilfully forecast and better than using a climatological forecast ($\text{BSS}_{med} = 0.28$, $\text{BSS}_{upper} = 0.30$, $\text{RPSS}_{ter} = 0.32$). Use of the linear regression model between hindcast climate index and observed demand, means forecasts are automatically bias adjusted and probabilities are reliable, for example see figure 5.7. Due to the small number of winters available, the reliability is only assessed across 4 probability bins. An operational forecast could therefore present the risk of an event using 4 categories, e.g. the probability (P) of above tercile demand is 'low' (P < 0.25), 'below median' ($0.25 \leq$ P < 0.5), 'above median' ($0.50 \leq$ P < 0.75) or 'high' (P ≥ 0.75), rather than giving actual probabilities.

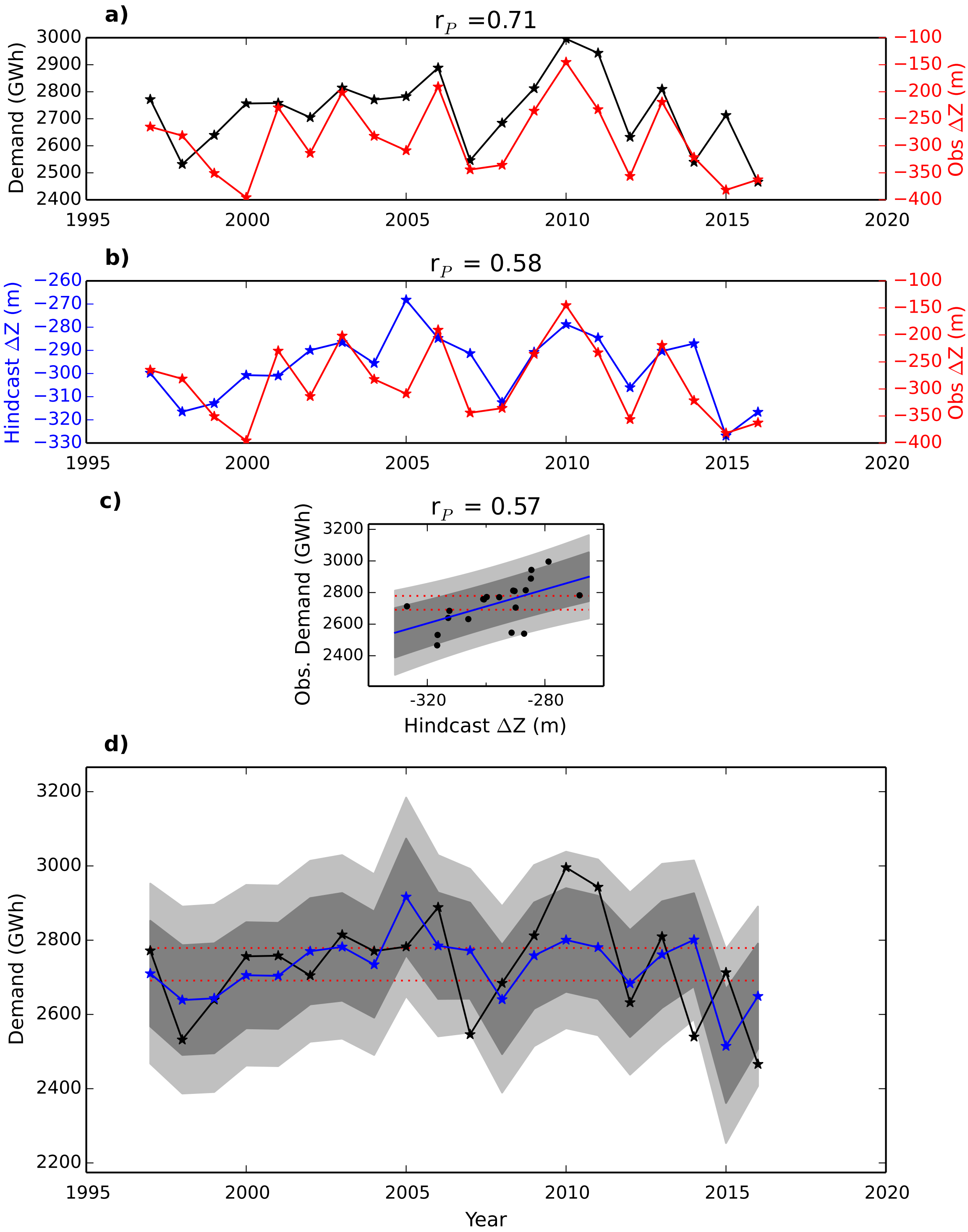

Figure 5.6: Using the winter mean Z500 North-South height difference (ΔZ) to predict winter mean gas demand. **a)** Timeseries of the winter mean GB gas demand and ΔZ. **b)** Timeseries of observed and hindcast ΔZ. **c)** Regression relationship between hindcast ΔZ and observed demand (blue) and the prediction interval (grey). **d)** Timeseries of winter mean gas demand (black) and central regression prediction (blue) and prediction interval (grey). See figure 5.3 for details.

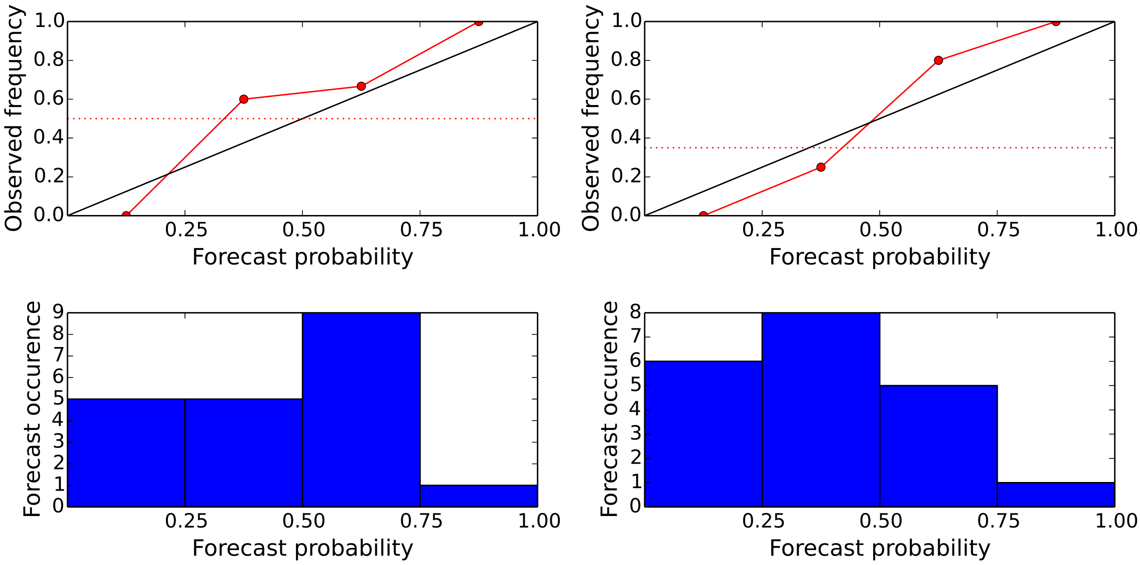

Figure 5.7: Reliability diagrams for probabilistic forecasts of winter mean gas demand using ΔZ as the climate predictor, for above median (left) and above upper tercile (right) demand. A perfectly reliable forecast would lie along the 1:1 line (black). The sample climatological probability is also given (red dotted). The lower bar charts show the distribution of forecast probabilities made during the hindcast period, ideally these would be flat, with each probability bin well sampled.

To explore how many ensemble members are needed to ensure a skilful forecast of gas demand, figure 5.8 shows how the prediction skill varies with ensemble size. Increasing the ensemble size from 1 to 30 leads to a rapid increase in prediction skill (the correlation increases from ∼0.1 to 0.5). Increasing the ensemble size even more leads to further improvements in the prediction skill, but at a much slower rate. Nevertheless, higher skill would likely be possible with more members.

In summary, skilful prediction of winter mean gas demand is possible using a forecast of the winter mean atmospheric circulation. The improvement over using a temperature forecast occurs because of the better prediction skill of the circulation indices. This may reflect the larger region over which the circulation indices are calculated, increasing the forecast signal strength over noise. The poorer forecast skill of the temperature index may also reflect the too weak NAO–temperature relationship in the ensemble mean forecasts (see figure 2 of Clark et al. 2017).

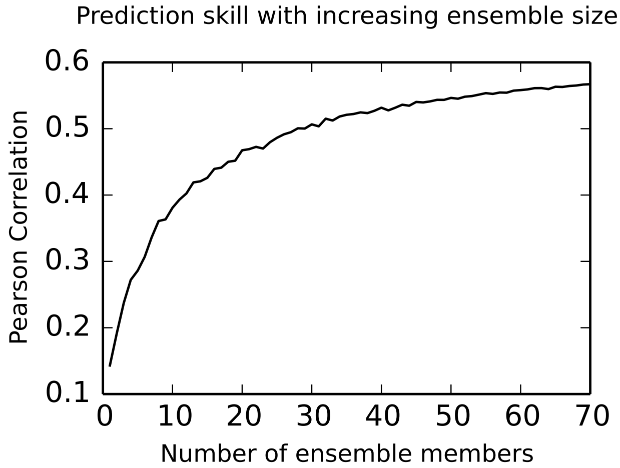

Figure 5.8: The impact of ensemble size on hindcast skill, when predicting winter mean gas demand using winter mean ΔZ. The skill is measured using the Pearson correlation coefficient. 1000 samples of the correlation have been generated by randomly sampling the ΔZ ensemble members each winter, to give alternative hindcast ensemble mean timeseries. The mean correlation of the bootstrap samples is shown. For a sample size of 20, statistical significance at the 5% level using a 1-sided Fisher Z test, is achieved with a correlation of at least 0.379.

5.4.3 Predicting the number of high gas demand days over the winter period

A day is classed as a high demand day if its demand is equal to or greater than the 95th percentile of daily winter demand calculated over all winters. Between 1997 and 2016 the observed number of high gas demand days per winter ('NG') varies between 0 and 15 (see black line, Figure 5.9a). Winters 2010 and 2011 had the largest number of high gas demand days, such that the energy system operator had to issue a number of gas balancing alerts (DECC, 2011; National Grid, 2011). These alerts encourage additional supplies of gas to become available, often following an increase in gas price. As these events stress the energy supply system an obvious question is whether their likelihood is predictable ahead of the winter. There is a strong correlation between winter mean gas demand and NG ($r_S = 0.70$). Consequently, if mean demand is skilfully predicted, NG may also be predictable to some extent.

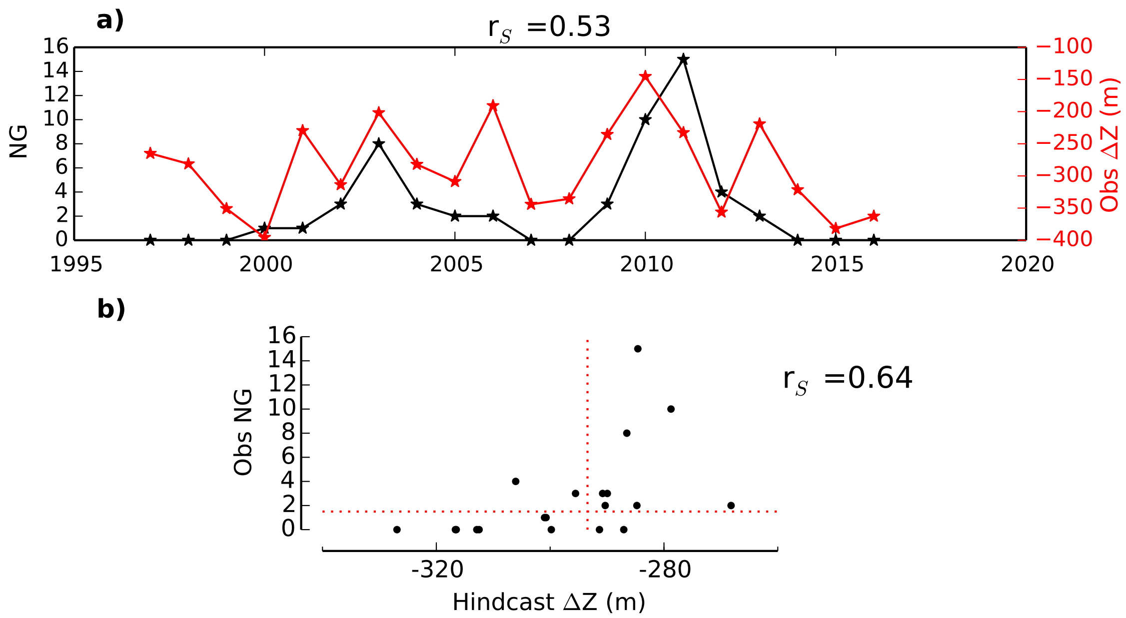

Figure 5.9: Using atmospheric circulation to predict the number of high gas demand days per winter (NG). **a)** Observed timeseries of NG and winter mean ΔZ. **b)** The relationship between hindcast ΔZ and observed NG. The median count and hindcast ΔZ are indicated with a dotted red line. The Spearman rank correlation coefficients are also given (r_S).

Although observed winter mean temperature has a reasonable relationship with

NG ($r_S = -0.55$), temperature is not a useful predictor of NG ($r_S = -0.11$ between NG and hindcast winter mean temperature, see Table 5.3, column 2). All circulation indices do however give skilful predictions of NG, with Spearman rank correlation magnitudes of approximately 0.4 to 0.6 (same Table).

Climate Index (C)	**Obs relationship** r_S (NG$_{obs}$, C_{obs})	**NG skill** $\lvert r_S \rvert$ (NG$_{obs}$, C_{hc})
Temperature	**-0.55**	0.11
NAO	**-0.49**	**0.42**
NAO$_{\mathbf{Z500}}$	**-0.47**	**0.63**
ΔP	**0.54**	**0.54**
ΔZ	**0.53**	**0.64**
N$_{\mathbf{WT}}$	**0.55**	**0.57**

Table 5.3: Column 1: Spearman rank correlation coefficient (r_S) between observed NG (NG$_{obs}$) and observed winter mean climate index (C_{obs}). Column 2: Hindcast skill in predicting NG (correlation magnitude between NG$_{obs}$ and C_{hc}). All data considers winters 1997–2016. Bold values indicate the correlation is significant at the 5% level using a 1-sided Fisher Z test.

A demonstration of the prediction skill of NG, using winter mean ΔZ as the predictor, is shown in figure 5.9. Given NG is discrete and limited to positive numbers, linear regression is not suitable for modelling its relationship with ΔZ. Due to the small sample size there is also considerable uncertainty in the form of the relationship between observed ΔZ and the NG. Consequently we do not try to model the relationship, rather we assess the prediction skill using a deterministic approach. Figure 5.9b shows the relationship between hindcast ΔZ and observed NG. As the predicted atmospheric flow over the UK becomes less westerly (i.e. ΔZ becomes less negative), NG increases. The contingency table for above median counts show that the hit rate is far higher than the false alarm rate (see Table 5.4), leading to a HSS of 0.6 (statistically significant at the 5% level using a 1000 member bootstrap as per Table 5.2). For above upper tercile counts, the HSS is positive (HSS = 0.34) but it is not statistically significant at either the 5% or 10% levels. Very similar results are found for the other atmospheric circulation predictors, whilst a temperature based prediction is no better than when using a random forecast (HSS ≤ 0).

In summary, given a forecast of the atmospheric circulation, we can give a skilful forecast of above median counts of the number of high gas demand days per winter. A longer timeseries is needed to assess the predictability of winters with a higher number of high demand days.

Above median count		Observed Yes	Observed No
Predicted	Yes	8 Hits	2 False alarms
	No	2 Misses	8 Correct rejections
Hit rate:		80%	
False alarm rate:		20%	

Table 5.4: Contingency table for above median count of the number of high demand days per winter, using ΔZ as the predictor.

5.5 Conclusions

The predictability of the weather-driven component of Britain's winter gas demand is assessed from early November using a range of climate predictors. Two components of gas demand are considered: winter mean gas demand and the number of high demand days over the winter period. The forecast skill is analysed from 1997 to 2016 using a large ensemble of retrospective climate forecasts from the Met Office's seasonal and decadal prediction systems. The climate predictors analysed are winter means of temperature, the NAO and a UK centred North-South pressure difference (at the surface and in the mid-troposphere). An additional predictor, based on the frequency of high demand weather types over the winter period, is also analysed. Forecast skill is assessed using a range of deterministic and probabilistic skill measures with a focus on the risk of higher demand winters. The main conclusions are:

- All circulation-based indices give skilful forecasts of winter mean gas demand. This is because such indices are both strongly correlated with gas demand and are skilfully predicted ahead of the winter period.
- A method for giving operational gas demand forecasts is demonstrated, based on a regression relationship between the climate predictor and observed gas demand. Skilful and reliable probabilistic forecasts of the risk of above median, above upper tercile and the correct tercile of winter mean demand are possible.
- A large ensemble of hindcast members is needed to give a skilful prediction of winter mean gas demand, reflecting the known signal to noise problem of seasonal forecasting in the Atlantic sector.

- Although winter mean temperature is the climate index most highly correlated with winter mean gas demand, due to the lower seasonal prediction skill of temperature, it does not give skilful predictions of winter mean demand.
- A skilful forecast of above median counts of the number of high gas demand days per winter is possible using a forecast of the winter mean atmospheric circulation.

The skilful prediction of winter gas demand demonstrated here, offers the potential for improved planning and resilience of Britain's energy system. For example, a more accurate forecast of winter demand could reduce the risk of gas supply shortages and related energy price spikes. It would be of interest to assess the skill of winter demand forecasts with a longer lead time, for example from early September or October, and when averaged over a shorter period, such as individual months, as both would clearly be useful. The use of an atmospheric circulation index to predict energy demand could also give skilful forecasts in other regions, provided demand is driven by the weather and skilful circulation forecasts are available. Seasonal weather forecasts offer the first outlook for the coming winter, but they should be used in conjunction with other nearer term forecasts, such as monthly outlooks through to day ahead forecasts, to maximise the preparedness of the energy industry for extreme demand events.

Chapter 6

Conclusions

This PhD aims to improve the understanding of the impacts of weather and atmospheric circulation on Britain's energy system in winter. It explores how atmospheric variability influences both the demand for electricity and gas and the availability of wind power. Particular attention is paid to weather-driven extremes of energy demand, due to their significant impact on the wider energy system. Their magnitude and likelihood is quantified and their driving atmospheric circulation patterns identified. To better understand the contribution that wind power can make to the security of energy supplies, the availability of wind power during extreme demand is analysed. In addition, to potentially improve the energy sector's preparedness for winter, the ability of seasonal climate forecasts to predict the weather-driven component of winter energy demand is explored. A summary of the findings for each thesis question posed and their place within the wider literature, is given below.

6.1 Energy demand variability

6.1.1 How has Britain's energy demand varied over the recent period and what has driven this variability?

Observed daily electricity and gas demand in GB have been analysed between 1975-2013 and 1996-2013 respectively. Long term trends in annual mean demand are seen, with demand peaking in the early to mid 2000s. Although temperature has been shown to be the dominant weather driver of demand variability in Britain (Psiloglou et al., 2009), it cannot explain the long-term trends seen here, rather socio-economic drivers are thought to be responsible. A strong correlation between demand and the strength of the economy is found prior to the peak in demand. However, after the demand peak, this relationship breaks down and other socio-economic drivers such as embedded generation and energy saving measures are thought to be responsible for the subsequent decline in demand. Once such low-frequency demand variability is removed, both electricity and gas demand are strongly anti-correlated with daily mean temperature (r_{elec} = -0.90 , r_{gas} = -0.94). After taking the annual cycles of temperature and demand into account, winter has the strongest demand-temperature relationship. Approximately two-thirds of electricity demand variability, and over four-fifths of gas demand variability are linearly accounted for by temperature variability. In winter there is also high temperature sensitivity, with a 1°C reduction in daily temperature typically giving a ~1% increase in daily electricity demand and a 3% – 4% increase in daily gas demand. Compared to electricity demand, gas demand is found to have a stronger anti-correlation with temperature, a larger relative annual cycle, a weaker weekly cycle and a greater sensitivity to temperature change. These differences are consistent with the higher proportion of gas demand that is consumed for domestic heating compared to electricity demand.

Advances relative to previous research (Hor et al. 2005, Psiloglou et al. 2009) include: a new method for removing non-weather driven demand variability; quantification of the demand-temperature relationship in each season and identification of the season with the strongest relationship; and a comparison of the influence of temperature on gas and electricity demand.

6.1.2 What is the risk and magnitude of weather-driven extreme demand events today?

Artificial estimates of daily demand have been made back to 1772 using detrended temperature observations and the modern demand–temperature regression relationships. The current risk and magnitude of weather-driven extreme demand events have then been quantified. The 1 in 20 year peak day electricity and gas demand estimates are approximately 15% and 45% above the last decade's average winter demand respectively. The coldest day over the last ~240 years (once the long term trend has been removed) would have resulted in an electricity and gas demand estimate of 17% and 57% above the average winter day respectively.

The month of December 2010 and the winter of 2009/2010 are recent examples of very cold GB conditions (Maidens et al. 2013, Cattiaux et al. 2010). The risk today of a month having at least as much electricity or gas demand as December

2010 is estimated to be one in $\sim$34 years (20–60 years). The risk of a winter having at least as much electricity or gas demand as the 2009/2010 winter is estimated to be one in $\sim$18 years (12–27 years). The long term trend in temperature means that the risk of a December 2010 or a winter 2009/2010 demand has approximately halved.

This appears to be the first assessment of weather-driven extreme energy demand risk in the published literature.

6.2 The balance of electricity demand and wind power

The availability of wind power during different electricity demand conditions in GB has been analysed between 1979 and 2013. Daily wind power availability has been estimated using reanalysis wind speeds and an idealised wind power model. This wind power estimate has then been compared with daily observations of total GB electricity demand.

6.2.1 What is the relationship between wind power and electricity demand and to what extent can it be explained by meteorology?

For the majority of the year, as demand increases, average available wind power also increases. This reflects the variation in temperatures and wind speeds with season, with calmer, warmer conditions in summer and cooler, windier conditions in late autumn and early spring. However in winter, average wind power reduces by a third between lower and higher demand. This winter relationship is shown to be driven by the large scale weather patterns affecting Northern Europe. The change from predominantly strong, warm, westerly winds, to colder, calmer, easterly winds explains the reduction in wind power supply as demand increases.

During highest winter demand a modest recovery in average wind power is found. This partial recovery is associated with a reversed north-south pressure gradient, the building of high pressure to the north of GB and strengthening easterly winds. These average relationships hide considerable daily variability, where for a given demand, a wide range of wind power availability is possible.

These results confirm the generally positive relationship between GB wind power and electricity demand across the year and the negative relationship in winter (Sinden, 2007), and the general influence of weather patterns on demand and wind power supply (Oswald et al. 2008, Leahy and Foley 2012, Brayshaw et al. 2012). Advances include: quantification of the reduction in wind power with increasing electricity demand, discovery of the partial recovery in wind power during highest demand; the dependence of the demand-wind power relationship on the north-south pressure difference across the UK; and the associated contrasting influence of westerly versus easterly weather patterns.

6.2.2 Can wind turbines provide power during high demand periods?

Approximately one-third of high demand days have wind power above the winter average, and two-thirds below. This is caused by a range of high pressure weather types which generate similarly cold conditions over GB, but varying wind power supply. For example, high pressure over Scandinavia typically produces high demand and above average wind power in GB, associated with cold, strong easterly winds. In contrast, high pressure over Greenland typically produces high demand but below average wind power, caused by cold, but weak northerly winds over GB. However, during peak demand, although days do exist with very little onshore and offshore wind power, half of days have above average wind power, due to more days with strong easterly winds.

These findings demonstrate that wind power can contribute to the supply mix during high and peak demand. However, the relationship is complex, such that certain weather types provide good wind power, whilst others limit availability. The spatial distribution of wind power availability varies across these weather types, indicating that a spread of wind turbines across Britain would maximise the average availability of wind power during high demand. Offshore wind power is also found to be more consistent, with a smaller percentage reduction in wind power supply with increasing demand.

The range in available wind power found during high electricity demand days, explains the range in results seen previously in the published literature (Oswald et al. 2008, Zachary and Dent 2012, Harrison et al. 2015, Sinden 2007, Zachary et al. 2011, Brayshaw et al. 2012), especially given the short data lengths often considered. Advances relative to previous research include: quantification of the likelihood of different wind power supply conditions during high electricity demand; identification of the variety of weather patterns responsible for generating high GB demand; and mapping of the spatial variation in wind power availability during the different high demand weather types.

6.2.3 Can interconnection help improve the security of energy supply?

There is a risk of concurrent high electricity demand and low wind power days across many parts of Europe, associated with extensive high pressure systems. Neighbouring countries may therefore struggle to provide additional capacity to GB when its demand is high and its wind power low. The Iberian Peninsula is the main exception, where demand is likely to be near normal and wind power higher than normal, when the British energy system is under strain.

Previous research has highlighted the north-south dipole in winter mean wind speeds across Europe under different phases of the NAO and its potential impacts on wind power (Hurrell 1995, Brayshaw et al. 2011, Ely et al. 2013, Jerez et al. 2013). The research here has demonstrated that at the daily timescale, under the different high GB demand weather types identified, the north-south dipole in wind speeds across Europe broadly remains. This variation in wind power across Europe under different weather regimes has subsequently been confirmed by Grams et al. (2017).

6.3 Seasonal predictability of energy demand

The predictability of the weather-driven component of Britain's winter gas demand has been assessed using climate forecasts beginning in early November. The forecast skill has been analysed from 1997 to 2016 using a large ensemble of retrospective climate forecasts from the Met Office's seasonal and decadal prediction systems. The climate predictors analysed include winter means of temperature, the NAO, a UK centred north-south pressure difference (at the surface and in the mid-troposphere) and the frequency of high demand weather types over the winter period. Low-frequency variability in gas demand, which is not driven by temperature but thought to relate to socio-economic changes, has been removed prior to analysis of prediction skill.

6.3.1 Can seasonal weather forecasts predict winter mean gas demand and the number of high gas demand days over the winter period?

Skilful forecasts of winter mean gas demand are possible using a prediction of winter mean atmospheric circulation. This skill arises because the circulation indices are both strongly correlated with gas demand in observations, and they are also skilfully predicted ahead of the winter period. Predictions of winter mean demand greater than the median or upper tercile are skilful, showing improvements over using a climatological forecast. Such skill is only achieved with a sufficiently large ensemble of hindcast members, reflecting the known signal to noise problem of seasonal forecasting in the Atlantic sector (Scaife and Smith, 2018). Although winter mean temperature is the climate index most highly correlated with winter mean gas demand, due to the lower seasonal prediction skill of temperature, it does not give skilful predictions of winter mean demand.

A skilful forecast of above median counts of the number of high gas demand days per winter ($\sim$ 1 per winter) is possible using a forecast of the winter mean atmospheric circulation. However, a longer timeseries of demand data and seasonal hindcasts is needed to assess the predictability of winters with a higher number of high demand days.

This is the first study to demonstrate skill in predicting winter mean GB gas demand and the number of high demand days over the winter period. The assessment builds on the electricity demand study of Clark et al. (2017) by extending the range of circulation predictors considered, assessing probabilistic skill and exploring extreme demand risk.

6.4 Implications and recommendations for future work

This research has shown that aspects of the British energy system are strongly influenced by the diverse range of weather conditions experienced in winter. The size of Britain's land mass and coastal regions means the energy system is highly sensitive to synoptic scale weather systems, which are a dominant feature of the winter climate in the North Atlantic region. The combination of synoptic weather systems and the strong meridional and zonal temperature gradients in the region produce a very variable winter climate in Britain. Energy demand and wind power supply are shown to be highly sensitive to meteorological conditions and consequently they are also highly variable.

6.4.1 Extreme energy demand

Understanding the risk of extreme demand periods is crucial for maintaining security of supply and resilience of the energy system. However given energy demand records are relatively short, gaining reliable extreme demand estimates is challenging. Here, the use of much longer climate records to better determine weather-driven demand risk is demonstrated. This could be further extended by use of initialised climate model simulations, referred to as the 'UNSEEN' methodology (Thompson et al., 2017). A large ensemble of hindcast runs from a coupled prediction system (e.g. GloSea5 or DePreSys3), for the recent period, could be mined to explore the risk of historical and unprecedented GB temperature extremes. The benefits of this method are twofold: the total length of the model simulations available is significantly longer than the observational record; and the use of a recent, initialised hindcast set means the simulations are representative of today's climate.

Given the weather types associated with high demand have been established, the risk of demand extremes could also be estimated using the frequency of high demand weather types in observational records or model simulations. A similar analysis could also be applied to climate model projections to assess the risk of high demand periods in the future. Operational memory of historical energy system events is relatively short, with mitigation efforts often focussed on the most recent extreme impacts. Through an improved estimation of weather-driven extreme demand risk, the resilience of the current energy system to climate variability can be better understood.

6.4.2 Supply - demand balance

The balancing of electricity supply and demand is becoming ever more complicated due to the increase in variable generation sources, such as wind power. The research in this PhD has highlighted the important role that atmospheric circulation plays in the balance between wind power and electricity demand. This improved understanding could help the industry and Government in the following ways: to improve the interpretation of how a particular weather forecast may impact the supply-demand balance; to better quantify the contribution that wind power can make within the wider energy system; and to better understand how the planned increase in both wind power capacity and electricity demand (associated with the electrification of heating), could influence the future management of the energy system.

The real-time balancing of electricity supply and demand is very complex, with multiple sources of generation needing to be considered and limited transmission capacity. Building on the research here, an improved assessment of the impact of weather and climate variability on the supply-demand balance could be achieved. Firstly, a more realistic GB wind power estimate could be determined by taking account of the current distribution and characteristics of the GB turbine fleet (for example as done by Cannon et al. 2015). Secondly, other renewable sources such as solar and hydro-power could be included in the assessment. Thirdly, the analysis of supply and demand could be undertaken at a higher temporal resolution, to better reflect the sub-hourly management of the system. For example, climate reanalyses at an hourly resolution are available and could be combined with sub-daily demand data, to better assess the energy balance across the day. Fourthly, climate data could be applied to more sophisticated models of the GB electricity system, to better account for transmission constraints.

This analysis of GB energy demand and wind power supply could also be repeated using climate projection data, to understand how the future energy balance in winter could be affected by anthropogenic climate change. In addition, if summer temperatures in Britain increase sufficiently into the future, then air-conditioning use could increase markedly. The availability of wind and solar power during heatwave-driven demand peaks could consequently become important and would also be worth investigation.

6.4.3 Forecasting of energy demand

The use of short-term weather forecasts in the management of the energy system is now common place. However the use of forecasts with a longer lead-time is much more limited, due to the increase in forecast uncertainty. Recent European Union funded research programs are helping to raise awareness of seasonal forecast skill and are encouraging the use of seasonal forecasts by the wider energy industry (e.g. Troccoli et al. 2018). This PhD highlights that even though seasonal predictions can only skilfully forecast the general characteristics of winter climate in the North Atlantic region, they can still provide information that is potentially useful for Britain's energy industry. This and other research (e.g. Clark et al. 2017), suggests it is timely to begin operational production of climate driven energy demand forecasts for Britain in winter. To ensure the effective use of such probabilistic forecasts, close collaboration between industry practitioners and climate forecast producers would be needed.

This research has focussed on the seasonal predictability of winter (December to February) energy demand, with forecasts initialised in early November. The current 'Winter Outlook' report produced by National Grid, is released in mid-October. To fully inform this report a winter forecast with a longer lead time would be beneficial, such as forecasts initialised in early September, or early October. An assessment of forecast skill for both longer lead times and for other periods during the winter (e.g. January to March) would therefore be worth undertaking.

Feedback from a recent Met Office trial where monthly and seasonal climate forecasts were shared with the energy industry, highlighted that monthly forecasts were deemed most useful. Monthly climate forecasts were used to better anticipate energy price fluctuations and energy system running costs, to inform trading positions and to estimate the risk of coming energy shortages. An assessment of the ability of climate forecasts to predict month ahead energy demand would consequently be worth undertaking. In addition, given blocking high pressure systems and their related cold-waves put Britain's energy system under significant strain, improved understanding of the mechanisms and predictability of such events at the monthly and seasonal timescale would also be very useful.

6.5 Concluding remarks

This PhD has highlighted the significant impact of weather and climate variability on the British energy system in winter. Atmospheric circulation is found to play an important role in the generation of weather-driven extreme demand events and in the contribution that wind power can make in meeting that demand. The better quantification of extreme demand risk and the availability of skilful winter demand forecasts, should help the energy industry better prepare for and manage weather-driven demand variability. With the drive to reduce the emissions of greenhouse gases and to increase renewable energy generation, knowledge of the impacts of weather on the energy system will become increasingly important.

6.6 Personal research ambitions

This PhD has given me a strong interest in our ability to forecast societally relevant impacts a season or more ahead. Within this PhD I have focussed on how to establish the underlying climate - impact relationship, explored the synoptic conditions associated with extreme impacts and investigated our ability to give a relevant seasonal forecast. I have shown that atmospheric circulation and dynamics are critical to many aspects of this work, although I have not spent much time exploring the underlying mechanisms of the climate system. The breadth of dynamical processes that can influence the winter in the North Atlantic and European region makes its study fascinating. I would consequently like to better understand the interaction of different forcing factors on European climate, such as the influence of the stratospheric polar vortex or the tropical Pacific. It would also be interesting to understand the role of these teleconnections in mid-latitude blocking and whether their contribution varies between Greenland and Scandinavian blocking events, given their differing impacts.

The ability of climate models to represent these key teleconnections is fundamental for successful forecasting of winter climate in the North Atlantic and European region. I am keen to better understand the current deficiencies of seasonal forecast models and to help investigate those that are particularly relevant for end user decision making. For example, a small change in the location of a persistent blocking high can greatly influence the weather experienced in the UK over an extended period. A study of the ability of current seasonal systems to forecast the details of the atmospheric circulation relevant for UK winter climate would therefore be very interesting. Also I would like to investigate the ability of models to forecast within season variability, for example if any large scale shifts during the season are expected, or if there is a changing risk of extreme events.

Decision makers often have a set timetable for making their decisions throughout the year, consequently an assessment of the skill of seasonal forecasts across the year, with differing lead times, would improve the usability of such forecasts. With the recent improvements in decadal forecasting of European climate, it would also be interesting to explore whether the current level of prediction skill is useful for societal decision making. For example, is the skill of forecasting annual mean temperature or accumulated rainfall, or their variation through the seasons, useful for energy demand or water resource planning? Alternatively, can a 2 to 5 year mean forecast of climate be informative? With the improving coordination and communication of seasonal and decadal forecasts, society will increasingly expect such forecasts to be used to reduce climate related impacts. I hope to play my part in helping improve the accuracy and the application of these forecasts.

Bibliography

Altenhoff, A. M., O. Martius, M. Croci-Maspoli, C. Schwierz, and H. C. Davies, 2008: Linkage of atmospheric blocks and synoptic-scale Rossby waves: a climatological analysis. *Tellus Series A - Dynamic Meteorology and Oceanography*, **60 (5)**, 1053–1063, doi: {10.1111/j.1600-0870.2008.00354.x}.

Anstey, J. A. and T. G. Shepherd, 2014: High-latitude influence of the quasi-biennial oscillation. *Quarterly Journal of the Royal Meterological Society*, **140 (678, A)**, 1–21, doi: {10.1002/qj.2132}.

Apadula, F., A. Bassini, A. Elli, and S. Scapin, 2012: Relationships between meteorological variables and monthly electricity demand. *Applied Energy*, **98**, 346–356, doi: {10.1016/j.apenergy.2012.03.053}.

Arvizu, D., et al., 2011: Direct Solar Energy: In IPCC Special Report on Renewable Energy Sources and Climate Change Mitigation. Cambridge University Press, Cambridge, United Kingdom and New York, NY, USA.

Athanasiadis, P. J., et al., 2014: The Representation of Atmospheric Blocking and the Associated Low-Frequency Variability in Two Seasonal Prediction Systems. *Journal of Climate*, **27 (24)**, 9082–9100, doi: {10.1175/JCLI-D-14-00291.1}.

Athanasiadis, P. J., et al., 2017: A Multisystem View of Wintertime NAO Seasonal Predictions. *Journal of Climate*, **30 (4)**, 1461–1475, doi: {10.1175/JCLI-D-16-0153.1}.

Bacon, S. and D. Carter, 1993: A connection between mean wave height and atmospheric-pressure gradient in the North-Atlantic. *International Journal of Climatology*, **13 (4)**, 423–436, doi: {10.1002/joc.3370130406}.

Baker, L. H., L. C. Shaffrey, R. T. Sutton, A. Weisheimer, and A. A. Scaife, 2018: An Intercomparison of Skill and Overconfidence/Underconfidence of the Wintertime North Atlantic Oscillation in Multimodel Seasonal Forecasts. *Geophysical Research Letters*, **45 (15)**, 7808–7817, doi: {10.1029/2018GL078838}.

Baldwin, M. and T. Dunkerton, 2001: Stratospheric harbingers of anomalous weather regimes. *Science*, **294 (5542)**, 581–584, doi: {10.1126/science.1063315}.

Barnston, A. G., M. K. Tippett, M. L. L'Heureux, S. Li, and D. G. DeWitt, 2012: Skill of Real-time Seasonal ENSO model predictions during 2002-11. Is our capability increasing? *Bulletin of the American Meteorological Society*, **93 (5)**, 631–651, doi: {10.1175/BAMS-D-11-00111.1}.

Beerli, R., H. Wernli, and C. M. Grams, 2017: Does the lower stratosphere provide predictability for month-ahead wind electricity generation in Europe? *Quarterly Journal of the Royal Meteorological Society*, **143 (709, B)**, 3025–3036, doi: {10.1002/qj.3158}.

BEIS, 2017: Energy Consumption in the UK, Department for Business, Energy and Industrial Strategy. `https://assets.publishing.service.gov.uk/government/uploads/system/uploads/attachment_data/file/633503/ECUK_2017.pdf`.

BEIS, 2018: Digest of United Kingdom Energy Statistics. `https://www.gov.uk/government/statistics/digest-of-uk-energy-statistics-dukes-2018-main-report`.

Bessec, M. and J. Fouquau, 2008: The non-linear link between electricity consumption and temperature in europe: A threshold panel approach. *Energy Economics*, **30 (5)**, 2705 – 2721, doi: {http://dx.doi.org/10.1016/j.eneco.2008.02.003}, URL `http://www.sciencedirect.com/science/article/pii/S0140988308000418`.

Best, M. J., et al., 2011: The Joint UK Land Environment Simulator (JULES), model description - Part 1: Energy and water fluxes. *Geoscientific Model Development*, **4 (3)**, 677–699, doi: {10.5194/gmd-4-677-2011}.

Bett, P. E. and H. E. Thornton, 2016: The climatological relationships between wind and solar energy supply in Britain. *Renewable Energy*, **87 (1)**, 96–110, doi: {10.1016/j.renene.2015.10.006}.

Bett, P. E., et al., 2017: Skill and Reliability of Seasonal Forecasts for the Chinese Energy Sector. *Journal of Applied Meteorology and Climatology*, **56 (11)**, 3099–3114, doi: {10.1175/JAMC-D-17-0070.1}.

Bett, P. E., et al., 2018: Seasonal forecasts of the summer 2016 yangtze river basin rainfall. *Advances in Atmospheric Sciences*, **35 (8)**, 918–926, doi: 10.1007/s00376-018-7210-y.

Bianco, V., F. Scarpa, and L. Tagliafico, 2014: Scenario analysis of nonresidential natural gas consumption in Italy. *Applied Energy*, **113 (SI)**, 392–403, doi: {10.1016/j.apenergy.2013.07.054}.

Bindoff, N. e. a., 2013: *Detection and Attribution of Climate Change: from Global to Regional*, chap. 10. Cambridge University Press, Cambridge, United Kingdom and New York, NY, USA.

Black, E., M. Blackburn, G. Harrison, B. Hoskins, and J. Methven, 2006: Factors contributing to the summer 2003 European heatwave. *Weather*, **59 (8)**, 217–223, doi: {10.1256/wea.74.04}.

Blackmon, M. L., 1976: A climatological spectral study of the 500mb geopotential height of the Northern Hemisphere. *Journal of Atmospheric Science*, **33**, 1607–1623.

Bloomfield, H., D. Brayshaw, L. Shaffrey, P. Coker, and H. Thornton, 2018: The changing sensitivity of power systems to meteorological drivers: a case study of Great Britain. *Environmental Research Letters*, **13 (054028)**, doi: 0.1088/1748-9326/aabff9.

Bloomfield, H. C., D. J. Brayshaw, L. C. Shaffrey, P. J. Coker, and H. E. Thornton, 2016: Quantifying the increasing sensitivity of power systems to climate variability. *Environmental Research Letters*, **11 (12)**, doi: {10.1088/1748-9326/11/12/124025}.

Boer, G. J. and K. Hamilton, 2008: QBO influence on extratropical predictive skill. *Climate Dynamics*, **31 (7-8)**, 987–1000, doi: {10.1007/s00382-008-0379-5}.

Branstator, G., 1995: Organization of storm track anomalies by recurring low-frequency circulation anomalies. *Journal of the Atmospheric Sciences*, **52 (2)**, 207–226, doi: 10.1175/1520-0469(1995)052⟨0207:OOSTAB⟩2.0.CO;2.

Brayshaw, D. J., C. Dent, and S. Zachary, 2012: Wind generation's contribution to supporting peak electricity demand - meteorological insights. *Proceedings of the Institution of Mechanical Engineers Part O - Journal of Risk and Reliability*, **226 (O1, SI)**, 44–50.

Brayshaw, D. J., B. Hoskins, and M. Blackburn, 2009: The Basic Ingredients of the North Atlantic Storm Track. Part I: Land-Sea Contrast and Orography. *Journal of the Atmospheric Sciences*, **66 (9)**, 2539–2558, doi: {10.1175/2009JAS3078.1}.

Brayshaw, D. J., A. Troccoli, R. Fordham, and J. Methven, 2011: The impact of large scale atmospheric circulation patterns on wind power generation and its potential predictability: A case study over the UK. *Renewable Energy*, **36 (8)**, 2087–2096, doi: {10.1016/j.renene.2011.01.025}.

Broennimann, S., 2007: Impact of El Nino Southern Oscillation on European climate. *Reviews of Geophysics*, **45 (2)**, doi: {10.1029/2006RG000199}.

Brown, S. J., J. Caesar, and C. A. T. Ferro, 2008: Global changes in extreme daily temperature since 1950. *Journal of Geophysical Research – Atmospheres*, **113**.

Butler, A. H., L. M. Polvani, and C. Deser, 2014: Separating the stratospheric and tropospheric pathways of El Nino-Southern Oscillation teleconnections. *Environmental Research Letters*, **9 (2)**, doi: {10.1088/1748-9326/9/2/024014}.

Cane, M., S. Zebiak, and S. Dolan, 1986: Experimental Forecasts of El-Nino. *Nature*, **321 (6073)**, 827–832, doi: {10.1038/321827a0}.

Cannon, D. J., D. J. Brayshaw, J. Methven, P. J. Coker, and D. Lenaghan, 2015: Using reanalysis data to quantify extreme wind power generation statistics: A 33 year case study in Great Britain. *Renewable Energy*, **75**, 767–778, doi: {10.1016/j.renene.2014.10.024}.

Cassou, C., L. Terray, J. Hurrell, and C. Deser, 2004: North Atlantic Winter Climate Regimes: Spatial Asymmetry, Stationarity with Time, and Oceanic Forcing. *Journal of Climate*, **17 (5)**, 1055–1068.

Cattiaux, J., R. Vautard, C. Cassou, P. Yiou, V. Masson-Delmotte, and F. Codron, 2010: Winter 2010 in Europe: A cold extreme in a warming climate. *Geophysical Research Letters*, **37**, doi: {10.1029/2010GL044613}.

Cho, H., Y. Goude, X. Brossat, and Q. Yao, 2013: Modeling and Forecasting Daily Electricity Load Curves: A Hybrid Approach. *Journal of the Americal Statistical Association*, **108**, 7–21.

Clark, R. T., P. E. Bett, H. E. Thornton, and A. A. Scaife, 2017: Skilful seasonal predictions for the European energy industry. *Environmental Research Letters*, **12 (2)**, doi: {10.1088/1748-9326/aa57ab}.

Climate Change Committee, 2009: Meeting carbon budgets - the need for a step change. `https://www.theccc.org.uk/publication/meeting-carbon-budgets-the-need-for-a-step-change-1st-progress-report/`.

Climate Change Committee, 2015: Power sector scenarios for the fifth carbon budget. https://www.theccc.org.uk/wp-content/uploads/2015/10/Power-sector-scenarios-for-the-fifth-carbon-budget.pdf.

Coles, S., 2001: An introduction to statistical modeling of extreme values. Springer-Verlag London, London.

Cradden, L. C., F. McDermott, L. Zubiate, C. Sweeney, and M. O'Malley, 2017: A 34-year simulation of wind generation potential for Ireland and the impact of large-scale atmospheric pressure patterns. *Renewable Energy*, **106**, 165–176, doi: {10.1016/j.renene.2016.12.079}.

Croci-Maspoli, M. and H. C. Davies, 2009: Key Dynamical Features of the 2005/06 European Winter. *Monthly Weather Review*, **137 (2)**, 664–678, doi: {10.1175/2008MWR2533.1}.

Croxton, P. J., K. Huber, N. Collinson, and T. H. Sparks, 2006: How well do the Central England Temperature and the England and Wales Precipitation Series represent the climate of the UK? *International Journal of Climatology*, **26**, 2287–2292.

Czaja, A. and C. Frankignoul, 2002: Observed impact of Atlantic SST anomalies on the North Atlantic oscillation. *Journal of Climate*, **15 (6)**, 606–623, doi: {10.1175/1520-0442(2002)015⟨0606:OIOASA⟩2.0.CO;2}.

De Felice, M., A. Alessandri, and F. Catalano, 2015: Seasonal climate forecasts for medium-term electricity demand forecasting. *Applied Energy*, **137**, 435–444, doi: {10.1016/j.apenergy.2014.10.030}.

De Felice, M., A. Alessandri, and P. M. Ruti, 2013: Electricity demand forecasting over Italy: Potential benefits using numerical weather prediction models. *Electric Power Systems Research*, **104**, 71–79.

DECC, 2009: The UK renewable energy strategy. https://www.gov.uk/government/publications/the-uk-renewable-energy-strategy.

DECC, 2011: Statutory Security of Supply Report, November 2010. https://assets.publishing.service.gov.uk/government/uploads/system/uploads/attachment_data/file/47960/803-security-of-supply-report.pdf.

DECC, 2012: Call for Evidence: Energy Efficiency, Office of Energy Efficiency. https://www.gov.uk/government/uploads/system/uploads/attachment_ data/file/42899/4286-call-for-evidence-energy-efficiency-deplyment-off.pdf.

DECC, 2013: Electricity Market Reform Delivery Plan. https://www.gov.uk/government/publications/electricity-market-reform-delivery-plan.

DECC, 2013: Energy consumption in the UK report. https://www.gov.uk/government/publications/energy-consumption-in-the-uk.

DECC, 2016: Electricity network delivery and access. https://www.gov.uk/guidance/electricity-network-delivery-and-access.

DECC, 2016: Energy Trends: June 2016, special feature article - Renewable energy in 2015. https://www.gov.uk/government/statistics/energy-trends-june-2016-special-feature-article-renewable-energy-in-2015.

Dee, D. P., et al., 2011: The ERA-Interim reanalysis: configuration and performance of the data assimilation system. *Quaterly Journal of the Royal Meteorological Society*, **137 (656, A)**, 553–597, doi: {10.1002/qj.828}.

Delworth, T. L., F. Zeng, L. Zhang, R. Zhang, G. A. Vecchi, and X. Yang, 2017: The Central Role of Ocean Dynamics in Connecting the North Atlantic Oscillation to the Extratropical Component of the Atlantic Multidecadal Oscillation. *Journal of Climate*, **30 (10)**, 3789–3805, doi: {10.1175/JCLI-D-16-0358.1}.

Deser, C., G. Magnusdottir, R. Saravanan, and A. Phillips, 2004: The effects of North Atlantic SST and sea ice anomalies on the winter circulation in CCM3. Part II: Direct and indirect components of the response. *Journal of Climate*, **17 (5)**, 877–889, doi: {10.1175/1520-0442(2004)017⟨0877:TEONAS⟩2.0.CO;2}.

Deser, C., R. A. Tomas, and S. Peng, 2007: The transient atmospheric circulation response to North Atlantic SST and sea ice anomalies. *Journal of Climate*, **20 (18)**, 4751–4767, doi: {10.1175/JCLI4278.1}.

Drake, B. and K. Hubacek, 2007: What to expect from a greater geographic dispersion of wind farms? - A risk portfolio approach. *Energy Policy*, **35 (8)**, 3999–4008, doi: {10.1016/j.enpol.2007.01.026}.

Drew, D., D. Cannon, D. Brayshaw, J. Barlow, and P. Coker, 2015: The impact of future offshore wind farms on wind power generation in great britain. *Resources Policy*, **4 (1)**, 155–171, URL http://centaur.reading.ac.uk/39743/.

DTU, 2015: Global wind atlas. https://globalwindatlas.info/about/introduction.

Duan, W. and C. Wei, 2013: The 'spring predictability barrier' for ENSO predictions and its possible mechanism: results from a fully coupled model. *International Journal of Climatology*, **33 (5)**, 1280–1292, doi: {10.1002/joc.3513}.

Dunn, R. J. H., K. M. Willett, P. W. Thorne, E. V. Woolley, I. Durre, A. Dai, D. E. Parker, and R. S. Vose, 2012: HadISD: a quality-controlled global synoptic report database for selected variables at long-term stations from 1973-2011. *Climate of the Past*, **8 (5)**, 1649–1679, doi: 10.5194/cp-8-1649-2012.

Dunstone, N., D. Smith, A. Scaife, L. Hermanson, R. Eade, N. Robinson, M. Andrews, and J. Knight, 2016: Skilful predictions of the winter North Atlantic Oscillation one year ahead. *Nature Geoscience*, **9 (11)**, 809+, doi: {10.1038/ngeo2824}.

Eade, R., D. Smith, A. Scaife, E. Wallace, N. Dunstone, L. Hermanson, and N. Robinson, 2014: Do seasonal-to-decadal climate predictions underestimate the predictability of the real world? *Geophysical Research Letters*, **41 (15)**, 5620–5628, doi: {10.1002/2014GL061146}.

Ely, C. R., D. J. Brayshaw, J. Methven, J. Cox, and O. Pearce, 2013: Implications of the North Atlantic Oscillation for a UK Norway Renewable power system. *Energy Policy*, **62**, 1420–1427, doi: {10.1016/j.enpol.2013.06.037}.

Engie, 2016: Understanding the capacity market. http://www.engie.co.uk/wp-content/uploads/2016/07/capacitymarketguide.pdf.

EU, 2009: Directive 2009/28/EC of the European Parliament and of the Council. http://eur-lex.europa.eu/legal-content/EN/TXT/?uri=CELEX%3A32009L0028.

European Commission, 2009: Directive 2009/28/ec of the european parliament and of the council of 23 april 2009 on the promotion of the use of energy from renewable sources. https://eur-lex.europa.eu/legal-content/EN/ALL/?uri=CELEX:32009L0028,.

Fereday, D., J. Knight, A. Scaife, C. Folland, and A. Philipp, 2008: Cluster analysis of North Atlantic-European circulation types and links with tropical Pacific sea surface temperatures. *Journal of Climate*, **21 (15)**, 3687–3703.

Fereday, D. R., A. Maidens, A. Arribas, A. A. Scaife, and J. R. Knight, 2012: Seasonal forecasts of northern hemisphere winter 2009/10. *Environmental Research Letters*, **7 (3)**, doi: {10.1088/1748-9326/7/3/034031}.

Fischer, E. M., S. I. Seneviratne, P. L. Vidale, D. Luethi, and C. Schaer, 2007: Soil moisture - Atmosphere interactions during the 2003 European summer heat wave. *Journal of Climate*, **20 (20)**, 5081–5099, doi: {10.1175/JCLI4288.1}.

Fischer, M., 2010: *Modelling and forecasting energy demand: principles and difficulties. In Management of Weather and Climate Risk in the Energy Industry*. doi: {10.1007/978-90-481-3692-6}.

Foley, A. M., P. G. Leahy, A. Marvuglia, and E. J. McKeogh, 2012: Current methods and advances in forecasting of wind power generation. *Renewable Energy*, **37 (1)**, 1–8, doi: {10.1016/j.renene.2011.05.033}.

Folland, C. K., A. A. Scaife, J. Lindesay, and D. B. Stephenson, 2012: How potentially predictable is northern European winter climate a season ahead? *International Journal of Climatology*, **32 (6)**, 801–818, doi: {10.1002/joc.2314}.

Fraedrich, K. and K. Muller, 1992: Climate anomalies in Europe associated with ENSO extremes. *International Journal of Climatology*, **12 (1)**, 25–31, doi: {10.1002/joc.3370120104}.

Grams, C. M., R. Beerli, S. Pfenninger, I. Staffell, and H. Wernli, 2017: Balancing Europe's wind-power output through spatial deployment informed by weather regimes. *Nature Climate Change*, **7 (8)**, 557–562, doi: {10.1038/NCLIMATE3338}.

Gray, L. J., et al., 2013: A lagged response to the 11 year solar cycle in observed winter Atlantic/European weather patterns. *Journal of Geophysical Research-Atmospheres*, **118 (24)**, 13 405–13 420, doi: {10.1002/2013JD020062}.

Grubb, M., L. Butler, and P. Twomey, 2006: Diversity and security in UK electricity generation: The influence of low-carbon objectives. *Energy Policy*, **34 (18)**, 4050–4062, doi: {10.1016/j.enpol.2005.09.004}.

Hahn, H., S. Meyer-Nieberg, and S. Pickl, 2009: Electric load forecasting methods: Tools for decision making. *European Journal of Operational Research*, **199**, 902–907.

Haigh, J. and P. Cargill, 2015: *The Sun's Influence on Climate*.

Hall, R. J., A. A. Scaife, E. Hanna, J. M. Jones, and R. Erdelyi, 2017: Simple Statistical Probabilistic Forecasts of the Winter NAO. *Weather and Forecasting*, **32 (4)**, 1585–1601, doi: {10.1175/WAF-D-16-0124.1}.

Harrison, G. P., S. L. Hawkins, D. Eager, and L. C. Cradden, 2015: Capacity value of offshore wind in Great Britain. *Proceedings of the Institution of Mechanical Engineers Part O - Journal of Risk and Reliability*, **229 (5, SI)**, 360–372, doi: {10.1177/1748006X15591619}.

Hartmann, D. e. a., 2013: *Observations: Atmosphere and Surface*, chap. 2, 159–254. Cambridge University Press, Cambridge, United Kingdom and New York, NY, USA.

Hekkenberg, M., R. Benders, H. Moll, and A. S. Uiterkamp, 2009: Indications for a changing electricity demand pattern: The temperature dependence of electricity demand in the netherlands. *Energy Policy*, **37 (4)**, 1542 – 1551, doi: http://dx.doi.org/10.1016/j.enpol.2008.12.030.

Henley, A. and J. Peirson, 1997: Non-linearities in electricity demand and temperature: Parametric versus non-parametric methods. *Oxford Bulletin of Economics and Statistics*, **59**, 149–&.

Holton, J. and H. Tan, 1980: The Influence of the Equatorial Quasi-Biennial Oscillation on the Global Circulation at 50 mb. *Journal of the Atmospheric Sciences*, **37 (2)**, 2200–2208.

Holton, J. R., 1992: *An Introduction to Dynamic Meteorology*. Academic Press Limited, Oval Road, London.

Hor, C., S. Watson, and S. Majithia, 2005: Analyzing the impact of weather variables on monthly electricity demand. *IEEE Transactions on Power Systems*, **20**, 2078–2085.

Hoskins, B. and I. James, 2014: *Fluid Dynamics of the Mid-Latitude Atmosphere*. Advancing Weather and Climate Science, Wiley, URL `https://books.google.co.uk/books?id=2o9ZBAAAQBAJ`.

Hoskins, B. and D. Karoly, 1981: The steady linear response of a spherical atmosphere to thermal and orographic forcing. *Journal of the Atmospheric Sciences*, **38 (6)**, 1179–1196, doi: {10.1175/1520-0469(1981)038⟨1179:TSLROA⟩2.0.CO;2}.

Hoskins, B. and P. Valdes, 1990: On the existence of storm-tracks. *Journal of the Atmospheric Sciences*, **47 (15)**, 1854–1864, doi: {10.1175/1520-0469(1990)047⟨1854:OTEOST⟩2.0.CO;2}.

Hunke, E. and W. Lipscomb, 2010: Cice: The sea ice model documentation and software users manual, version 4.1. Technical report LA-CC-06-012. Los Alamos National Laboratory: Los Alamos, NM.

Huntingford, C., et al., 2014: Potential influences on the United Kingdom's floods of winter 2013/14. *Nature Climate Change*, **4 (9)**, 769–777, doi: {10.1038/NCLIMATE2314}.

Huntington, H., 2007: Industrial Natural Gas Consumption in the United States: An Empirical Model for Evaluating Future Trends. *Energy Economics*, **29 (4)**, 743–759.

Hurrell, J. and C. Deser, 2009: North atlantic climate variability: The role of the north atlantic oscillation. *Journal of Marine Systems*, **78**, doi: 10.1016/j.jmarsys.2008.11.026.

Hurrell, J. W., 1995: Decadal trends in the North Atlantic Oscillation - regional temperatures and precipitation. *Science*, **269 (5224)**, 676–679, doi: 10.1126/science.269.5224.676.

Huth, R., 1996: An intercomparison of computer-assisted circulation classification methods. *International Journal of Climatology*, **16 (8)**, 893–922, doi: {10.1002/(SICI)1097-0088(199608)16:8⟨893::AID-JOC51⟩3.0.CO;2-Q}.

Ineson, S., A. A. Scaife, J. R. Knight, J. C. Manners, N. J. Dunstone, L. J. Gray, and J. D. Haigh, 2011: Solar forcing of winter climate variability in the Northern Hemisphere. *Nature Geoscience*, **4 (11)**, 753–757, doi: {10.1038/NGEO1282}.

International Energy Agency, 2016: Energy policites of iea countries, france, 2016 review. `https://webstore.iea.org/download/direct/307`.

James, I., 1994: *Introduction to Circulating Atmospheres*. Cambridge University Press.

Jerez, S., R. M. Trigo, S. M. Vicente-Serrano, D. Pozo-Vazquez, R. Lorente-Plazas, J. Lorenzo-Lacruz, F. Santos-Alamillos, and J. P. Montavez, 2013: The Impact of the North Atlantic Oscillation on Renewable Energy Resources in Southwestern

Europe. *Journal of Applied Meteorology and Climatology*, **52 (10)**, 2204–2225, doi: {10.1175/JAMC-D-12-0257.1}.

Kang, D., et al., 2014: Prediction of the Arctic Oscillation in boreal winter by dynamical seasonal forecasting systems. *Geophysical Research Letters*, **41 (10)**, 3577–3585, doi: {10.1002/2014GL060011}.

Karpechko, A. Y., K. A. Peterson, A. A. Scaife, J. Vainio, and H. Gregow, 2015: Skilful seasonal predictions of Baltic Sea ice cover. *Environmental Research Letters*, **10 (4)**, doi: {10.1088/1748-9326/10/4/044007}.

Kendon, M. and M. McCarthy, 2015: The UK's wet and stormy winter of 2013/2014. *Weather*, **70 (2, SI)**, 40–47, doi: {10.1002/wea.2465}.

Kerr, R., 2000: A North Atlantic climate pacemaker for the centuries. *Science*, **288 (5473)**, 1984–1986, doi: {10.1126/science.288.5473.1984}.

Kidston, J., A. A. Scaife, S. C. Hardiman, D. M. Mitchell, N. Butchart, M. P. Baldwin, and L. J. Gray, 2015: Stratospheric influence on tropospheric jet streams, storm tracks and surface weather. *Nature Geoscience*, **8 (6)**, 433–440, doi: {10.1038/NGEO2424}.

Kirtman, B. P., et al., 2014: The North American Multimodel Ensemble Phase-1 Seasonal-to-Interannual Prediction; Phase-2 toward Developing Intraseasonal Prediction. *Bulletin of the American Meteorological Society*, **95 (4)**, 585–601, doi: {10.1175/BAMS-D-12-00050.1}.

Knight, J., R. Allan, C. Folland, M. Vellinga, and M. Mann, 2005: A signature of persistent natural thermohaline circulation cycles in observed climate. *Geophysical Research Letters*, **32 (20)**, doi: {10.1029/2005GL024233}.

Knight, J. R., C. K. Folland, and A. A. Scaife, 2006: Climate impacts of the Atlantic Multidecadal Oscillation. *Geophysical Research Letters*, **33 (17)**, doi: {10.1029/2006GL026242}.

Knight, J. R., et al., 2017: Global meteorological influences on the record UK rainfall of winter 2013-14. *Environmental Research Letters*, **12 (7)**, doi: {10.1088/1748-9326/aa693c}.

Koster, R. and M. Suarez, 2003: Impact of land surface initialization on seasonal precipitation and temperature prediction. *Journal of Hydrometeorology*, **4 (2)**, 408–423, doi: {10.1175/1525-7541}.

Kumar, A., et al., 2011: Hydropower: In IPCC Special Report on Renewable Energy Sources and Climate Change Mitigation. Cambridge University Press, Cambridge, United Kingdom and New York, NY, USA.

Lamb, H. H., 1972: British isles weather types and a register of daily sequence of circulation patterns, 1861-1971. *Geophysical Memoir*, **116 (7)**, 85.

Lau, N.-C., 1988: Variability of the observed midlatitude storm tracks in relation to low-frequency changes in the circulation pattern. *Journal of the Atmospheric Sciences*, **45 (19)**, 2718–2743, doi: 10.1175/1520-0469(1988)045⟨2718:VOTOMS⟩2.0.CO;2.

Le Comte, D. and H. Warren, 1981: Modeling the Impact of Summer Temperatures on National Electricity Consumption. *Journal of Applied Meteorology*, **20 (12)**, 1415–1419, doi: {10.1175/1520-0450(1981)020⟨1415:MTIOST⟩2.0.CO;2}.

Leahy, P. and A. Foley, 2012: Wind generation output during cold weather-driven electricity demand peaks in Ireland. *Energy*, **39 (1)**, 48 – 53, doi: http://dx.doi.org/10.1016/j.energy.2011.07.013.

Leahy, P. G. and E. J. McKeogh, 2013: Persistence of low wind speed conditions and implications for wind power variability. *Wind Energy*, **16 (4)**, 575–586, doi: {10.1002/we.1509}.

Lockwood, M., R. G. Harrison, T. Woollings, and S. K. Solanki, 2010: Are cold winters in Europe associated with low solar activity? *Environmental Research Letters*, **5 (2)**, doi: {10.1088/1748-9326/5/2/024001}.

Lopes, F. M., H. G. Silva, R. Salgado, A. Cavaco, P. Canhoto, and M. Collares-Pereira, 2018: Short-term forecasts of GHI and DNI for solar energy systems operation: assessment of the ECMWF integrated forecasting system in southern Portugal. *Solar Energy*, **170**, 14–30, doi: {10.1016/j.solener.2018.05.039}.

Luo, J.-J., S. Masson, S. K. Behera, and T. Yamagata, 2008: Extended ENSO predictions using a fully coupled ocean-atmosphere model. *Journal of Climate*, **21 (1)**, 84–93, doi: {10.1175/2007JCLI1412.1}.

Lynch, K. J., D. J. Brayshaw, and A. Charlton-Perez, 2014: Verification of European Subseasonal Wind Speed Forecasts. *Monthly Weather Review*, **142 (8)**, 2978–2990, doi: {10.1175/MWR-D-13-00341.1}.

MacLachlan, C., et al., 2015: Global Seasonal forecast system version 5 (GloSea5): a high-resolution seasonal forecast system. *Quarterly Journal of the Royal Meteorological Society*, **141 (689, B)**, 1072–1084, doi: {10.1002/qj.2396}.

Madec, G., 2008: *NEMO ocean engine*. Note du Pole de modelisation, Institut Pierre-Simon Laplace (IPSL), France, No 27, ISSN No 1288-1619.

Maidens, A., A. Arribas, A. A. Scaife, C. MacLachlan, D. Peterson, and J. Knight, 2013: The Influence of Surface Forcings on Prediction of the North Atlantic Oscillation Regime of Winter 2010/11. *Monthly Weather Review* , **141 (11)**, 3801–3813, doi: {10.1175/MWR-D-13-00033.1}.

Manwell, J. F., J. G. McGowan, and A. L. Rogers, 2002: *Wind Energy Explained*. John Wiley & Sons, Ltd, doi: {10.1002/0470846127}.

Marshall, A. G. and A. A. Scaife, 2009: Impact of the QBO on surface winter climate. *Journal of Geophysical Research-Atmospheres*, **114**, doi: {10.1029/2009JD011737}.

Marshall, A. G. and A. A. Scaife, 2010: Improved predictability of stratospheric sudden warming events in an atmospheric general circulation model with enhanced stratospheric resolution. *Journal of Geophysical Research-Atmospheres*, **115**, doi: {10.1029/2009JD012643}.

Marshall, J., et al., 2001: North Atlantic climate variability: Phenomena, impacts and mechanisms. *International Journal of Climatology*, **21 (15)**, 1863–1898, doi: {10.1002/joc.693}.

Matthews, T., C. Murphy, R. L. Wilby, and S. Harrigan, 2014: Stormiest winter on record for Ireland and UK. *Nature Climate Change*, **4 (9)**, 738–740, doi: {10.1038/nclimate2336}.

McColl, L., E. Palin, H. Thornton, D. Sexton, R. Betts, and K. Mylne, 2012: Assessing the potential impact of climate change on the UK's electricity network. *Climatic Change*, **115**, 821–835.

Merkel, U. and M. Latif, 2002: A high resolution AGCM study of the El Nino impact on the North Atlantic/European sector. *Geophysical Research Letters*, **29 (9)**, doi: {10.1029/2001GL013726}.

Mirasgedis, S., Y. Sarafidis, E. Georgopoulou, D. Lalas, A. Moschovits, F. Karagiannis, and D. Papakonstantinou, 2006: Models for mid-term electricity demand forecasting incorporating weather influences. *Energy*, **31**, 208–227.

Mitchell, J., P. Beck, and M. Grubb, 1996: The new geopolitics of energy. Royal Institute of International Affairs/Earthscan, London.

Miyakoda, J. S. R. F. S., K. and G. D. Hembree, 1969: Experimental extended predictions with a nine-level hemispheric model. *Monthly Weather Review*, **97**, 1–76.

Molteni, F., et al., 2011: The new ECMWF seasonal forecast system (system 4). ECMWF, Technical Memorandum 656.

Monforti, F., M. Gaetani, and E. Vignati, 2016: How synchronous is wind energy production among European countries? *Renewable & Sustainable Energy Reviews*, **59**, 1622–1638, doi: {10.1016/j.rser.2015.12.318}.

Myhre, G., et al., 2013: *Anthropogenic and natural radiative forcing*, 659–740. Cambridge University Press, Cambridge, UK, doi: 10.1017%2FCBO9781107415324.018.

National Academy of Sciences, 2010: Assessment of Intraseasonal to Interannual Climate Prediction and Predictability. https://www.nap.edu/initiative/committee-on-assessment-of-intraseasonal-to-interannual-climate-prediction-and-predictability.

National Grid, 2011: Winter consultation, 2011/12. https://www.nationalgrideso.com/document/63831/download.

National Grid, 2012a: Gas Demand Forecasting Methodology. https://www.nationalgrid.com/NR/rdonlyres/71CFD0F6-3607-474B-9F37-0952404976FB/52071/GasDemandForecastingMethodologyFeb12.pdf.

National Grid, 2012b: Nets Security and Quality of Supply Standard. http://www2.nationalgrid.com/UK/Industry-information/Electricity-codes/SQSS/The-SQSS/.

National Grid, 2013: Winter Outlook 2013/2014. https://www.nationalgrideso.com/document/63796/download.

National Grid, 2014: Winter Outlook 2014/2015. https:http://www2.nationalgrid.com/UK/Industry-information/Future-of-Energy/FES/Winter-Outlook/.

National Grid, 2016: Gas Demand Forecasting Methodology. https://www.nationalgrid.com/sites/default/files/documents/8589937808-Gas%20Demand%20Forecasting%20Methodology.pdf.

National Grid, 2017: Winter outlook report, 2017/2018. https://www.nationalgrid.com/sites/default/files/documents/Winter%20Outlook%202017.pdf.

National Grid, 2018: Winter Review and Consultation. https://www.nationalgrideso.com/sites/eso/files/documents/2018%20Winter%20Review%20and%20Consultation.pdf.

National Grid, 2018: Winter review and consultation, june 2018. https://www.nationalgrid.com/sites/default/files/documents/2018%20Winter%20Review%20and%20Consultation%20FINAL%20v2.pdf.

National Grid, 2019: Future energy scenarios. http://fes.nationalgrid.com/media/1409/fes-2019.pdf.

NCIC, 2018: National Climate Information Centre, UK Climate Statistics. https://www.metoffice.gov.uk/climate.

Ofgem, 2015: Electricity security of supply. https://www.ofgem.gov.uk/electricity/wholesale-market/electricity-security-supply.

Osborn, T., D. Conway, M. Hulme, J. Gregory, and P. Jones, 1999: Air flow influences on local climate: observed and simulated mean relationships for the United Kingdom. *CLIMATE RESEARCH*, **13 (3)**, 173–191, doi: {10.3354/cr013173}.

Oswald, J., M. Raine, and H. Ashraf-Ball, 2008: Will British weather provide reliable electricity? *Energy Policy*, **36 (8)**, 3212–3225, doi: {10.1016/j.enpol.2008.04.033}.

Palin, E. J., A. A. Scaife, E. Wallace, E. C. D. Pope, A. Arribas, and A. Brookshaw, 2016: Skillful Seasonal Forecasts of Winter Disruption to the U.K. Transport System. *Journal of Applied Meteorology and Climatology*, **55 (2)**, 325–344, doi: {10.1175/JAMC-D-15-0102.1}.

Palmer, T., et al., 2004: Development of a European multimodel ensemble system for seasonal-to-interannual prediction (DEMETER). *Bulletin of the American Meteorological Society*, **85 (6)**, 853+, doi: {10.1175/BAMS-85-6-853}.

Parker, D., T. Legg, and C. Folland, 1992: A new daily central England temperature series, 1772-1991. *International Journal of Climatology*, **12**, 317–342.

Pelly, J., 2001: The predictability of atmospheric blocking. Phd thesis, Reading University. `http://www.met.rdg.ac.uk/phdtheses/Thepredictabilityofatmosphericblocking.pdf`.

Pfahl, S., C. Schwierz, M. Croci-Maspoli, C. M. Grams, and H. Wernli, 2015: Importance of latent heat release in ascending air streams for atmospheric blocking. *Nature Geoscience*, **8 (8)**, 610+, doi: {10.1038/NGEO2487}.

Philander, S., 1989: *El Nino, La Nina and the Southern Oscillation*. Academic Press.

Pinheiro, M. C., P. A. Ullrich, and R. Grotjahn, 2019: Atmospheric blocking and intercomparison of objective detection methods: flow field characteristics. *Climate Dynamics*, **53 (7-8)**, 4189–4216, doi: {10.1007/s00382-019-04782-5}.

Pohlmann, H., et al., 2013: Improved forecast skill in the tropics in the new MiKlip decadal climate predictions. *Geophysical Research Letters*, **40 (21)**, 5798–5802, doi: {10.1002/2013GL058051}.

Pozo-Vazquez, D., M. Esteban-Parra, F. Rodrigo, and Y. Castro-Diez, 2001: The association between ENSO and winter atmospheric circulation and temperature in the North Atlantic region. *Journal of Climate*, **14 (16)**, 3408–3420, doi: {10.1175/1520-0442(2001)014⟨3408:TABEAW⟩2.0.CO;2}.

Prior, J. and M. Kendon, 2011: The UK winter of 2009/2010 compared with severe winters of the last 100 years. *Weather*, **66 (1)**, 4–10, doi: {10.1002/wea.735}.

Psiloglou, B., C. Giannakopoulos, S. Majithia, and M. Petrakis, 2009: Factors affecting electricity demand in Athens, Greece and London, UK: A comparative assessment. *Energy*, **34**, 1855 – 1863.

Rex, D., 1950: Blocking Action in the Middle Troposphere and its Effect upon Regional Climate. II. The Climatology of Blocking Action. *Tellus*, **2**, 275–301.

Riddle, E. E., A. H. Butler, J. C. Furtado, J. L. Cohen, and A. Kumar, 2013: CFSv2 ensemble prediction of the wintertime Arctic Oscillation. *Climate Dynamics*, **41 (3-4)**, 1099–1116, doi: {10.1007/s00382-013-1850-5}.

Robock, A., 2000: Volcanic eruptions and climate. *Reviews of Geophysics*, **38 (2)**, 191–219, doi: {10.1029/1998RG000054}.

Rodwell, M. and C. Folland, 2002: Atlantic air-sea interaction and seasonal predictability. *Quarterly Journal of the Royal Meteorological Society*, **128 (583, A)**, 1413–1443, doi: {10.1256/00359000260247291}.

Rodwell, M., D. Rowell, and C. Folland, 1999: Oceanic forcing of the wintertime North Atlantic Oscillation and European climate. *Nature*, **398 (6725)**, 320–323, doi: {10.1038/18648}.

Rodwell, M. J. and F. J. Doblas-Reyes, 2006: Medium-range, monthly, and seasonal prediction for Europe and the use of forecast information. *Journal of Climate*, **19 (23)**, 6025–6046, doi: {10.1175/JCLI3944.1}, Climate Variability and Predictability Workshop on Atlantic Predictability, Univ Reading, Reading, ENGLAND, APR, 2004.

Rogers, J., 1990: Patterns of low-frequency monthly sea-level pressure variability (1899-1986) and associated wave cyclone frequencies. *Journal of Climate*, **3 (12)**, 1364–1379, doi: {10.1175/1520-0442(1990)003⟨1364:POLFMS⟩2.0.CO;2}.

Royal Academy of Engineering, 2013: Gb electricity capacity margin. `https://www.raeng.org.uk/publications/reports/gb-electricity-capacity-margin`.

Saha, S., et al., 2006: The NCEP Climate Forecast System. *Journal of Climate*, **19 (15)**, 3483–3517, doi: {10.1175/JCLI3812.1}.

Sailor, D. and J. Munoz, 1997: Sensitivity of electricity and natural gas consumption to climate in the USA - Methodology and results for eight states. *ENERGY*, **22 (10)**, 987–998, doi: {10.1016/S0360-5442(97)00034-0}.

Sailor, D., J. Rosen, and J. Munoz, 1998: Natural gas consumption and climate: A comprehensive set of predictive state-level models for the United States. *Energy*, **23**, 91–103.

Santos-Alamillos, F. J., D. Pozo-Vazquez, J. A. Ruiz-Arias, V. Lara-Fanego, and J. Tovar-Pescador, 2014: A methodology for evaluating the spatial variability of wind energy resources: Application to assess the potential contribution of wind energy to baseload power. *Renewable Energy*, **69**, 147–156, doi: {10.1016/j.renene.2014.03.006}.

Scaife, A. A. and D. Smith, 2018: A signal-to-noise paradox in climate science. *npj Clim. Atm. Sci.*, doi: {10.1038/s41612-018-0038-4}.

Scaife, A. A., et al., 2011: Improved Atlantic winter blocking in a climate model. *Geophysical Research Letters*, **38**, doi: {10.1029/2011GL049573}.

Scaife, A. A., et al., 2014a: Predictability of the quasi-biennial oscillation and its northern winter teleconnection on seasonal to decadal timescales. *Geophysical Research Letters*, **41 (5)**, 1752–1758, doi: {10.1002/2013GL059160}.

Scaife, A. A., et al., 2014b: Skillful long-range prediction of European and North American winters. *Geophysical Research Letters*, **41 (7)**, 2514–2519, doi: {10.1002/2014GL059637}.

Scaife, A. A., et al., 2017: Tropical rainfall, Rossby waves and regional winter climate predictions. *Quarterly Journal of the Royal Meteorological Society*, **143 (702)**, 1–11, doi: {10.1002/qj.2910}.

Screen, J. A., 2017: The missing Northern European winter cooling response to Arctic sea ice loss. *Nature Communications*, **8**, doi: {10.1038/ncomms14603}.

Shabbar, A., J. Huang, and K. Higuchi, 2001: The relationship between the wintertime North Atlantic Oscillation and blocking episodes in the North Atlantic. *International Journal of Climatology*, **21 (3)**, 355+, doi: {10.1002/joc.612}.

Shutts, G., 1983: The propagation of eddies in diffulent jetstreams - eddy vorticity forcing of blocking flow-fields. *Quarterly Journal of the Royal Meteorological Society*, **109 (462)**, 737–761, doi: {10.1002/qj.49710946204}.

Siegert, S., D. B. Stephenson, P. G. Sansom, A. A. Scaife, R. Eade, and A. Arribas, 2016: A Bayesian Framework for Verification and Recalibration of Ensemble Forecasts: How Uncertain is NAO Predictability? *Journal of Climate*, **29 (3)**, 995–1012, doi: {10.1175/JCLI-D-15-0196.1}.

Sigmond, M., J. F. Scinocca, V. V. Kharin, and T. G. Shepherd, 2013: Enhanced seasonal forecast skill following stratospheric sudden warmings. *Nature Geoscience*, **6 (2)**, 98–102, doi: {10.1038/NGEO1698}.

Sinden, G., 2007: Characteristics of the UK wind resource: Long-term patterns and relationship to electricity demand. *Energy Policy*, **35 (1)**, 112 – 127, doi: http://dx.doi.org/10.1016/j.enpol.2005.10.003.

Smith, D. M., A. A. Scaife, and B. P. Kirtman, 2012: What is the current state of scientific knowledge with regard to seasonal and decadal forecasting? *Environmental Research Letters*, **7 (1)**, 015 602, URL `http://stacks.iop.org/1748-9326/7/i=1/a=015602`.

Soldo, B., 2012: Forecasting natural gas consumption. *Applied Energy*, **92**, 26–37.

Stockdale, T. N., F. Molteni, and L. Ferranti, 2015: Atmospheric initial conditions and the predictability of the Arctic Oscillation. *Geophysical Research Letters*, **42 (4)**, 1173–1179, doi: {10.1002/2014GL062681}.

Summerfield, A., T. Oreszczyn, I. Hamilton, D. Shipworth, G. Huebner, R. Lowe, and P. Ruyssevelt, 2015: Empirical variation in 24-h profiles of delivered power for a sample of UK dwellings: Implications for evaluating energy savings. *Energy and Buildings*, **88**, 193–202.

Svensson, C., et al., 2015: Long-range forecasts of UK winter hydrology. *Environmental Research Letters*, **10 (6)**, doi: {10.1088/1748-9326/10/6/064006}.

Szoplik, J., 2015: Forecasting of natural gas consumption with artificial neural networks. *Energy*, **85**, 208–220, doi: 10.1016/j.energy.2015.03.084.

Taylor, J., 2010: Triple seasonal methods for short-term electricity demand forecasting. *European Journal of Operational Research*, **204**, 139–152.

Taylor, J. and R. Buizza, 2003: Using weather ensemble predictions in electricity demand forecasting. *International Journal of Forecasting*, **19**, 57 – 70.

Thompson, D., M. Baldwin, and J. Wallace, 2002: Stratospheric connection to Northern Hemisphere wintertime weather: Implications for prediction. *Journal of Climate*, **15 (12)**, 1421–1428, doi: {10.1175/1520-0442(2002)015⟨1421:SCTNHW⟩2.0.CO;2}.

Thompson, V., N. J. Dunstone, A. A. Scaife, D. M. Smith, J. M. Slingo, S. Brown, and S. E. Belcher, 2017: High risk of unprecedented UK rainfall in the current climate. *Nature Communications*, **8**, doi: {10.1038/s41467-017-00275-3}.

Thornton, H. E., B. J. Hoskins, and A. A. Scaife, 2016: The role of temperature in the variability and extremes of electricity and gas demand in Great Britain. *Environmental Research Letters*, **11 (114015)**, doi: {10.1088/1748-9326/11/11/114015}.

Thornton, H. E., A. A. Scaife, B. J. Hoskins, and D. J. Brayshaw, 2017: The relationship between wind power, electricity demand and winter weather patterns in Great Britain. *Environmental Research Letters*, **12 (6)**, doi: {10.1088/1748-9326/aa69c6}.

Tibaldi, S. and F. Molteni, 1990: On the operational predictability of blocking. *Tellus*, **42A**, 343–365.

Timmer, R. and P. Lamb, 2007: Relations between temperature and residential natural gas consumption in the central and eastern United States. *Journal of Applied Meteorology and Climatology*, **46**.

Toniazzo, T. and A. A. Scaife, 2006: The influence of ENSO on winter North Atlantic climate. *Geophysical Research Letters*, **33 (24)**, doi: {10.1029/2006GL027881}.

Torralba, V., F. J. Doblas-Reyes, D. MacLeod, I. Christel, and M. Davis, 2017: Seasonal Climate Prediction: A New Source of Information for the Management of Wind Energy Resources. *Journal of Applied Meteorology and Climatology*, **56 (5)**, 1231–1247, doi: {10.1175/JAMC-D-16-0204.1}.

Trenberth, K. E. and J. T. Fasullo, 2012: Climate extremes and climate change: The Russian heat wave and other climate extremes of 2010. *Journal of Geophysical Research-Atmospheres*, **117**, doi: {10.1029/2012JD018020}.

Trenberth, K. E. and J. T. Fasullo, 2017: Atlantic meridional heat transports computed from balancing Earth's energy locally. *Geophysical Research Letters*, **44 (4)**, 1919–1927, doi: {10.1002/2016GL072475}.

Trenberth, K. E. and A. Solomon, 1994: The global heat balance - heat transports in the atmosphere and ocean. *Climate Dynamics*, **10 (3)**, 107–134, doi: {10.1007/BF00210625}.

Trigo, R., I. Trigo, C. DaCamara, and T. Osborn, 2004: Climate impact of the European winter blocking episodes from the NCEP/NCAR Reanalyses. *Climate Dynamics*, **23 (1)**, 17–28, doi: {10.1007/s00382-004-0410-4}.

Troccoli, A., 2010: Seasonal climate forecasting. *Meteorological Applications*, **17 (3)**, 251–268, doi: {10.1002/met.184}.

Troccoli, A., et al., 2018: Creating a proof-of-concept climate service to assess future renewable energy mixes in Europe: An overview of the C3S ECEM project. *Advances in Science and Research*, **15**, 191–205, doi: {10.5194/asr-15-191-2018}, 17th EMS Annual Meeting / European Conference for Applied Meteorology and Climatology, Dublin, IRELAND, SEP 04-08, 2017.

UK Government, 2008: Climate change act 2008. `https://www.legislation.gov.uk/ukpga/2008/27/contents`.

UNFCCC, 1997: Kyoto protocol. `https://unfccc.int/resource/docs/publications/08_unfccc_kp_ref_manual.pdf`.

UNFCCC, 2015: Paris agreement. `https://bigpicture.unfccc.int/#content-the-paris-agreemen`.

US Department of Energy, 2008: 20energy's contribution to u.s. electricity supply. 248 pp.

Vallis, G. K., E. P. Gerber, P. J. Kushner, and B. A. Cash, 2004: A mechanism and simple dynamical model of the north atlantic oscillation and annular modes. *Journal of the Atmospheric Sciences*, **61 (3)**, 264–280, doi: 10.1175/1520-0469(2004)061⟨0264:AMASDM⟩2.0.CO;2.

van Goor, H. and B. Scholtens, 2014: Modeling natural gas price volatility: The case of the UK gas market. *Energy*, **72**, 126–134.

Visbeck, M., E. Chassignet, R. Curry, T. Delworth, R. Dickson, and G. Krahmann, 2003: *Chapter: The Ocean's response to North Atlantic Oscillation variability. In The North Atlantic Oscillation: Climatic significance and environmental impact.* American Geophysical Union, Washington, DC, doi: {10.1029/134GM06}.

Wallace, J. and D. Gutzler, 1981: Teleconnections in the geopotential height field during the northern hemisphere winter. *Monthly Weather Review*, **109 (4)**, 784–812.

Wallace, J. M. and P. V. Hobbs, 1977: *Atmospheric Science: An Introductory Survey*. Academic Press, Inc.

Wang, B., et al., 2009: Advance and prospectus of seasonal prediction: assessment of the APCC/CliPAS 14-model ensemble retrospective seasonal prediction (1980-2004). *Climate Dynamics*, **33 (1)**, 93–117, doi: {10.1007/s00382-008-0460-0}.

Wang, L. and W. Chen, 2010: ownward Arctic Oscillation signal associated with moderate weak stratospheric polar vortex and the cold December 2009. *Geophysical Research Letters*, **37 (3)**, doi: {10.1029/2010GL042659}.

Wangpattarapong, K., S. Maneewan, N. Ketjoy, and W. Rakwichian, 2008: The impacts of climatic and economic factors on residential electricity consumption of Bangkok Metropolis. *Energy and Buildings*, **40 (8)**, 1419–1425, doi: {10.1016/j.enbuild.2008.01.006}.

Watson, S., 2014: Quantifying the variability of wind energy. *Wiley Interdisciplinary Reviews - Energy and Environment*, **3 (4)**, 330–342, doi: {10.1002/wene.95}.

Wilks, D., 2006: *Statistical Methods in the Atmospheric Sciences, Second Addition*. International Geophysics Series, Academic Press, Elsevier.

Williams, K. D., et al., 2015: The Met Office Global Coupled model 2.0 (GC2) configuration. *Geoscientific Model Development*, **8 (5)**, 1509–1524, doi: {10.5194/gmd-88-1509-2015}.

Wilson, I., A. Rennie, Y. Ding, P. Eames, P. Hall, and N. Kelly, 2013: Historical daily gas and electrical energy flows through Great Britain's transmission networks and the decarbonisation of domestic heat. *Energy Policy*, **61**, 301–305.

Wiser, R., et al., 2011: Wind energy: In IPCC Special Report on Renewable Energy Sources and Climate Change Mitigation. Cambridge University Press, Cambridge, United Kingdom and New York, NY, USA.

Woollings, T., 2010: Dynamical influences on European climate: an uncertain future. *Philosophical Transactions of the Royal Society A - Mathematical, Physical and Engineering Sciences*, **368 (1924)**, 3733–3756, doi: {10.1098/rsta.2010.0040}.

Woollings, T., A. Hannachi, and B. Hoskins, 2010: Variability of the North Atlantic eddy-driven jet stream. *Quarterly Journal of the Royal Meteorological Society*, **136 (649, B)**, 856–868, doi: {10.1002/qj.625}.

Woollings, T., et al., 2018: Blocking and its response to climate change. *Current Climate Change Reports*, **4 (3)**, 287–300, URL `https://doi.org/10.1007/s40641-018-0108-z`.

Zachary, S. and C. J. Dent, 2012: Probability theory of capacity value of additional generation. *Proceedings of the Institute of Mechanical Engineers Part O- Journal of Risk and Reliability*, **226 (O1, SI)**, 33–43, doi: {10.1177/1748006X11418288}.

Zachary, S., C. J. Dent, and D. J. Brayshaw, 2011: Challenges in Quantifying Wind Generation's Contribution to Securing Peak Demand. *2011 IEEE Power and Energy Society General Meeting*, IEEE Power & Energy Soc (PES); IEEE, IEEE Power and Energy Society General Meeting PESGM, General Meeting of the IEEE-Power-and-Energy-Society (PES), Detroit, MI, JUL 24-28, 2011.

Zebiak, S. and M. Cane, 1987: A model El-Nino Southern Oscillation. *Monthly Weather Review*, **115 (10)**, 2262–2278, doi: {10.1175/1520-0493(1987)115⟨2262:AMENO⟩2.0.CO;2}.

Zeng, N., J. Neelin, K. Lau, and C. Tucker, 1999: Enhancement of interdecadal climate variability in the Sahel by vegetation interaction. *Science*, **286 (5444)**, 1537–1540, doi: {10.1126/science.286.5444.1537}.

Zubiate, L., F. McDermott, C. Sweeney, and M. O'Malley, 2017: Spatial variability in winter NAO-wind speed relationships in western Europe linked to concomitant states of the East Atlantic and Scandinavian patterns. *Quarterly Journal of the Royal Meteorological Society*, **143 (702)**, 552–562, doi: {10.1002/qj.2943}.